NAVAL POSTGRADUATE SCHOOL

MONTEREY, CALIFORNIA

THESIS

EVALUATION OF CAUSES OF LARGE 96-H AND 120-H TRACK ERRORS IN THE WESTERN NORTH PACIFIC

by

Kathryn A. Payne

June 2006

Thesis Advisor:	Russell L. Elsberry
Second Reader:	Mark A. Boothe

Approved for public release; distribution is unlimited

THIS PAGE INTENTIONALLY LEFT BLANK

REPORT DOCUMENTATION PAGE		*Form Approved OMB No. 0704-0188*
Public reporting burden for this collection of information is estimated to average 1 hour per response, including the time for reviewing instruction, searching existing data sources, gathering and maintaining the data needed, and completing and reviewing the collection of information. Send comments regarding this burden estimate or any other aspect of this collection of information, including suggestions for reducing this burden, to Washington headquarters Services, Directorate for Information Operations and Reports, 1215 Jefferson Davis Highway, Suite 1204, Arlington, VA 22202-4302, and to the Office of Management and Budget, Paperwork Reduction Project (0704-0188) Washington DC 20503.		
1. AGENCY USE ONLY *(Leave blank)*	**2. REPORT DATE** June 2006	**3. REPORT TYPE AND DATES COVERED** Master's Thesis
4. TITLE AND SUBTITLE Evaluation of Causes of Large 96-h and 120-h Track Errors in the Western North Pacific		**5. FUNDING NUMBERS**
6. AUTHOR(S) Kathryn A. Payne		
7. PERFORMING ORGANIZATION NAME(S) AND ADDRESS(ES) Naval Postgraduate School Monterey, CA 93943-5000		**8. PERFORMING ORGANIZATION REPORT NUMBER**
9. SPONSORING /MONITORING AGENCY NAME(S) AND ADDRESS(ES) N/A		**10. SPONSORING/MONITORING AGENCY REPORT NUMBER**
11. SUPPLEMENTARY NOTES The views expressed in this thesis are those of the author and do not reflect the official policy or position of the Department of Defense or the U.S. Government.		
12a. DISTRIBUTION / AVAILABILITY STATEMENT Approved for public release; distribution is unlimited		**12b. DISTRIBUTION CODE**

13. ABSTRACT (maximum 200 words)

Whereas the Joint Typhoon Warning Center (JTWC) has ten track forecasts to 72 h, only four dynamical model forecasts are available at 96 h and 120 h. Forming a selective consensus (SCON) by proper removal of a likely erroneous track forecast is hypothesized to be more accurate than the non-selective consensus (NCON) of all four models. Conceptual models describing large track error mechanisms, which are related to known tropical cyclone motion processes being misrepresented in the dynamical fields, are applied to forecasts by the Navy Operational Global Atmospheric Prediction System (NOGAPS), U.S. Navy version of the Geophysical Fluid Dynamics Laboratory Model (GFDN), United Kingdom Meteorological Office (UKMO), and National Centers for Environmental Prediction (NCEP) Global Forecast System (GFS) during the 2005 western North Pacific typhoon season. A systematic error in the GFDN was identified in which the model built a false anticyclone downstream of the Tibetan Plateau, which explained over 50% of the large GFDN track errors. In the GFS model, 95% of the large errors occurred due to an incorrect depiction of the vertical structure of the tropical cyclone. The majority of NOGAPS and UKMO large errors were caused by an incorrect depiction of the midlatitude system evolutions. Characteristics of the erroneous forecast tracks and corresponding model fields are documented and illustrative case studies are presented. By applying rules of the Systematic Approach, the average SCON error was 222 n mi (382 n mi) less than NCON (JTWC) in 20% of all 120-h forecasts.

14. SUBJECT TERMS Tropical Cyclone Track Forecasting, Systematic Approach, Track Error Mechanisms Conceptual Models, Joint Typhoon Warning Center, Western North Pacific Typhoons		**15. NUMBER OF PAGES** 109
		16. PRICE CODE
17. SECURITY CLASSIFICATION OF REPORT Unclassified	**18. SECURITY CLASSIFICATION OF THIS PAGE** Unclassified	**19. SECURITY CLASSIFICATION OF ABSTRACT** Unclassified

| | | | **20. LIMITATION OF ABSTRACT** UL |

NSN 7540-01-280-5500

Standard Form 298 (Rev. 2-89)
Prescribed by ANSI Std. 239-18

THIS PAGE INTENTIONALLY LEFT BLANK

EVALUATION OF CAUSES OF LARGE 96-H AND 120-H TRACK ERRORS IN THE WESTERN NORTH PACIFIC

Kathryn A. Payne
Captain, United States Air Force
B.A., University of Virginia, 2000
B.S., Texas A&M University, 2001

Submitted in partial fulfillment of the
requirements for the degree of

MASTER OF SCIENCE IN METEOROLOGY

from the

**NAVAL POSTGRADUATE SCHOOL
June 2006**

Author: Kathryn A. Payne

Approved by: Russell L. Elsberry
                 Thesis Advisor

                 Mark A. Boothe
                 Second Reader

                 Philip A. Durkee
                 Chairman, Department of Meteorology

THIS PAGE INTENTIONALLY LEFT BLANK

ABSTRACT

Whereas the Joint Typhoon Warning Center (JTWC) has ten track forecasts to 72 h, only four dynamical model forecasts are available at 96 h and 120 h. Forming a selective consensus (SCON) by proper removal of a likely erroneous track forecast is hypothesized to be more accurate than the non-selective consensus (NCON) of all four models. Conceptual models describing large track error mechanisms, which are related to known tropical cyclone motion processes being misrepresented in the dynamical fields, are applied to forecasts by the Navy Operational Global Atmospheric Prediction System (NOGAPS), U.S. Navy version of the Geophysical Fluid Dynamics Laboratory Model (GFDN), United Kingdom Meteorological Office (UKMO), and National Centers for Environmental Prediction (NCEP) Global Forecast System (GFS) during the 2005 western North Pacific typhoon season. A systematic error in the GFDN was identified in which the model built a false anticyclone downstream of the Tibetan Plateau, which explained over 50% of the large GFDN track errors. In the GFS model, 95% of the large errors occurred due to an incorrect depiction of the vertical structure of the tropical cyclone. The majority of NOGAPS and UKMO large errors were caused by an incorrect depiction of the midlatitude system evolutions. Characteristics of the erroneous forecast tracks and corresponding model fields are documented and illustrative case studies are presented. By applying rules of the Systematic Approach, the average SCON error was 222 n mi (382 n mi) less than NCON (JTWC) in 20% of all 120-h forecasts.

THIS PAGE INTENTIONALLY LEFT BLANK

TABLE OF CONTENTS

LIST OF FIGURES

LIST OF TABLES

THIS PAGE INTENTIONALLY LEFT BLANK

ACKNOWLEDGMENTS

I would like to extend my sincerest thanks to my advisor Professor Russell Elsberry and my second reader Mark Boothe for their time and expertise in answering my hundreds of questions while I finished my thesis. My time at NPS has been an incredible experience that will help me for the rest of my Air Force career and feel so fortunate to have worked with both of you.

A special thanks to Mary Jordan for all her hard work developing and perfecting the MATLAB program used in Chapter IV. Also, I would like to thank Bob Creasey and Lt Col Karl Pfeiffer for their help with locating and manipulating the model data fields that were essential to this thesis.

THIS PAGE INTENTIONALLY LEFT BLANK

I. INTRODUCTION

A. MOTIVATION

The western North Pacific Ocean holds the distinction as not only being a key strategic region for the United States military, but also as the world's hotbed of tropical cyclone (TC) activity. Thus, billions of dollars in Department of Defense (DoD) assets in mainland Japan, Okinawa, Guam, and the Korean Peninsula are threatened each year by TCs. Military commanders in the region require as much advance notice as possible to make decisions as whether to sortie ships and aircraft, and how to protect base personnel and assets. In the past decade, dynamical models and forecasting techniques have improved such that 120-h TC track errors today are comparable with 72-h TC track errors of ten years ago (approximately 300 n mi.) Therefore, in recent years, accurate five-day forecasts have become the benchmark of advanced warning for military decision-makers.

The Joint Typhoon Warning Center (JTWC) provides official TC support to all DoD resources in the western North Pacific basin. The JTWC official TC warnings include a 120-h track forecast provided every six hours. The primary guidance used by JTWC in track forecasting is a consensus, or average, of dynamical model tracks, which is a method first described by Goerss (2000). The JTWC uses a consensus of ten dynamical models called CONW at 72 h. Given the success of 72-h forecasting (Jeffries and Fukada 2002), and after a three-year test period, the JTWC officially began issuing 120-h forecasts in May 2003. However, only four dynamical models are available for the 96-h and 120-h consensus: Naval Operational Global Atmospheric Prediction System (NOGAPS); Geophysical Fluid Dynamics Laboratory-Navy version (GFDN); National Centers for Environmental Prediction (NCEP); Global Forecast System (GFS); and United Kingdom Meteorological Office (UKMO) (Jeffries and Fukada 2002).

The JTWC average track forecast errors at 72 h, 96 h, and 120 h for the last six seasons are summarized in Fig. 1. Note that average 120-h track errors have remained at approximately 300 n mi since 2003.
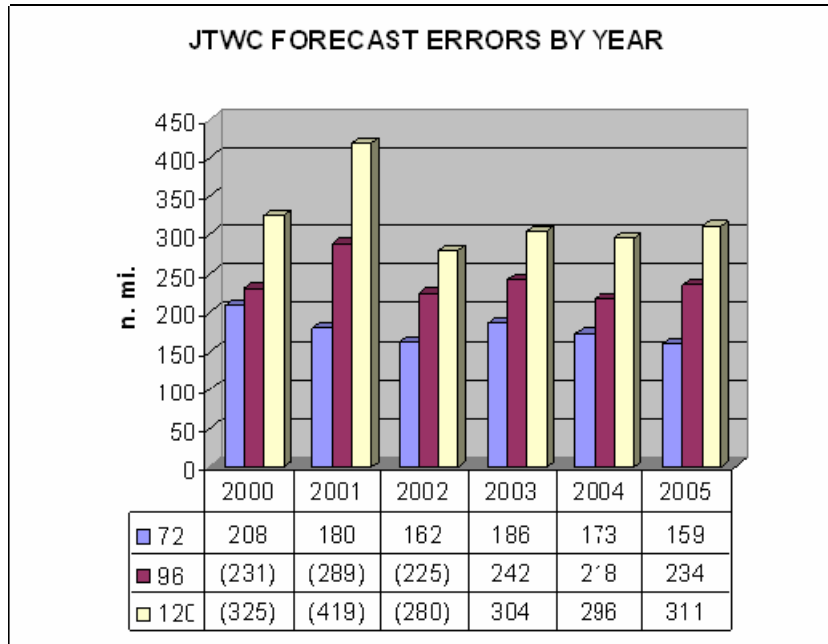
Figure 1.   Average 72-, 96-, 120-h track errors (n mi) of JTWC forecasts during 2000-2005. Data were obtained from the JTWC error statistics on their website and from Jeffries and Fukada (2002) for the 2000-2002 period when the 96-h and 120-h track forecasts were in a test mode (numbers in parentheses).

A homogenous comparison of 120-h forecast errors for the 2005 western North Pacific season is given in Fig. 2. The usefulness of consensus (CONW) track forecasting is evident at 72 h. Whereas the four dynamical models that are also used for longer forecasts have 72-h errors on the order of 175-200 n mi, when these four model tracks are combined with six other models, the CONW is about 125 n mi (Fig. 2) for this sample.

Notice that the 96-h and 120-h track errors increase significantly, and the variability among the four model tracks also increases, relative to the 72-h track errors. Whereas the GFS (UKMO) model had the superior (poorer) performance at 96 h and 120 h during 2004 (Kehoe 2005), the GFS (UKMO) had the poorest (superior) performance during 2005. Although dynamical models have greatly improved in past years, they occasionally produce TC track forecasts with large errors. Having just one member with a large error in a four-member consensus introduces uncertainty and can greatly degrade the consensus forecast accuracy. In addition, JTWC did not improve upon the CONW at 96 h and 120 h during the 2005 season.
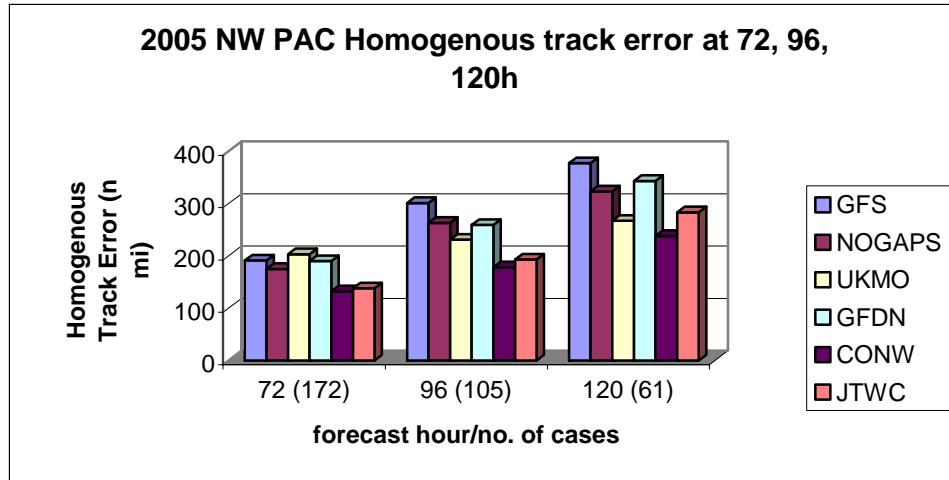
Figure 2. Homogenous track error comparison for 2005 season for the various models (see inset), the consensus (CONW), and the JTWC calculated from JTWC aids and best-track files. The number of cases is indicated in parentheses.

For these reasons, it is desirable to study the sources of these large 96-h and 120-h track errors by the various models and give guidance to the JTWC forecaster as to when to trust the model track guidance. It is hypothesized that operational track forecasts can be improved if forecasters can identify in "real time" if a large error is occurring in a dynamical model.

B. BRIEF HISTORY OF CONSENSUS TRACK FORECASTING

1. Goerss (2000)

Based primarily on the improvements to global and regional dynamical models, Goerss (2000) noted the significant increase in skill of track forecast guidance in the 1990s. Whereas ensemble model forecasts had previously been used in extratropical numerical weather prediction (NWP) by creating a series of perturbations to the initial conditions of a single model, Goerss (2000) suggested using an ensemble of multiple NWP models to reduce TC track forecast errors. Elsberry and Carr (2000) later characterized such an average of multiple NWP center TC tracks as a "non-selective consensus," which will be used hereafter. The mean consensus forecast error over some sample is expected to be smaller than the mean forecast errors of the individual models (if the individual models are independent) because the random errors will be reduced in the averaging. The smaller the correlation between the model forecast errors, i.e., larger

3

the effective degrees of freedom, the smaller the mean consensus error will be compared to means of the individual model forecast errors.

Goerss (2000) produced a consensus track forecast using the forecast positions of the Geophysical Fluid Dynamics Laboratory (GFDL) model plus NOGAPS and UKMO from the 1995-1996 Atlantic season, since the models were known to have roughly equal accuracies. The consensus error was improved (statistical improvement to 99% level) at 24, 48, and 72 h compared to the best individual model. Similarly, Goerss created a consensus for the western North Pacific, using UKMO, NOGAPS, and the Japanese Global Spectral Model (JGSM). In this case, the NOGAPS errors were larger than for the other two models. However, the consensus still showed statistically significant improvement over the best model (JGSM) at greater than the 90% level at all forecast intervals. Goerss found that the three-model track consensus was slightly better than a consensus of UKMO and JGSM (removing NOGAPS, the poorest performer), although the improvement was not statistically significant. A second consensus of two regional models in the western North Pacific, the Navy version of the GFDL model called GFDN and the Japan Typhoon Model (JTYM) also had superior performance to the better of the two models at 24 h, 48 h, and 72 h.

Goerss (2000) calculated the means and standard deviations of the across-track and along-track errors of each individual model and the consensus, and found mean consensus errors to be neither the best nor the worst. However, the standard deviations of along-track/across-track errors for the consensus were smaller than for each individual model. He concluded the smaller error distribution of the consensus accounted for its improvement in forecast error versus the individual models. Thus, consensus forecasts could be used operationally as an improvement on the guidance of individual models.
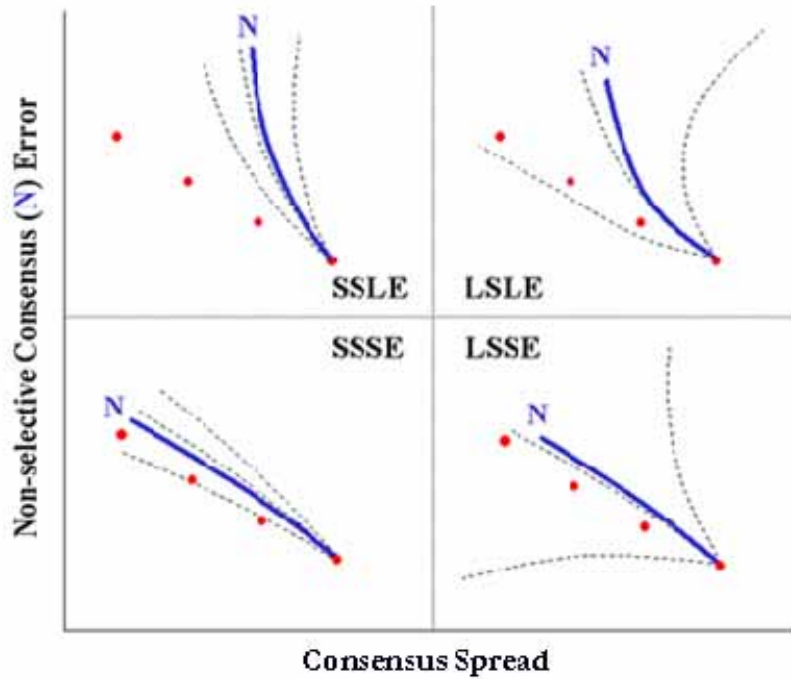
Figure 3.   Schematics of non-selective (N) consensus tracks (solid) from three member tracks (small dotted lines) and the actual 24-, 48-, and 72-h positions (large dots) in four possible scenarios: small spread and large error (SSLE); small spread and small error (SSSE); large spread and large error (LSLE); and large spread and small error (LSSE) (from Elsberry and Carr 2000).

2.   Carr and Elsberry Studies

In an extension of the work by Goerss (2000), Elsberry and Carr (2000) sought a relationship between the consensus spread and the error of the consensus. They created a five-member consensus of the operationally available versions of three global and two regional models (NOGAPS, JGSM, UKMO, GFDN, and JTYM) by translating the forecast track from the dynamical model such that the starting position 6 h or 12 h later agreed with the new warning position. Spread was defined as the maximum displacement of an individual model forecast from the consensus forecast position. Based on a sample of 381 cases from the western North Pacific in 1997, the authors divided consensus forecasts into four possibilities (Fig. 3): (i) small spread, small error (SSSE); (ii) small spread, large error (SSLE); (iii) large spread, large error (LSLE); and (iv) large spread, small error (LSSE). For these 72-h track forecasts, "large" was defined to be in excess of 300 n mi spread or error.

The SSSE is the ideal scenario in which all of the model tracks and the consensus track provide sound guidance. The SSLE case is perhaps the nightmare scenario in which all the forecast guidance departs from reality. The LSLE case results from a bifurcation of model guidance (e.g., between a straight-running and recurvature path) in which one of these paths is actually correct and a consensus between the two clusters would result in large error. In the final LSSE scenario, the actual TC path is between bifurcation of two guidance tracks, and the compensating errors for those two tracks still leads to a small consensus error.

Elsberry and Carr (2000) explored two ways that an operational forecaster can "add value" to a non-selective consensus (NCON) forecast: (i) identify the model with the minimum track error among the consensus; or (ii) identify the model with the maximum track error. In the first case, identifying the best model track is extremely difficult in that no model is best in every scenario and no guidance exists to aid the forecaster in identifying the best model track. In the second case, if a forecaster could remove a model track suspected to have a large track error, he/she could then make a selective consensus (SCON) of the remaining forecast models. The authors suggest a SCON could make the most improvement in a LSLE case (bifurcation scenario) by eliminating the wrongly forecast branch. To remove the erroneous forecast, a forecaster must have a knowledge base of conceptual model errors, and characteristic errors of the individual models within the consensus.

Thus, Carr and Elsberry (2000a, b) reviewed cases of large track errors at 72 h (greater than 300 n mi) in the NOGAPS and GFDN models during the 1997 western North Pacific typhoon season. From this study, they developed a set of conceptual models for the physical mechanisms that cause large track errors, which almost always resulted when the models improperly forecast a physical mechanism determining the TC motion. This knowledge base of frequent model track errors was designed to help operational forecasters detect when dynamical model guidance was likely to be erroneous. By identifying that a characteristic error mechanism was occurring, a forecaster could eliminate the offending model and create a SCON track forecast that should be more accurate than the NCON track forecast.

Carr et al. (2001) used cases from the 1999 western North Pacific season to conduct a beta test of the production of a SCON track forecast. A team of researchers attempted to create SCON TC track forecasts using the knowledge base of GFDN and NOGAPS model error characteristics developed by Carr and Elsberry (2000a, b). Carr et al. (2001) concluded it was not advisable to create a SCON forecast over a non-selective consensus (NCON) when the consensus spread was less than 250 n mi. The study found 14 (out of 31) cases in which a 72-h SCON forecast improved upon the NCON by 10%, which the authors felt indicated a forecaster could indeed "add value" via a SCON forecast. The authors further suggested that a complete knowledge base of all the models, as well as data fields for all models in the consensus, could improve the success of the SCON.

In 2000, the JTWC implemented the Systematic Approach Forecasting Aid (SAFA) defined by Carr and Elsberry (2000a, b), and identified the use of NCON as the top contributor to decreased forecast error at 72 h (Jeffries and Fukada 2002). During the first year, forecasters had difficulty creating a SCON that improved upon NCON. Post-season analysis determined that a SCON forecast was often created by JTWC forecasters when none was required (Jeffries and Fukada 2002). It is hypothesized that a more careful application of model characteristic errors traits and a set of error mechanisms for all models in the consensus will enable forecasters to create an SCON that improves upon a NCON. Since Jeffries and Fukada (2002) found that NCON skill was increased if more than three dynamic models were included in the consensus, and only four models are available at 96-h and 120-h, eliminating one or more model tracks may also cause problems.

3.   Kehoe 2005

With the extension of JTWC official forecasts to 120 h, a new investigation of model characteristics and error mechanisms was desirable since despite reductions in average track forecast errors, dynamical models still produce forecasts with large errors. Following the methods of Carr and Elsberry (2000a, b), Kehoe (2005) examined 2004 western North Pacific model forecasts and best-track data from the 2004 season to identify characteristic errors of the NOGAPS and GFDN models that lead to large 96-h and 120-h track errors. A summary of Kehoe's findings is given in Appendix A.

C.   THESIS OBJECTIVES

As dynamical models are constantly being upgraded and improved (Appendix B), the frequency of the track error mechanisms in each model may change from year to year. Thus, studying these models fields to determine error mechanisms is essential to assess the usefulness of track guidance supplied to JTWC forecasters. This research will continue the efforts of Kehoe (2005) to produce a set of error mechanism conceptual models for the NOGAPS and GFDN models applicable to 120-h track forecasts by studying the 2005 western North Pacific season. In addition, frequently occurring mechanisms in the UKMO and GFS models will be assessed for the first time. This combined study of large track error mechanisms will add to the meteorological knowledge base that may be exploited by JTWC forecasters. Finally, an estimate of 120-h predictability based on these four models will be calculated assuming a forecaster can perfectly eliminate a dynamical model track containing a large error. This metric will provide a goal to achieve optimum benefit from the four-model guidance in improving tropical cyclone support to the U.S. military in the western North Pacific.

II.   METHODS

A.   EVALUATION OF LARGE TRACK ERRORS

Following the procedures established by Carr and Elsberry (2000 a, b) and Kehoe (2005), large track errors (exceeding 400 n mi at 96 h and 500 n mi at 120 h) were identified for NOGAPS, GFDN, GFS, and UKMO in the western North Pacific during 2005. Large track errors were determined by comparing the interpolated model track forecasts (as used operationally by JTWC and described by Goerss et al. 2004) with the best track. The numbers of large 96-h and 120-h track errors that occurred in NOGAPS, GFDN, GFS, and UKMO were 60, 66, 40, and 38, respectively. Forecast fields through 120 h were then reviewed to determine the mechanism leading to each large error. While Kehoe (2005) studied frequent error characteristics during the 2004 season for the NOGAPS and GFDN models, this is the first study in which GFS and UKMO fields were available for review of large track errors.   Error mechanisms were described (if appropriate) by conceptual models (Carr and Elsberry 2000 a, b) that were related to known tropical cyclone motion processes being misrepresented in the dynamical fields. In an extension of the previous research, the model depiction of TC structure and vertical extent in each large error case was documented in addition to the large error mechanism.

The lack of availability of archived model fields was a major obstacle for this research. While the vast majority of NOGAPS and GFS fields for large error cases were attainable (54 out of 60, and 45 out of 53, respectively), large gaps in fields existed for the GFDN and UKMO. For the GFDN model, only 06 UTC and 18 UTC forecast fields are currently archived in the Navy Master Environmental Library (MEL) at the Naval Research Laboratory - Monterey. Large track errors for the 00 UTC and 12 UTC forecasts had to be inferred from the preceding and following model forecasts. However, 16 (out of 66) large error cases remained in which an error mechanism could not be determined. For the UKMO model, 14 out of 45 fields for large error cases could not be accessed. As a result, no error mechanism could be determined in three of the ten TCs in which large track errors occurred in the UKMO model. Additionally, UKMO fields were only available through the 120-h forecast. Since the interpolated forecasts use the 126-h and 132-h forecasts from the available 00 UTC or 12 UTC forecast to get an interpolated

track forecast, these fields were not available for review. The appropriate error mechanism was inferred from the accessible fields through 120 h.

Due to the nature of the data files, the forecast fields had to be reviewed in two separate software programs. The NOGAPS and GFDN fields were reviewed in the SAFA system, but the UKMO and GFS fields were reviewed using GEMPAK Analysis and Rendering Program (GARP). The GARP displayed the model fields in 1º lat. and long. resolution. In both SAFA and GARP, models fields and verifying analyses were reviewed within the same software program to allow for easier comparison of meteorological features. For consistency and due to its availability, NOGAPS 0-h and 6-h fields were used as the verifying analysis for all model comparisons.

The primary model and verifying analysis fields used to determine large error mechanisms were winds (streamlines) and geopotential heights (GPH) at 200, 500, 700, and 850 mb and mean sea-level (MSL) pressure. However, no GPH fields were archived in MEL for the GFDN model. The 500- and 700-mb GPH fields were used to determine the strength of midlatitude features impacting the TC steering environment. Streamlines at 850 through 500 mb were essential in determining possible interaction between two adjacent cyclones that could be either tropical or midlatitude in nature. In addition, GARP contained a function that calculated and displayed vertical wind shear from 850 to 200 mb, which allowed an assessment of impact of such shear on the TC. The MSL pressure fields and 500-mb GPH were used to determine TC size, structure, and vertical extent.

B.   ESTIMATION OF 120-H PREDICTABILITY

Predictability for 120-h forecasts based on optimum use of available dynamical model guidance was estimated assuming that a forecaster could identify a frequently occurring error mechanism in real time. The optimum use of the model guidance focuses on the LSLE cases in Fig. 3, since the forecaster should accept the NCON for the SSSE and LSSE (compensating errors) cases and must necessarily accept the NCON of the SSLE cases in lieu of other guidance. Following procedures established by Elsberry and Carr (2000), the spread of the consensus was calculated for each 120-h forecast for the 2005 western North Pacific season via the MATLAB program. The MATLAB program

10

was also used to calculate a selective consensus (SCON) when appropriate, and then calculate the SCON error versus the best-track data.

THIS PAGE INTENTIONALLY LEFT BLANK

III. ANALYSIS OF LARGE TRACK ERROR CASES

A. CONCEPTUAL MODEL ERROR MECHANISMS

Following the procedures established in Carr and Elsberry (2000a, b) and Kehoe (2005), conceptual models of the sources of large errors were matched to each case, and the summary is presented in Table 1. Large track errors were divided into those due to tropical influences and those due to midlatitude influences. In addition to assigning the error mechanism, the model depiction of the TC structure and its possible contribution to the track error for each TC was noted in each large error case.

Error mechanisms due to tropical influences included Direct Cyclone Interaction (DCI-t), Indirect Cyclone Interaction (ICI), and Ridge Modification by the Tropical Cyclone (RMT). Tropical error mechanisms accounted for only 5%, 11%, 13%, and 11% of all large 96-h and 120-h errors in NOGAPS, GFDN, GFS, and UKMO, respectively (Table 1). Supporting Kehoe's conclusions from the 2004 season analysis, midlatitude error mechanisms also dominated the large track error cases in the 2005 season: 95%, 89%, 87%, and 89% of all large errors in NOGAPS, GFDN, GFS, and UKMO, respectively. Midlatitude error mechanisms contributing to large errors were Direct Cyclone Interaction-midlatitude (DCI-m), Response to Vertical wind Shear (RVS), Midlatitude Cyclogenesis (MCG), Midlatitude Cyclolysis (MCL), Midlatitude Anticyclogenesis (MAG), and Midlatitude Anticyclolysis (MAL). In 16 cases, the large error was caused by a mechanism not previously described by Carr and Elsberry (2000 a, b) or Kehoe (2005). Two large errors in GFDN were caused when the TC failed to decay after making landfall, and 14 cases occurred in GFS in which the TC excessively dissipated without the presence of vertical wind shear. In four, 16, eight, and 14 cases in NOGAPS, GFDN, GFS, and UKMO, respectively, no error mechanisms could be assigned due to a lack of model fields. Hereafter, error mechanisms will be referred to by their three letter acronym as defined in Table 1 with a prefix of E (excessive) or I (insufficient).

In the following sections, the most frequently occurring tropical and midlatitude mechanisms in NOGAPS, GFDN, GFS, and UKMO will be highlighted.

Table 1. 96-h and 120-h error mechanisms for NOGAPS, GFDN, GFS, and UKMO occurring in 2005. *The first (second) number listed is the number of times the phenomenon occurred excessively (insufficiently). ** Two "Other" GFDN errors occurred due to the model TC failing to decay over land. *** Fourteen "Other" GFS errors occurred when the TC excessively dissipated with no vertical shear involved.

2005 96-h and 120-h Error Mechanisms					
Phenomenon name	Acronym	No. of NOGAPS forecasts*	No. of GFDN forecasts*	No. of GFS forecasts*	No. of UKMO forecasts*
Large Errors due to Tropical Influences					
Direct Cyclone Interaction(tropical)	DCI	2-0	7-0	6-0	4-0
Indirect Cyclone Interaction (West TC)	ICI-W	0-0	0-0	1-0	0-0
Ridge Modification by TC	RMT	1-0	0-0	0-0	0-0
Large Errors due to Midlatitude Influences					
Direct Cyclone Interaction(midlatitude)	DCI-m	1-0	0-0	12-0	4-0
Response to vertical wind shear	RVS	6-0	0-0	9-0	0-0
Midlatitude cyclogenesis	MCG	21-9	4-1	0-2	2-14
Midlatitude cyclolysis	MCL	4-0	0-1	0-1	0-0
Midlatitude anticyclogenesis	MAG	7-5	31-0	0-0	7-0
Midlatitude anticyclolysis	MAL	0-0	4-0	0-0	0-0
Other		0	2**	14***	0
Fields not available		4	16	8	14
Total		60	66	53	45
* The first (second) number listed is the number of times the phenomenon occurred excessively (insufficiently)					
** two "Other" GFDN errors occurred due to the model TC failing to decay overland					
*** Fourteen "Other" GFS errors occurred when TC excessively dissipated with no vertical wind shear involved					

B. TROPICAL INTERACTION ERROR MECHANISMS

The only tropical mechanism to frequently cause large errors during the 2005 season was Excessive Direct Cyclone Interaction (E-DCI-t). In agreement with the previous research by Carr and Elsberry (2000a) and Kehoe (2005), no insufficient cases of DCI occurred during the 2005 season.

1. Description

In the conceptual model of DCI (Fig. 4), two tropical cyclones rotate about one another cyclonically, with a possible merger into one circulation. Carr and Elsberry (2000a) previously found that one third of all large track errors at 72 h were due to E-DCI (occurring in both the tropics and in the midlatitudes). The E-DCI-t errors occurred when a TC was forecast to either falsely or too vigorously interact with an adjacent cyclonic circulation (Carr and Elsberry 2000a). Kehoe found through analysis of the 2004 season that the smaller of the two circulations was usually accelerated as it rotated counter-clockwise (CCW) around the larger circulation, while the larger circulation displayed little CCW rotation, but had a slowing of its westward track.
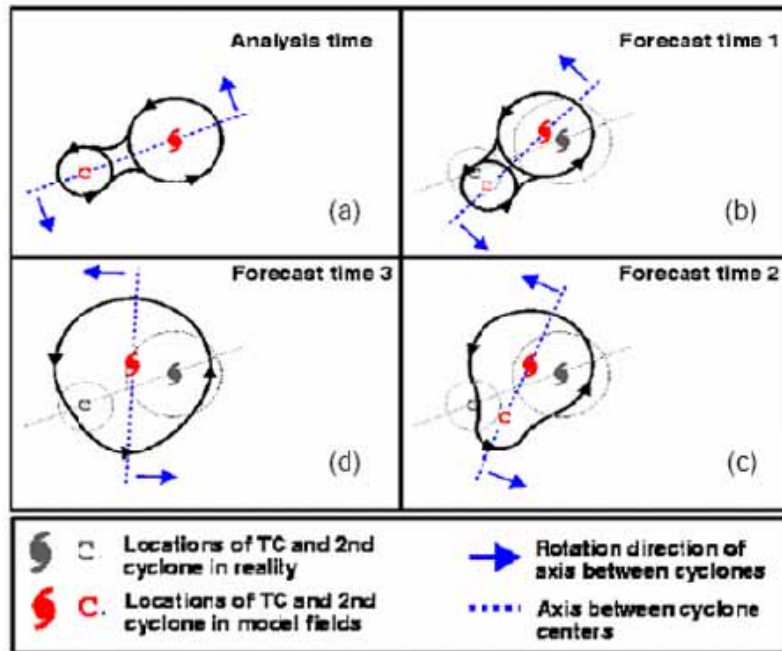
Figure 4.   Conceptual model of DCI in which a TC circulation interacts with another cyclone (C) to cause a counterclockwise rotation of the axis between the cyclone centers (heavy dashed line) and a possible merger of the two cyclones in which the combined circulation becomes larger with time [(c) and (d)]. The TC may also be the smaller of the two cyclones, or the model may be applied to two TCs of similar sizes in which the tracks of both TCs will be affected (from Carr and Elsberry 2000a).

Kehoe (2005) further noted three reasons why the models falsely predicted E-DCI-t: (i) either the TC or the other cyclone was predicted to have too large a horizontal extent; (ii) either the TC or the other cyclone was misplaced such that the separation distance between the two was too small; or (iii) the TC was predicted by the model to be weaker than reality, such that its steering was controlled by the correctly forecast cyclone. Both Carr and Elsberry (2000a) and Kehoe (2005) determined that for all cases of model-predicted tropical E-DCI in the 1997 and 2004 respectively, DCI failed to occur in reality. Given this fact, both studies concluded that if the forecaster can diagnose the occurrence of DCI in the numerical model, the forecast interaction is most likely false.

2.   Frequency and Characteristics

The E-DCI-t mechanism caused large errors in all four models (Table 1): NOGAPS (2 cases), GFDN (7), GFS (6), and UKMO (4). All E-DCI-t errors occurred in TY Khanun (15W). In every case, the model TC interacted with a tropical low to the

west of the Philippines such that the TC rotated counter-clockwise around the tropical low or merged with it. This interaction caused model forecast tracks that were south of the actual track. In reality, Khanun had sufficient intensity to escape the influence of the tropical low and continue a northwestward track under the influence of the subtropical ridge to the east. The GFS and NOGAPS models both under-forecast the structure of Khanun, which (as described in Carr and Elsberry 2000a) likely contributed to the false interaction with the second circulation. Although the depiction of the TC structure in the UKMO model was more accurate, it was still slightly under-forecast. However, the UKMO model over-forecast the strength of the second low, and the separation between the second low and the TC was much smaller in the model than in reality. In contrast, the high-resolution GFDN model predicted a merger with the tropical low to form a larger TC over the Philippines. The GFDN and GFS forecasts will be examined in more detail in the case study below.

Kehoe (2005) found E-DCI-t errors occurred more frequently during the 2004 western North Pacific season, with 11 GFDN cases and 20 NOGAPS cases in five TCs. For the majority of the NOGAPS cases, Kehoe noted that an incorrect intensity forecast led to a false interaction with a second cyclone. Whereas E-DCI-t occurred less frequently during the 2005 season, this difference may be explained by the formation of fewer TCs in comparison to 2004. In four of the five 2004 E-DCI-t cases, the model TC interacted with another TC. Only one instance occurred in which two TCs were within 500 n mi of one another during the 2005 season, and E-DCI-t did not occur. Given the continued propensity of the global models to under-forecast TC structure, such TCs are still likely to falsely interact with a second cyclone if it is too close to the TC.

3.   Case Studies

For the 1800 UTC 7 September forecasts of TC Khanun, all four models provided poor guidance at 96 h for JTWC forecasters. All model tracks had large forecast errors (greater than 400 n mi), and the non-selective consensus (CONW) forecast had an error of 545 n mi. This case study will illustrate the E-DCI-t error (706 n mi) occurring in GFS, which is similar in nature to the NOGAPS (438 n mi) and UKMO (474 n mi) forecast errors. The E-DCI-t large error (713 n mi) occurring in GFDN will also be described.
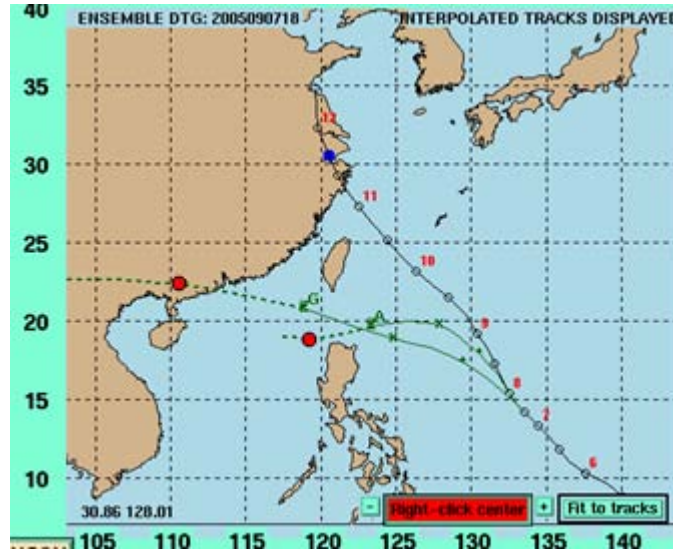
Figure 5.   Interpolated forecast tracks for 15W (Khanun) by GFDN (G) and GFS (A) for the 1800 UTC 7 September 2005 forecasts. The solid sections of the forecast tracks represent the 00-h through 72-h forecast while the dashed sections represent the 72-h through 120-h forecast. The solid line with open circles and corresponding dates represents the TC best track. The verifying 96-h position is indicated by the blue circle, while the 96-h interpolated forecasts are indicated by the corresponding red circles.

a.   GFS E-DCI-t error

The GFS forecast track for Khanun (Fig. 5) changes from a northwestward track to an almost westward track, which takes the TC just north of the Philippines. In reality, Khanun moves north of Taiwan and makes landfall near Shanghai. At the initial time, Khanun has an intensity of 60 kt. However, the GFS depiction of the initial TC structure is too weak (not shown). Although the GFS TC undergoes slight intensification in the first 12 h, it then remains at constant intensity. The E-DCI in the GFS model is caused by the fact that the model TC is too weak to be steered by the midlatitude ridge to its north, and thus cannot escape the circulation of the second low. This results in the model TC being too close to the second circulation, further exacerbating the E-DCI.

17
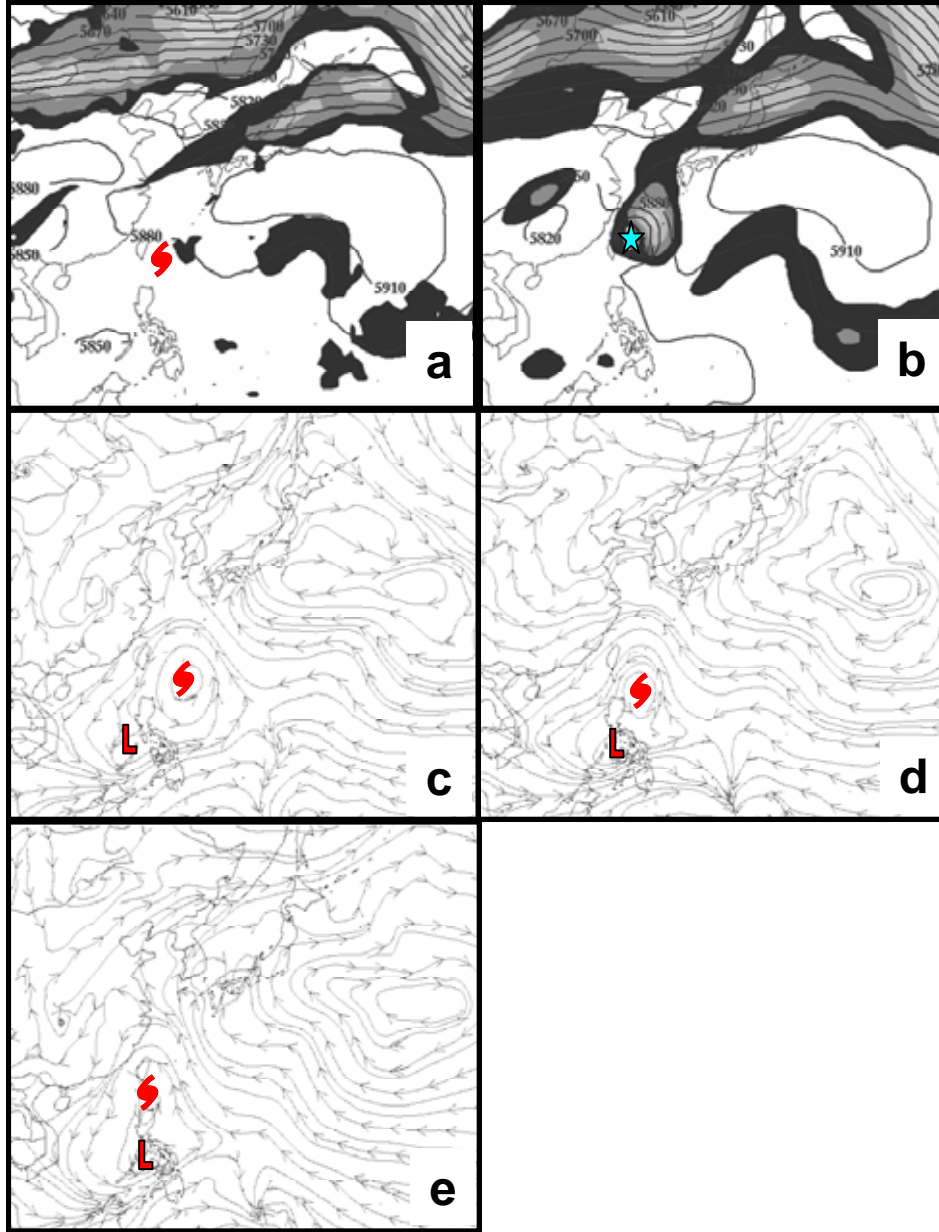
Figure 6.   Forecast 500-mb geopotential heights (m) and isotach (contour interval of 20 kt beginning at 20 kt) field for 15W (Khanun) predicted by (a) GFS and (b) verifying NOGAPS analysis for tau 66 of 1800 UTC 7 September 2005 forecast. Verifying TC position indicated by star. Forecast 850-mb wind fields predicted by the GFS for taus (c) 54, (d) 66, and (e) 78. The forecast TC position is indicated by the red TC symbol, and the second cyclone is indicated by the red "L".

A comparison of the 66-h 500-mb geopotential height fields reveals several concentric isopleths around the verifying (NOGAPS) analysis of the TC (Fig. 6b), while no closed vortex is evident in the GFS model fields (Fig. 6a). An isotach maximum

to the northeast of the TC in the verifying analysis indicates the strong steering environment provided by the subtropical ridge to the northeast of the storm. Although the subtropical ridge has a comparable intensity in the 500-mb GFS fields, almost no isotach maximum is evident. By 54 h (not shown) in the forecast, Khanun is already well to the northeast of the TC in the GFS forecast and is not being influenced by the second circulation west of the Philippines. The weaker TC in the GFS forecast is migrating toward the second low circulation, as opposed to being steered by the subtropical ridge at 500 mb. An examination of the GFS 850-mb streamlines from 54 h to 78 h (Fig. 6c-e) shows the counterclockwise rotation of the model TC about a low over the Philippines.

b.   GFDN E-DCI-t error

The GFDN model forecast takes Khanun south of Taiwan (Fig. 5). In contrast to the GFS model forecast of Khanun, the GFDN model properly depicts the initial intensity of the TC (not shown). Given its vertical structure, the model TC should be able to escape any possible rotation about a weaker cyclone. Examination of the 54-h MSL pressure forecast (Fig. 7a) reveals a lobe of low pressure on the western coast of the Philippines. By 60 h (Fig. 7c), the lobe has intensified, and by 66 h (Fig. 7e) this lobe has been absorbed into the core of the model TC. This evolution is a characteristic signature of E-DCI. In the NOGAPS analyses, the second cyclone is well to the west of the Philippines (Figs. 7d, e, f).

The 850-mb GFDN model streamlines (Figs. 8a, c, e) further depict the merger of the two cyclones into one massive cyclone stretching from Vietnam to Okinawa. While some interaction between the wind fields of the two cyclones is apparent in the verifying NOGAPS analyses, no merger occurs (Figs. 8b, d, f). Such an E-DCI occurrence in the GFDN occurs because the second circulation is much closer to the TC than in reality. Due to the orientation of the 500-mb anticyclone to the north (not shown), the model TC encounters a more westerly than northwesterly steering, which brings it closer to the Philippines.
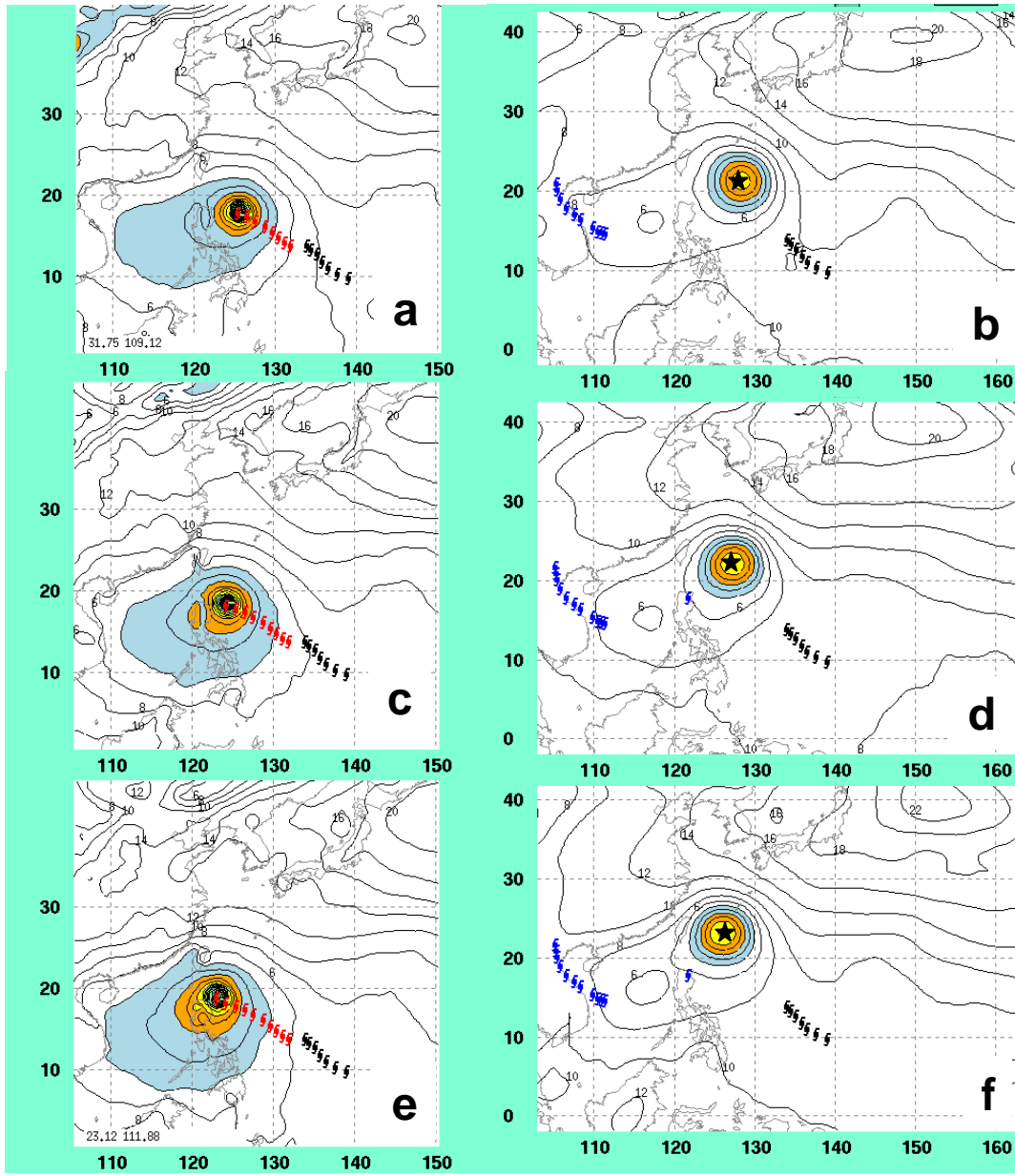
Figure 7.   Forecast mean sea-level pressure (mb) forecast fields for 15W (Khanun) by GFDN for taus (a) 54, (c) 60, and (e) 66 for 1800 UTC 7 September 2005 and the corresponding verifying 00-h NOGAPS analyses (b, d, and f). The verifying TC position is indicated by a black star. Pressure values below 1004 mb are shaded.
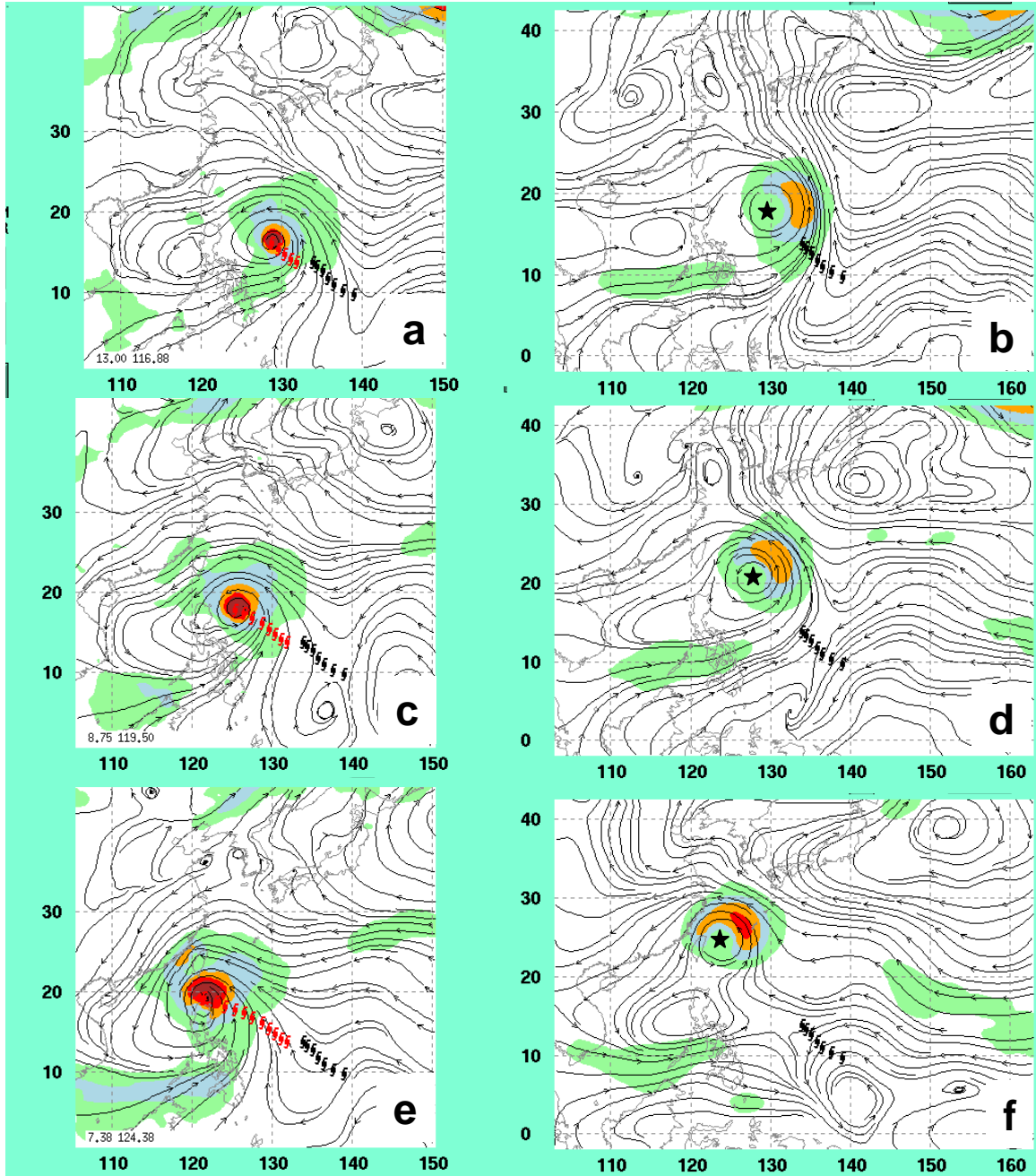
Figure 8.   Forecast 850-mb streamline and isotach (contour interval of 20 kt starting at 20 kt) fields for 15W (Khanun) by GFDN for taus (a) 36, (c) 54, and (e) 72 for 1800 UTC 7 September 2005 and the corresponding verifying 00-h NOGAPS analyses (b, d, and f). The verifying TC position is indicated by a black star.

While the GFDN initially depicted the second cyclonic circulation to the west of the Philippines accurately (not shown), as the TC approached, the center of the second cyclone was relocated over the northern island of Luzon (Fig. 7a,c).   It is

hypothesized that interaction of the flow with the high terrain over the Philippines in the high resolution GFDN model led to the spin up of this cyclone in a location much closer to the model TC than in reality. Similar interaction with the tropical cyclone and higher terrain is sometimes predicted over Taiwan in the GFDN. Once the TC began to rotate around the terrain-induced cyclone (as is evident in the 850-mb streamlines), the forecast track became more westerly than northwesterly.

C. MIDLATITUDE INTERACTIONS

As previously mentioned, midlatitude error mechanisms accounted for the overwhelming majority of large track errors at 96 h and 120 h in both the 2004 (Kehoe 2005) and 2005 seasons. This midlatitude dominance might be expected since TCs tend to recurve into the midlatitudes within five days. The most frequent midlatitude-related error mechanisms during the 2005 seasons (Table 1) were the midlatitude DCI, Response to Vertical Shear (RVS), and the Midlatitude System Evolutions (MSE): Midlatitude Cyclogenesis (MCG), Midlatitude Cyclolysis (MCL), Midlatitude Anticylogenesis (MAG), and Midlatitude Anticyclolysis (MAL). These conceptual models were defined by Carr and Elsberry (2000b) and are briefly described below.

1. Midlatitude System Evolutions (MSE)

a. *Description*

According to Carr and Elsberry (2000b), an MSE occurs when a change to the TC steering flow involved the development, dissipation, and/or movement of a midlatitude circulation (cyclone, trough, anticyclone, or ridge). The MSE conceptual error mechanisms are illustrated in Fig. 9. These errors may occur either excessively (E), or insufficiently (I). For a dynamical model to correctly forecast TC recurvature, it must also correctly forecast MSEs affecting the TC steering environment.

Consider the TC located south of the subtropical ridge prior to a MCG event (Fig. 9). The MCG will cause a break in the subtropical ridge, and thus possibly affect both the direction and speed of the TC (Carr and Elsberry 2000b). During E-MCG, the model midlatitude trough amplitude is often over-forecast such that the TC undergoes an accelerated recurvature versus the actual track. During I-MCG, the model depiction of the midlatitude trough amplitude is under-forecast such that recurvature does not occur or is too slow.

22
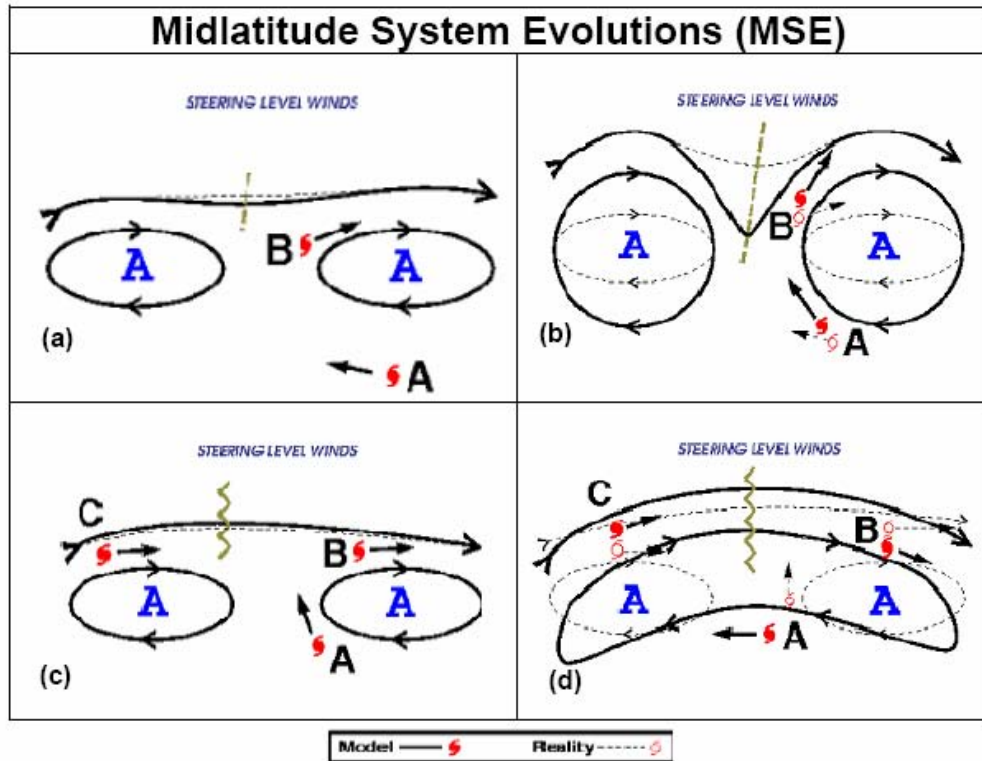
Figure 9.   Schematics of the MSEs that may lead to large TC track errors.   The deepening of the midlatitude trough from (a) to (b) depicts the MCG and the reverse order [(b) to (a)] implies MCL.   Similarly, the midlatitude anticyclone change poleward of the TC from (c) to (d) depicts MAG and the reverse order [(d) to (c)] implies MAL (from Carr and Elsberry 2000b.)

The process of MCL can be described by reversing the order of MCG events [i.e., (b) to (a) in Fig. 9] (Carr and Elsberry 2000b). An E-MCL error may occur when a midlatitude trough moves too quickly, or weakens too rapidly, to influence the steering of the TC. In contrast, I-MCL occurs when a midlatitude trough does not move quickly enough or fills prematurely, and thus falsely influences the steering for the TC.

In the MAG conceptual model, the TC is tracking poleward along the periphery of the subtropical ridge when the ridge builds sufficiently to inhibit the poleward track of the TC, or force the TC to transition to a westward track (Carr and Elsberry 2000b).   For E-MAG, the steering ridge is depicted as too strong in the model compared to reality, which prevents the TC from turning poleward and/or undergoing recurvature at the appropriate time and location. For I-MAG, the TC poleward track is delayed in reality,

but in the model the steering ridge is depicted as too weak, and thus recurvature occurs too soon.

The MAL error mechanism is described by reversing the order of MAG events [i.e., (d) to (c) in Fig. 9] (Carr and Elsberry 2000b). If the steering ridge in the model weakens too rapidly, the TC is falsely translated poleward/ recurves and E-MAL is occurring. In contrast, I-MAL occurs when the steering ridge weakens rapidly in reality (thus allowing the TC to move poleward), but the ridge in the model is too strong and the TC remains below the subtropical ridge axis.

b.   *Frequency and Characteristics-Global Models*

Midlatitude System Evolutions accounted for 82% (46 of 56 cases with fields available) of large errors in NOGAPS, and 74% (23 of 31 cases with fields available) of large errors in UKMO (Table 1). Kehoe (2005) found that 51% of 2004 season large errors in NOGAPS were due to MSEs, although the sample size for 2004 was much larger than for 2005. In contrast, only three instances (of 31 cases with fields available) of MSE errors were observed in the GFS during 2005.

Midlatitude Cyclogenesis was the most commonly occurring large error in NOGAPS, as it occurred excessively (E) in 21 cases in four TCs and insufficiently (I) in nine cases in two TCs (Table 1). The two-sided (both excessively and insufficiently) nature of this error in NOGAPS will make it difficult for forecasters to assess the nature of the error in real time. Fourteen of the E-MCG cases involved an overly deep midlatitude trough that caused an acceleration of the TC to the northeast too quickly, and resulted in large along-track errors. Conversely, for nine cases of I-MCG involving two TCs, NOGAPS failed to sufficiently deepen a midlatitude trough, which resulted in the TC not translating to the northwest quickly enough. The other seven E-MCG cases involved two TCs in which the NOGAPS model spun up a false cyclone in the vicinity of the remnants of a decaying second circulation, which could be either another TC or a midlatitude circulation. In these NOGAPS forecasts, the TC then interacted with the false circulation in such a way as to create a large track error. In both TCs, the structure of the model TC was falsely depicted as being too shallow, which exacerbated the interaction between the two cyclones. One such interaction in Banyan (07W) is described in the case study below.

Whereas Kehoe (2005) also found MCG-related errors to be the most commonly occurring error mechanism in NOGAPS in 2004, he found I-MCG (53 cases) occurred much more frequently than E-MCG (six cases). Kehoe did not note any cases in which NOGAPS spun up a false midlatitude low.

The most frequent MSE-related error mechanism attributed to the UKMO model was I-MCG (Table 1), although 12 of the 14 cases occurred consecutively in Banyan (to be described below). For these 12 I-MCG cases, a migratory shortwave trough was predicted to be insufficiently deep. By contrast, only two UKMO cases of E-MCG occurred in which a migratory shortwave trough was too deep. As was the case for NOGAPS, the two-sided nature of the MCG error will make it difficult for forecasters to identify the error in real time.

Midlatitude anticyclogenesis errors also occurred both excessively and insufficiently in the NOGAPS model. All seven cases of E-MAG in three TCs involved an overly strong subtropical ridge east of Japan, which caused a TC track forecast that was too far to the west. In contrast, four of the five cases of I-MAG involved an under-forecast of the building of a mid-level subtropical steering ridge over southern China.

In the UKMO model, six of the seven cases of E-MAG (although all occurred in one storm) involved the over-amplification of a migratory midlatitude ridge that then merged with the eastern subtropical ridge to produce a more westward TC track than in reality. In contrast, the E-MAG cases in the NOGAPS forecasts occurred when the subtropical ridge built excessively. No cases of I-MAG were predicted by the UKMO model during the 2005 season.

In three TCs in which an MSE was assigned as the primary error mechanism in the UKMO model, a slow and southward bias was predicted in the first 24 to 48 hours. The slow bias accounted for approximately 1°-2° lat. in track error while the model TC was south of the subtropical ridge axis. Carr and Elsberry (1997) described a Beta Effect Propagation (BEP) error mechanism related to the TC propagation west-northwestward due to beta gyres formed from latitudinal variation of the Coriolis parameter. The BEP is larger for larger tropical cyclones. Thus, if a model significantly over- or under-forecasts the size of a TC, it may have a significant effect on the TC

motion. Such an error may be difficult for the forecaster to detect unless the TC is in relatively weak flow. In strong environmental flow, the error could be obscured (Carr and Elsberry 2000a). In several large error cases, the size of the TC in the UKMO model was noticeably smaller than the TC in the verifying analysis, which would account for the slow and southward bias. In other cases, a size error was hard to detect subjectively. In all of these UKMO large-error cases, the incorrect prediction of the midlatitude circulation would still have been the dominant contribution to the large error. The midlatitude contribution would have just been easier to detect if the TC had been forecast farther to the north during the early hours. Thus, a MSE was assigned as the primary error mechanism even though the MSE errors were most likely exacerbated by an earlier I-BEP.

Note in Table 1 that only three instances of MSEs were found in the GFS model. In the majority of large error cases in which a forecast TC in the GFS approached the midlatitudes, the TC vertical structure was insufficient to interact with the midlatitude steering environment. Thus, any possible contribution of inaccurate forecasts of midlatitude features and their effect on the TC track errors could not be assessed.

The correct prediction of midlatitude systems by the dynamical models is essential to successfully forecast TCs undergoing recurvature. Unfortunately, a review of these large error mechanisms in the NOGAPS and UKMO models has revealed both NOGAPS and UKMO have difficulty predicting the midlatitude steering environment, especially at 96 h and 120 h. Whereas the majority of MSE cases in UKMO were characterized by an incorrect depiction of a migratory trough-ridge couplet, both migratory troughs and the subtropical ridge were frequently incorrectly predicted in the NOGAPS model. Consequently, forecasters assessing potential UKMO and NOGAPS track errors should pay close attention to the model prediction of the midlatitude features.

While the UKMO had the smallest average 120-h track errors of all models for the 2005 season (Fig. 2), it was also available to JTWC forecasters the fewest number of times. Since the sample size for large errors for UKMO was relatively small, the above conclusions as to its error characteristics should be regarded as tentative.

26

Examination of UKMO errors for subsequent western North Pacific seasons will be essential.

c.   Case Studies-Global Models

(1) E-MCG (NOGAPS) - Banyan (7W). According to the best track for Banyan, the storm moved due north before taking a sharp turn to the northeast and skirting eastern Japan as it underwent extratropical transition (Fig. 10). The 0600 UTC 22 July NOGAPS interpolated forecast has Banyan turning eastward well south of Japan. At the initial forecast hour (not shown), Banyan is a tropical storm south of Japan with a large horizontal extent. A second tropical cyclone Nalgae (06W) is much smaller and weaker in extent, and is located to the northeast of Banyan. In the NOGAPS MSL pressure 48-h forecast (Fig. 11a), Nalgae has dissipated and is no longer represented by a closed vortex, while the verifying NOGAPS analysis (Fig. 11b) still has Nalgae as a closed vortex near 33º N, 162º E moving slowly eastward. By the 60-h NOGAPS forecast (Fig. 11c), the model has developed a small cyclone near 30º N, 150º E adjacent to Banyan, in the region that NOGAPS had decayed Nalgae. Although vorticity fields are not available, it is hypothesized that NOGAPS spun up this low in response to remnant vorticity from the dissipated Nalgae. NOGAPS continues to intensify the false secondary low in the 72-h forecast (Fig. 11e), while no such feature is evident in the verifying analysis (Figs. 11d, f).

27

Figure 10.   Interpolated NOGAPS (N) forecast track for 7W (Banyan) for the 0600 UTC 22 July 2005 E-MCG case study. The solid sections of the forecast tracks represent the 0-h through 72-h forecast while the dashed sections represent the 72-h through 120-h forecast. The solid line with open circles and corresponding dates represents the TC best track. The verifying 120-h interpolated position is indicated by the blue circle, while the 120-h interpolated forecast is indicated by the red circle.

The 700-mb streamlines at 72 h (Fig. 12a) indicate that the false cyclone is inhibiting the strength of the subtropical ridge that is providing the northward steering environment for Banyan as is evident in the NOGAPS analysis (Fig. 12b). In the verifying NOGAPS analysis (Fig. 12b), Nalgae is almost 30º longitude east of Banyan near 37º N, 165º E. By the 96-h forecast (Fig. 12c), the NOGAPS TC is being steered east-northeastward toward the false cyclone on the northwestern periphery of the subtropical ridge. In the 96-h MSL pressure forecast (not shown), Banyan is predicted to weaken and have relatively the same intensity as the false cyclone. In the 120-h NOGAPS forecast (Fig. 12e), Banyan is merging with the false cyclone as the two cyclones continue to move east. In the verifying NOGAPS analysis (Fig. 12f), Banyan has gone extratropical and has accelerated to the northeast toward Hokkaido.

28

Figure 11.   Forecast mean sea-level pressure (mb) for 7W (Banyan) by NOGAPS for taus (a) 48, (c) 60, and (e) 72 for 0600 UTC 22 July 2005 and the corresponding verifying 00-h NOGAPS analyses (b, d, and f).   The verifying TC position is indicated by a black star.

Because Banyan was improperly steered in the NOGAPS forecast by the subtropical ridge modified by the false cyclone, the ultimate source of the large error was E-MCG, even though the E-MCG later led to an E-DCI at the end of the forecast period. A forecaster should be able to recognize the spin up of the spurious low in NOGAPS, and thus question the validity of the steering environment it produces.

(2) I-MAG (NOGAPS) - Longwang (19W). In the 0000 UTC 28 September NOGAPS interpolated forecast, Longwang was predicted to have a northwestward track north of Okinawa before recurving and making landfall in Kyushu after 108 h (Fig. 13). In reality, the best track of Longwang is a westward track with landfall over Taiwan after 96 h.

During the first 24 h, both the NOGAPS forecast and the verifying analysis have Longwang in a weak steering environment between two subtropical ridges (not shown). By 48 h, the western subtropical ridge has built eastward and now extends south of Japan in the verifying analysis (Fig. 14b). While the analysis has a strong isotach maximum to the north of the TC, a much weaker isotach maximum exists in the model forecast (Fig. 14a). In the 60-h verifying analysis, the eastern and western subtropical ridges have merged, which led to the strong westerly steering on the TC (Fig. 14d). In the 60-h forecast, the subtropical ridges remain separate (Fig. 14c). The 72-h NOGAPS forecast has the model TC under the northwesterly steering influence of the stronger eastern subtropical ridge (Fig. 15a). A clear break between the two subtropical ridges in the forecast differs from the analysis, which has one merged ridge oriented east-west (Fig. 15b). In the NOGAPS forecast, the TC is accelerated toward the break in the ridge, while Longwang is actually increasing in translation speed under the strong westerly steering. At 96 h, the model TC has reached the subtropical ridge axis (Fig. 15c), while Longwang has actually made landfall over Taiwan (Fig. 15d). In the 120-h forecast, the model TC is north of the ridge axis and has accelerated in conjunction with a midlatitude trough (Fig. 15e). Longwang is actually well south of the ridge axis, and has made a second landfall in China (Fig. 15f). In this case study, the failure of the western subtropical ridge to build eastward and merge with the eastern subtropical ridge led to the assignment of the I-MAG error mechanism.
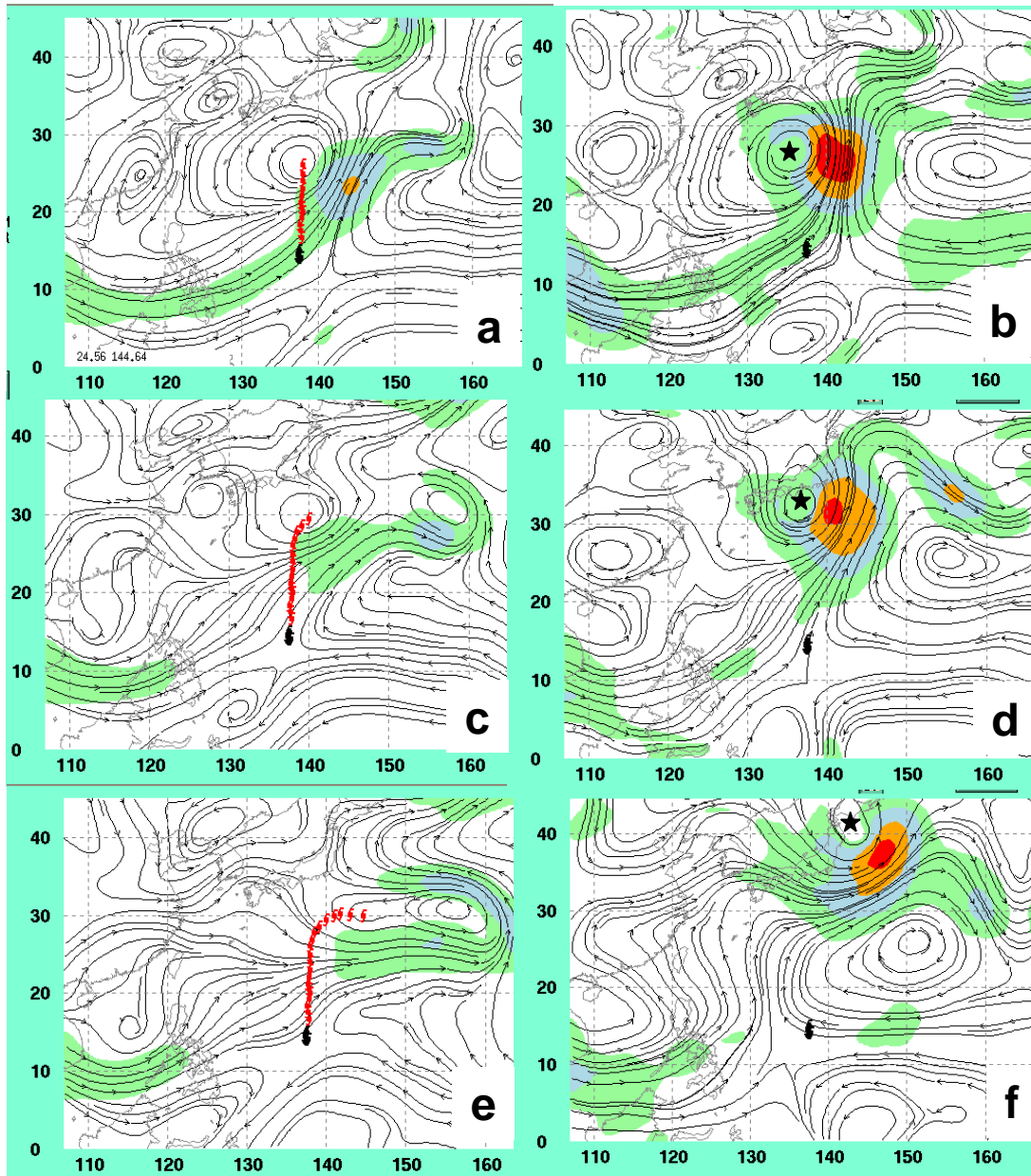
Figure 12.   Forecast 700-mb streamline and isotach (contour interval of 20 kt beginning at 20 kt) fields for 07W by NOGAPS for taus (a) 72, (c) 96, and (e) 120 for 0600 UTC 22 July 2005 and the corresponding verifying 00-h NOGAPS analyses (b, d, and f). The verifying TC position is indicated by a black star.

31
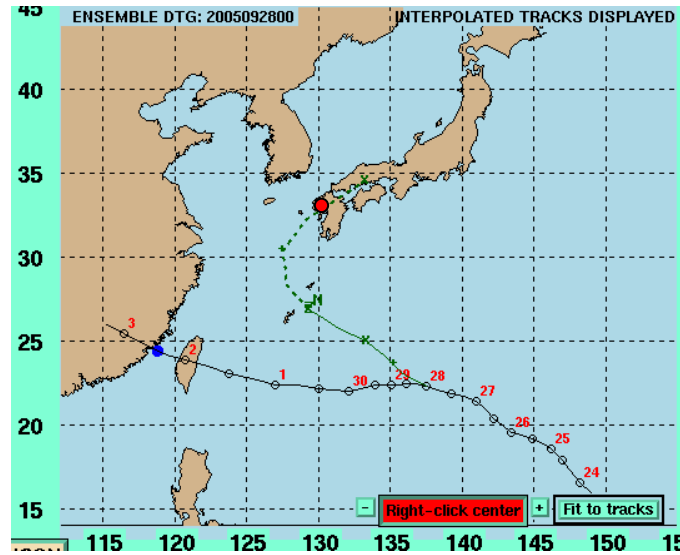
Figure 13. Interpolated NOGAPS (N) forecast track for 19W (Longwang) for the 0000 UTC 28 September 2005 I-MAG case study. The solid sections of the forecast tracks represent the 0-h through 72-h forecast while the dashed sections represent the 72-h through 120-h forecast. The solid line with open circles and corresponding dates represents the TC best track. The verifying 120-h position is indicated by the blue circle, while the 120-h interpolated forecast is indicated by the red circle.

(1) I-MCG (UKMO) - Banyan (7W). In the 1800 UTC 23 July UKMO forecast, TC Banyan is predicted to move poleward and recurve south of Japan (Fig. 16). In reality, Banyan recurved farther north and moved northeastward to near 50ºN as an extratropical system. The 24-h UKMO forecast and the NOGAPS verifying analysis both depict positively tilted midlatitude troughs of comparable depth over the Gulf of Pohai (not shown). At 42 h, the trough in the UKMO forecast has translated eastward and maintained a positive tilt with a northeast-southwest axis through the Sea of Japan (Fig. 17a). Although the trough in the verifying analysis has deepened, it has a neutral orientation, and is just northwest of Banyan (Fig. 17b).
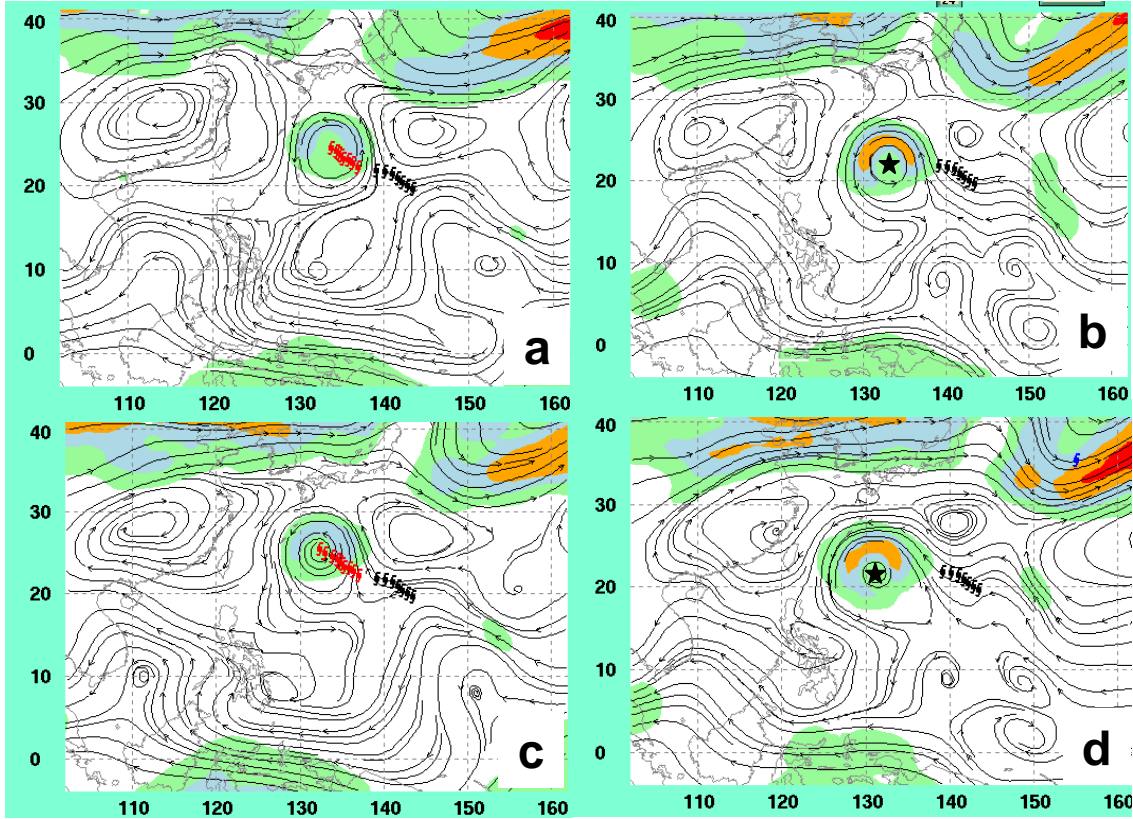
Figure 14.   Forecast 500-mb streamline and isotach (contour interval 20 kt beginning at 20 kt) fields for 19W (Longwang) by NOGAPS for taus (a) 48, (c) 60 for 0000 UTC 28 September 2005 and the corresponding verifying 00-h NOGAPS analyses (b and d). The verifying TC position is indicated by a black star.

Twelve hours later, the 54-h verifying analysis has the 5790 m GPH isopleth enveloping the TC (Fig. 17d). In the UKMO forecast, the 5790 m isopleth is still located in the northern Sea of Japan (Fig. 17c). Since the midlatitude trough in the UKMO model is not forecast to deepen, it also fails to interact with and lead to the extratropical transition of Banyan. Instead of predicting an acceleration to the northeast as the extratropical system deepens, the 90-h UKMO forecast has the TC just off the east coast of Japan moving in the midlatitude westerly regime on the northern periphery of the subtropical ridge (Fig. 18a). In the 90-h verifying analysis, the extratropical system is over Hokkaido (Fig. 18b). At 114 h, the UKMO forecast has the TC continuing its eastward movement (Fig. 18c), while in reality the tropical cyclone is over the Kuril Islands (Fig. 18d). From this case study, it is clear that for a model to properly handle the extratropical transition of a tropical cyclone, it must first depict the midlatitude

trough/cyclone with the appropriate amplitude. The shortwave trough in the UKMO forecast for this case was under-predicted, and thus I-MCG was assigned as the primary error mechanism.
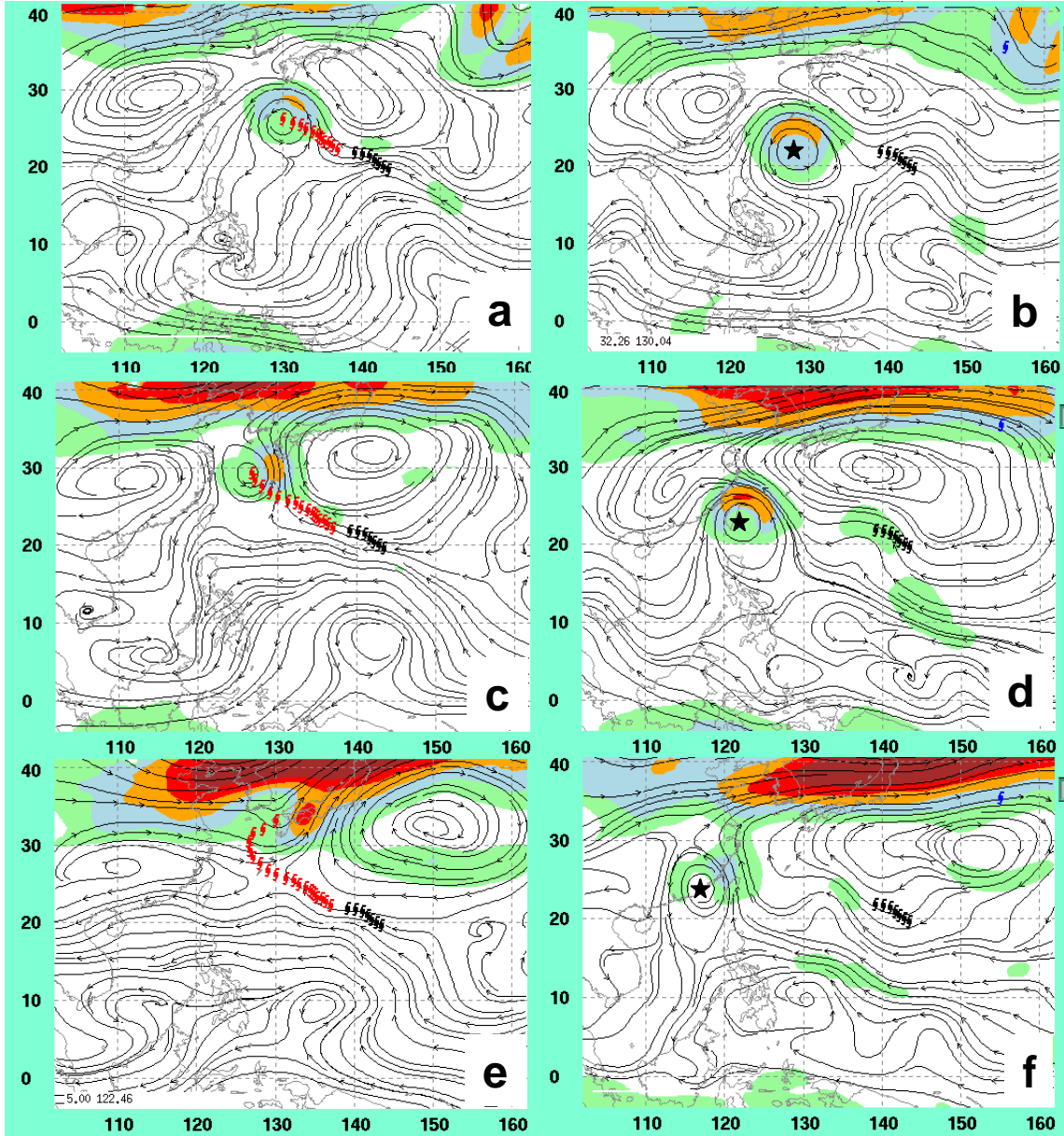
Figure 15. Forecast 500-mb streamline and isotach (contour interval 20 kt beginning at 20 kt) fields for 19W (Longwang) by NOGAPS for taus (a) 72, (c) 96, and (e) 120 for 0000 UTC 28 September 2005 and the corresponding verifying 00-h NOGAPS analyses (b, d, and f). The verifying TC position is indicated by a black star.
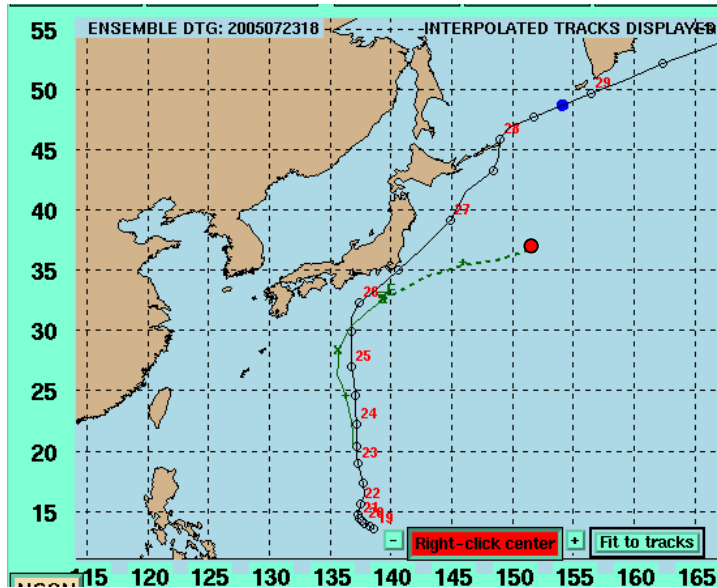
Figure 16. Interpolated UKMO (E) forecast track for 07W (Banyan) for the 1800 UTC 23 July 2005 I-MCG case study. The solid sections of the forecast tracks represent the 0-h through 72-h forecast while the dashed sections represent the 72-h through 120-h forecast. The solid line with open circles and corresponding dates represents the TC best track. The verifying 120-h position is indicated by the blue circle, while the 120-h interpolated forecast is indicated by the red circle.

(1) E-MAG (UKMO) – Nabi (14W). In the 1200 UTC 1 September UKMO forecast, Nabi is predicted to have a similar path as the best track through the first 84 h, although with a southward bias (Fig. 19). Between 84 h and 120 h, Nabi undergoes recurvature over Kyushu, while the UKMO-predicted track continues toward the northwest.

The early southward track bias can most likely be explained by Insufficient-Beta-Effect Propagation (I-BEP). Note the smaller size of the TC in the UKMO model MSL pressure fields (Fig. 20a) compared to the verifying NOGAPS analysis at 12 h (Fig. 20b). In the absence of strong environmental steering, it is likely that I-BEP contributed to the 143 n mi error through 48 h. In the 72-h wind forecast, the UKMO representation of Banyan has reached a size comparable to the verifying analysis (not shown).
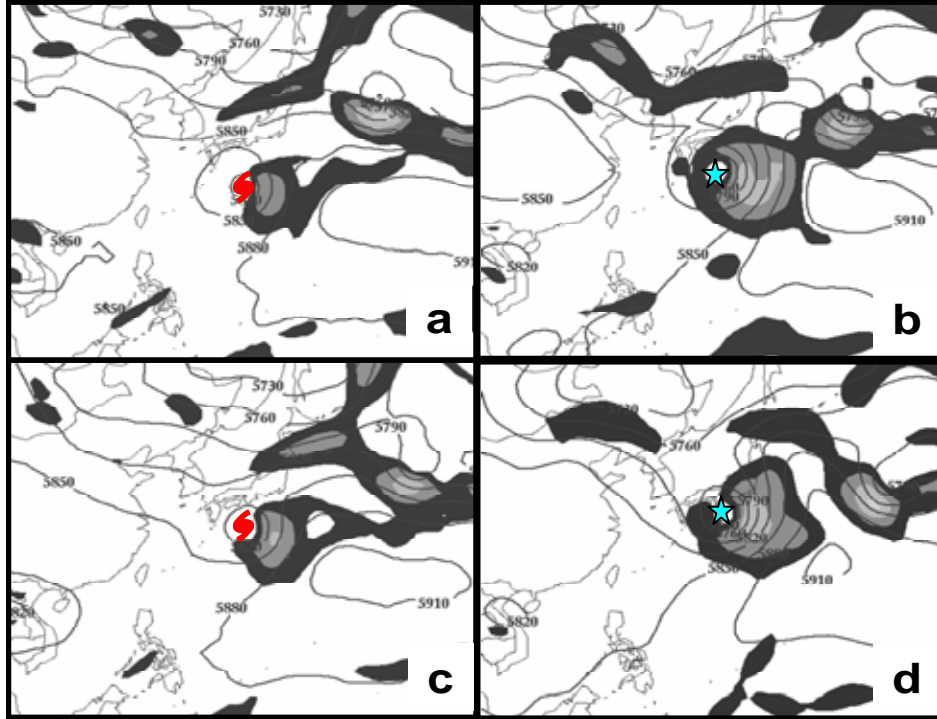
Figure 17.   Forecast 500-mb geopotential heights and isotach (contour interval 20 kt beginning at 20 kt) field for 7W (Banyan) predicted by UKMO for taus (a) 42 and (c) 54 for 1800 UTC 23 July 2005 and the corresponding verifying 00-h NOGAPS analyses (b and d). The forecasted position is indicated by a red TC symbol, and the verifying TC position is indicated by a blue star.

By 72 h, the subtropical ridge east of Japan is still predicted to be connected to the subtropical ridge in eastern China (Fig. 20c). In the verifying analysis, a break exists between the two ridges, which allows the TC to translate poleward (Fig. 20d). At 84 h, an over-predicted high amplitude migratory ridge over the Korean Peninsula has merged with the eastern subtropical ridge, which then blocked a northward turn by the TC in the UKMO model (Fig. 21a). The verifying analysis indicates that the migratory ridge has much lower amplitude and does not merge with the eastern subtropical ridge (Fig. 21b).
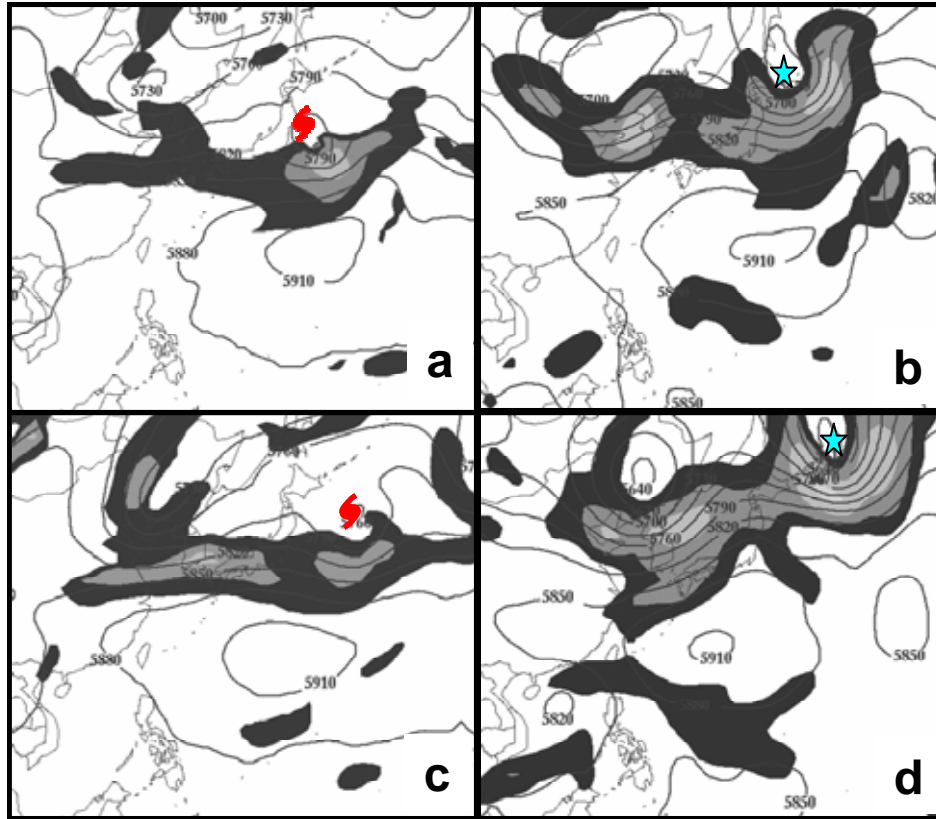
Figure 18.   Forecast 500-mb geopotential heights and isotach (contour interval 20 kt beginning at 20 kt) field for 7W (Banyan) predicted by UKMO for taus (a) 90 and (c) 114 for 1800 UTC 23 July 2005 and the corresponding verifying 00-h NOGAPS analyses (b and d). The forecast position is indicated by a red TC symbol, and the verifying TC position is indicated by a blue star.

By 108 h, the migratory ridge in the UKMO has moved eastward, and the forecast TC is finally on the western periphery of the subtropical ridge (Fig. 21c) and is moving north-northwestward (Fig. 19). At this time, the TC in the UKMO model is predicted to be south of the Korean Peninsula, whereas in reality Nabi is about to make landfall in Kyushu (Fig. 21d). Although model fields are not available for the 120-h forecast, it can be inferred from the interpolated track that Nabi was not in the position (too far south) to undergo a recurvature over the Sea of Japan, or be influenced by the shortwave trough over the Gulf of Pohai.

The E-MAG error in this case study is operationally significant because the UKMO track brought Nabi directly south of Okinawa at 96 h. In reality, the center of Nabi passed well to the east of Okinawa, and the closest point of approach had already occurred at 72 h.
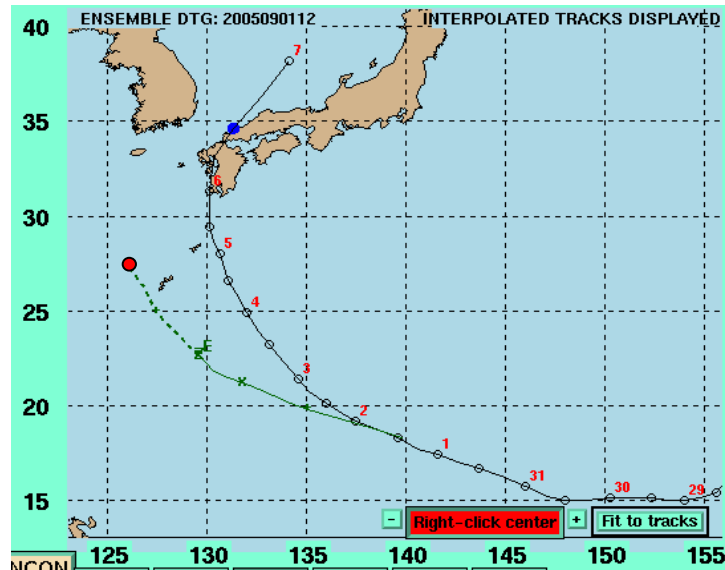
Figure 19.   Interpolated UKMO (E) forecast track for 14W (Nabi) for the 1200 UTC 1 September 2005 E-MAG case study. The solid sections of the forecast tracks represent the 0-h through 72-h forecast while the dashed sections represent the 72-h through 120-h forecast. The solid line with open circles and corresponding dates represents the TC best track. The verifying 120-h position is indicated by the blue circle, while the 120-h interpolated forecast is indicated by the red circle.
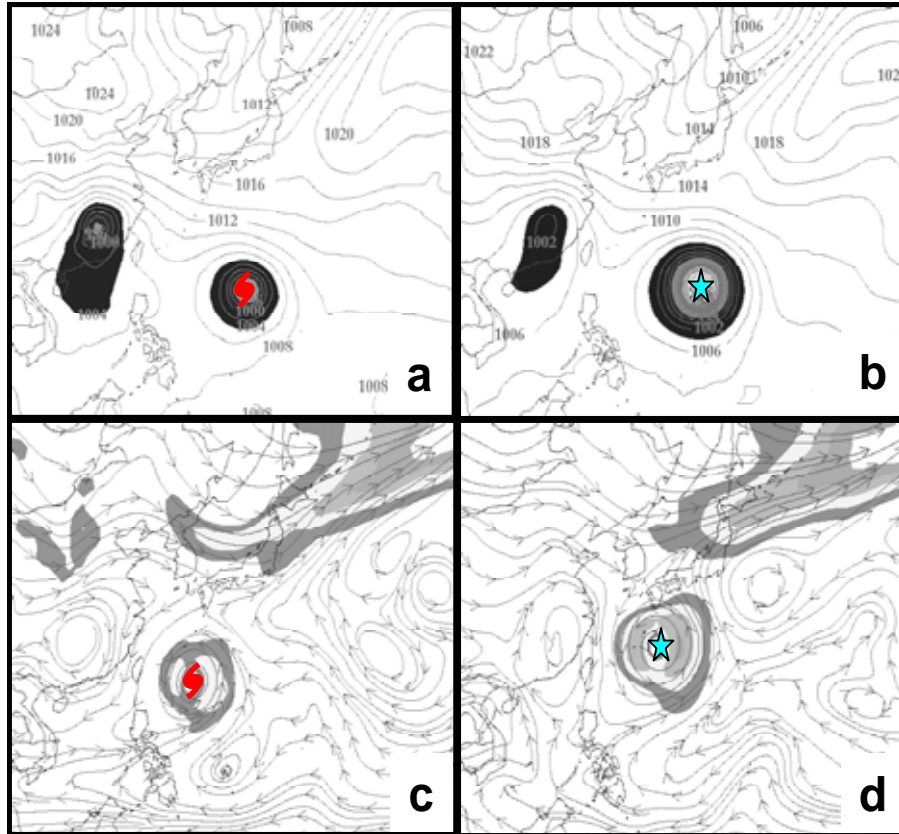
Figure 20.   Forecast mean sea-level pressure field for 14W (Nabi) predicted by (a) UKMO and (b) verifying NOGAPS analysis for tau 12 of 1200 UTC 1 September 2005 forecast. Forecast 500-mb streamlines and isotach (contour interval 20 kt beginning at 20 kt) field predicted by (c) UKMO for tau 72 and (d) the corresponding verifying 00-h NOGAPS analyses. The forecast position is indicated by a red TC symbol, and the verifying TC position is indicated by a blue star.
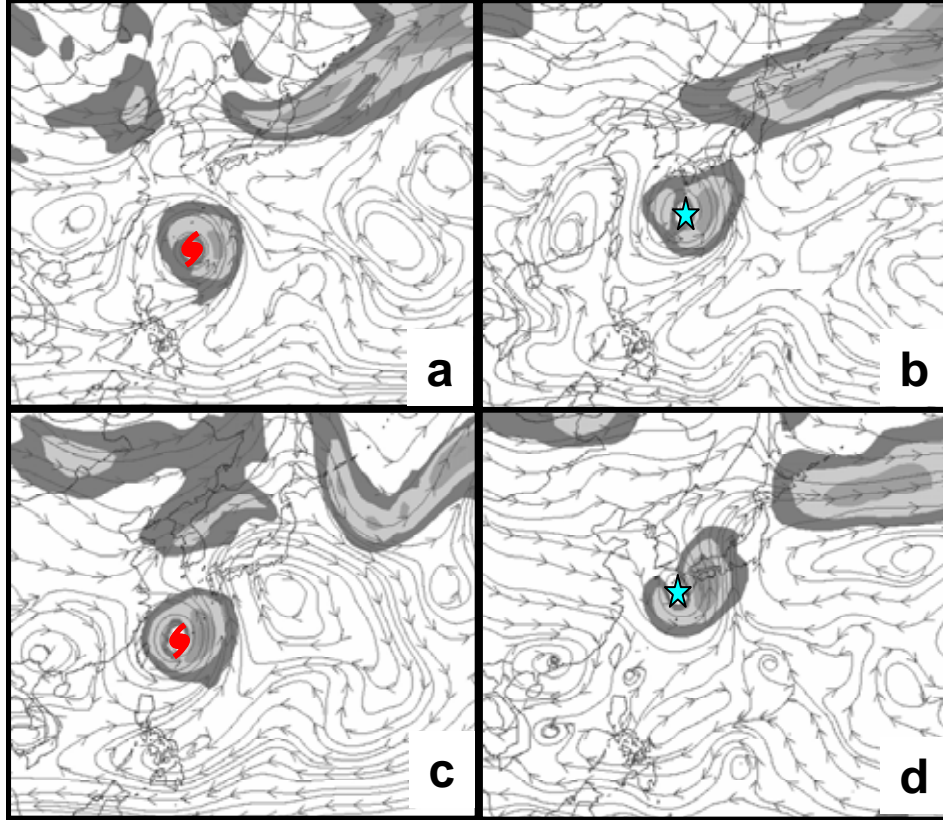
Figure 21.   Forecast 500-mb streamlines and isotach (contour interval 20 kt beginning at 20 kt) field for 14W (Nabi) predicted by UKMO for taus (a) 84 and (c) 108 for 1200 UTC 1 September 2005 and the corresponding verifying 00-h NOGAPS analyses (b and d). The forecast position is indicated by a red TC symbol, and the verifying TC position is indicated by a blue star.

d.   *Frequency and Characteristics-Regional Model (GFDN)*

Although the GFDN model also had difficulty forecasting the midlatitude steering environment, one systematic error could explain a large majority of the large track errors. In 31 of the 50 large error cases at 96 h or 120 h with GFDN fields available (Table 1), excessive (E) midlatitude anticyclogenesis (E-MAG) was predicted in which the GFDN built a false anticyclone at 500 mb and 700 mb over central China to the east of the Tibetan Plateau. At longer forecast intervals, the anticyclone migrated over the Korean Peninsula and toward the northern Sea of Japan. In some cases, the existence of this Tibetan anticyclone falsely affected the downstream midlatitude pattern by propagating energy along a wave train to the east. This wave train resulted in a perturbation that falsely displaced the subtropical ridge that normally is centered off the east coast of Japan (hereafter, eastern subtropical ridge) too far east. Since the false

40

anticyclone generally formed in the same position, it is hypothesized that the interaction between the GFDN outer nest boundary and the high elevation of the Tibetan Plateau (approximately 500-700 mb) contributes to the formation of the anticyclone.

In multiple model runs without large track errors, the GFDN model predicted a similar Tibetan anticyclone, but the feature either did not lead to incorrect steering of the TC, or was similar enough to an anticyclone in reality that it did not cause a large error. Nevertheless, the cause of the frequent false anticyclogenesis in the GFDN needs to be understood and corrected so that TCs approaching this region do not have large track errors due to the false anticyclone modifying the steering flow.

Although E-MAG was assigned as the primary error mechanism for 31 GFDN cases, the location of the TCs relative to this erroneous feature, as well as the varying downstream effects of the false anticyclone, resulted in different erroneous track forecasts. The false Tibetan anticyclone led to large track errors in four ways with the following secondary error mechanism assignments (not counted in Table 1): (i) incorrect steering of the TC on the southern periphery of the false anticyclone (E-MAG, nine cases in four TCs); (ii) incorrect steering of the TC caused by a merger of the false anticyclone and the eastern subtropical ridge (E-MAG, ten cases in three TCs); (iii) insufficient development of the short-wave trough that actually affected the TC (insufficient midlatitude cyclogenesis (I-MCG, seven cases in two TCs)); and (iv) incorrect steering of the TC due to the false eastward displacement of the eastern subtropical ridge (insufficient midlatitude anticyclogenesis (I-MAG), five cases in three TCs).

In four GFDN predictions of one TC, E-MAL was attributed as the primary error mechanism (Table 1). In these cases, the GFDN model accurately forecast the presence of an anticyclone, but the anticyclone propagated eastward too rapidly, and failed to slow the northward movement of the TC as occurred in reality. Since the rapid eastward propagation that occurred in all of these cases also involved the false Tibetan anticyclone, it is hypothesized that these four E-MAL cases might be a symptom of the previously described systematic anticylogenesis error.

Review of some of the GFDN forecast fields for the large track errors during 2004 studied by Kehoe (2005) indicated that the false Tibetan anticyclone was

41

also predicted in multiple cases. However, Kehoe assigned E-MAG as a primary mechanism in only nine large-error cases. However, I-MCG (which may be a secondary error mechanism in some cases due to the presence of the false Tibetan anticyclone) was named as an error mechanism in 46 cases during 2004. It is possible that in most of these cases, the presence of the false anticyclone may have led to the I-MCG, which would make E-MAG the primary error mechanism.

e.   Case studies- Regional Model (GFDN)

The following case studies will describe the two most common secondary error mechanisms that resulted from the presence of the false Tibetan anticyclone: a merger between the false anticyclone and the eastern subtropical ridge, and the steering of the TC on the southeast periphery of the anticyclone.

(1) E-MAG (GFDN) - Nabi (14W). The 1200 UTC 2 September GFDN interpolated forecast track indicates that TC Nabi will continue on a track to the northwest with a final turn to the north toward the Korean Peninsula at 120 h (Fig. 22). However, the JTWC best track reveals TC Nabi recurved much earlier and made landfall over the Japanese island of Kyushu at 96 h. From an operational standpoint, the TC actually impacted Sasebo Naval Station and Iwakuni MCAS in Japan. By contrast, the GFDN forecast would indicate that the DOD assets on the Korean Peninsula were under threat.

An anticyclone induced downstream of the Tibetan plateau is predicted near 40ºN, 115ºE in the 500-mb GFDN fields at 48 h (Fig. 23a). Although the verifying NOGAPS analysis (Fig. 23b) has a migratory ridge in roughly the same location, the GFDN-predicted anticyclone is of much larger extent and is already merging with the subtropical ridge east of Japan. By 72 h (Fig. 23c), the GFDN has predicted the anticyclone to have completely merged with the eastern subtropical ridge. In the 72-h NOGAPS analysis (Fig. 23d), a short-wave trough is present in the northern Sea of Japan between the migratory ridge and the eastern subtropical ridge. This migratory trough is contributing to a break in the eastern subtropical ridge that allows Nabi to recurve northward along the western periphery of the eastern subtropical ridge. In the GFDN forecast, no shortwave trough is evident at 500 mb, and the model TC is predicted to move northwestward along the southern periphery of the merged anticyclones. At 96 h

(Fig. 23e), the false anticyclone is predicted to propagate northeast of Hokkaido and become connected with the eastern subtropical ridge in a north-south orientation. In the GFDN forecast, the TC remains south of the falsely merged 500-mb anticyclones, which has also left a trailing ridge that extends westward north of the Korean peninsula. In the verifying NOGAPS analysis, a clear break exists between the subtropical ridge and a newly developing anticyclone north of Korea, which allows the poleward translation of Nabi (Fig. 23f).

   (2) E-MAG (GFDN) - Kai-tak (22W). In the interpolated GFDN forecast from 1200 UTC 29 October, TC Kai-tak is predicted to take a due west track and make landfall over Vietnam within 36 h (Fig. 24). In contrast, Kai-tak actually moved very slowly north and northwest over the first 48 h, and then moved parallel to the northern Vietnam coast before making landfall. By 96 h, the GFDN forecast has Kai-tak in the Gulf of Thailand, while the TC is actually making landfall in northern Vietnam, yielding a track error of 610 n mi.
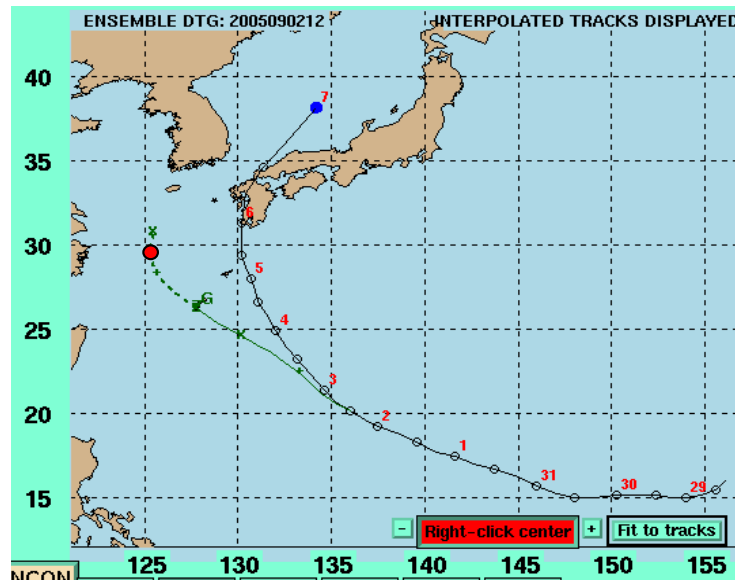
Figure 22. Interpolated GFDN (G) forecast track for 14W (Nabi) for the 1200 UTC 2 September 2005 E-MAG case study. The solid sections of the forecast tracks represent the 0-h through 72-h forecast while the dashed sections represent the 72-h through 120-h forecast. The solid line with open circles and corresponding dates represents the TC best track. The verifying 108-h position is indicated by the blue circle, while the 108-h interpolated forecast is indicated by the red circle.
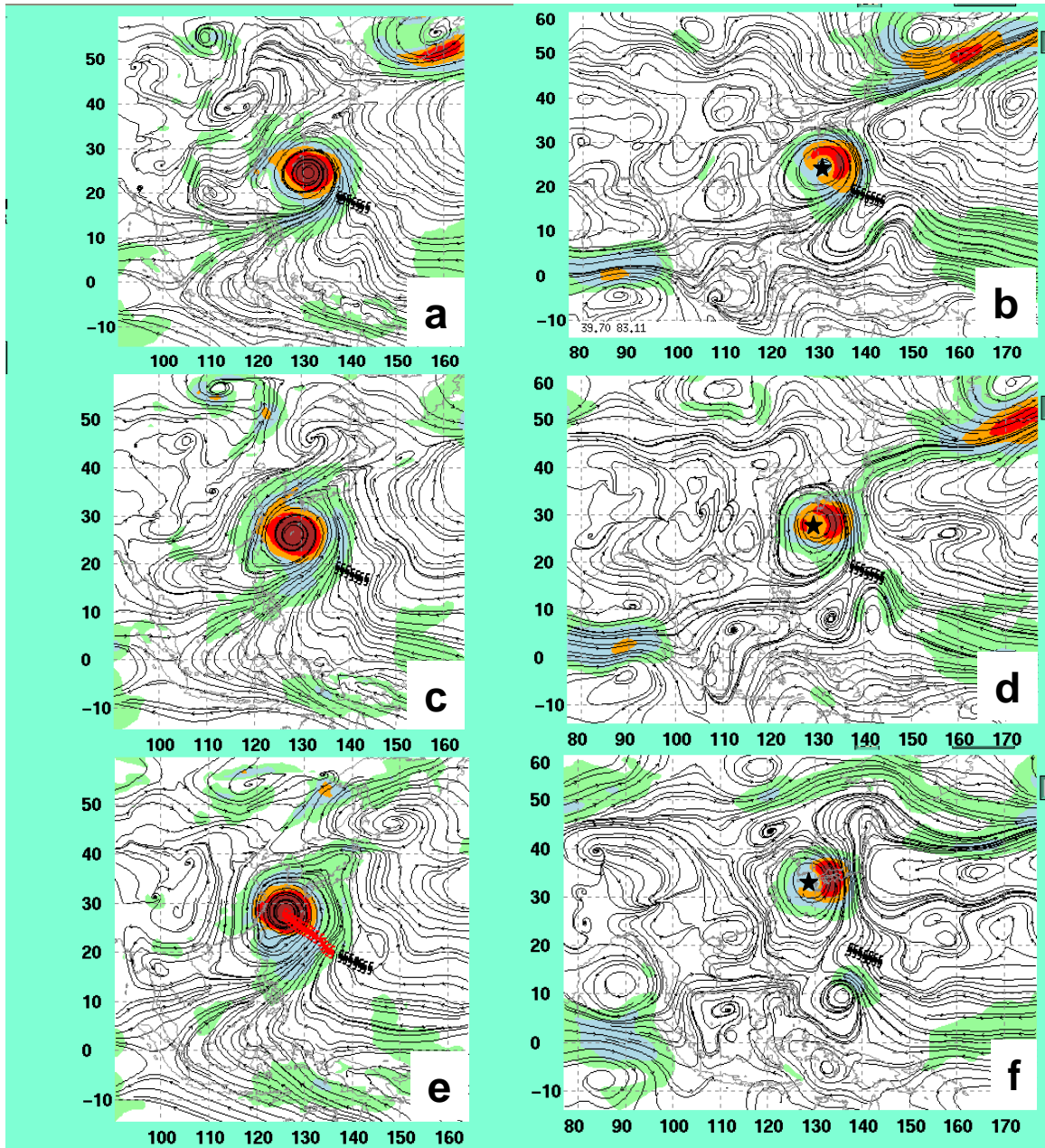
Figure 23.   Forecast 500-mb streamline and isotach (contour interval 20 kt beginning at 20 kt) fields for 14W (Nabi) by GFDN for taus (a) 48, (c) 72, and (e) 96 for 1200 UTC 2 September 2005 and the corresponding verifying 00-h NOGAPS analyses (b, d, and f). The verifying TC position is indicated by a black star.

In the initial 0-h GFDN 700-mb wind field (not shown), the midlatitude ridge over northern China matches well with the verifying analysis (not shown), but excessive ridging exists to the north of the TC when compared to reality. In the 24 h GFDN 700-mb forecast (Fig. 25a), the previous ridge features are now predicted as a huge false Tibetan anticyclone in central China. This anticyclone extends from central China to western Japan and entirely engulfs the model domain such that the shortwave trough over Korea and the anticyclone centered near Okinawa in the verifying analysis (Fig. 25b) are non-existent in the GFDN forecast (Fig. 25a). The smaller anticyclone centered near Okinawa in the NOGAPS verifying analysis builds northwestward over central China by 48 h (Fig. 25d), and provides a stronger northwesterly steering for the TC. By 48 h (Fig. 25c), the false anticyclone is predicted to have a northeast-southwest orientation from Japan to northern Thailand. Notice that the anticyclone in the East China Sea is not present in the GFDN forecast. By 72 h, the center of the false anticyclone has propagated eastward and is centered over western Japan. However, the trailing ridge is still providing strong steering for the GFDN TC, which is now in the Gulf of Thailand (Fig. 25e). Such an eastward propagation of the false anticyclone was typical of all the cases examined in the GFDN model. In the 72-h verifying NOGAPS analysis, Kai-Tak continues to move northwestward, and has yet to make landfall over northern Vietnam (Fig. 25f).

Since the TC intensity is approximately 50 kt, it is reasonable to expect that Kai-tak is being steered at the 700-mb level, and the GFDN track in Fig. 24 is consistent with the steering flow along the southern periphery of the false anticyclone. In reality, the verifying NOGAPS analysis at 24 h (Fig. 25b) has the TC in a region of weak steering between anticyclones over China and the East China Sea which is consistent with the initial slow movement of Kai-tak. This case study illustrates how the GFDN model's incorrect depiction of the steering environment in the first 48 h of the GFDN prediction can have significant effects on the model track error through 96 h.

In summary, a false Tibetan anticyclone is a feature that should be easy for JTWC forecasters to recognize. In the case of a weaker TC, forecasters will

have to assess the effects of the 700-mb anticyclone on the direct steering of the TC. In the case of a strong TC, forecasters will need to assess if the false anticyclogenesis is affecting the steering flow at 500 mb.

2. Vertical Structure Related Errors

a. Description of E-RVS, E-DCI-m, Excessive Dissipation

The remaining midlatitude error mechanisms, Excessive Response to Vertical Shear (E-RVS) and Excessive Direct Cyclone Interaction-midlatitude (E-DCI-m) can be attributed to an incorrect depiction of the TC structure by the model that then led to the large errors. A previously unobserved error mechanism, excessive dissipation of the TC, occurred only in the GFS model and will be described below.
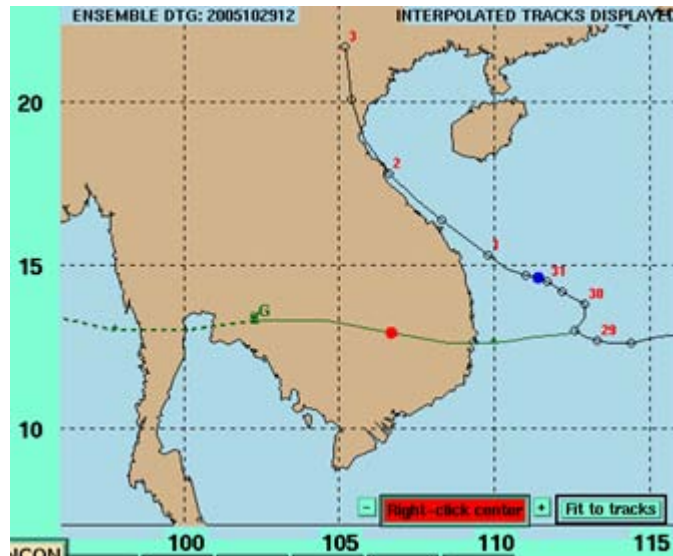
Figure 24. Interpolated GFDN (G) forecast track for 22W (Kai-Tak) for the 1200 UTC 29 October 2005 E-MAG case study. The solid sections of the forecast tracks represent the 0-h through 72-h forecast while the dashed sections represent the 72-h through 120-h forecast. The solid line with open circles and corresponding dates represents the TC best track. The verifying 48-h position is indicated by the blue circle, while the 48-h interpolated forecast is indicated by the red circle.
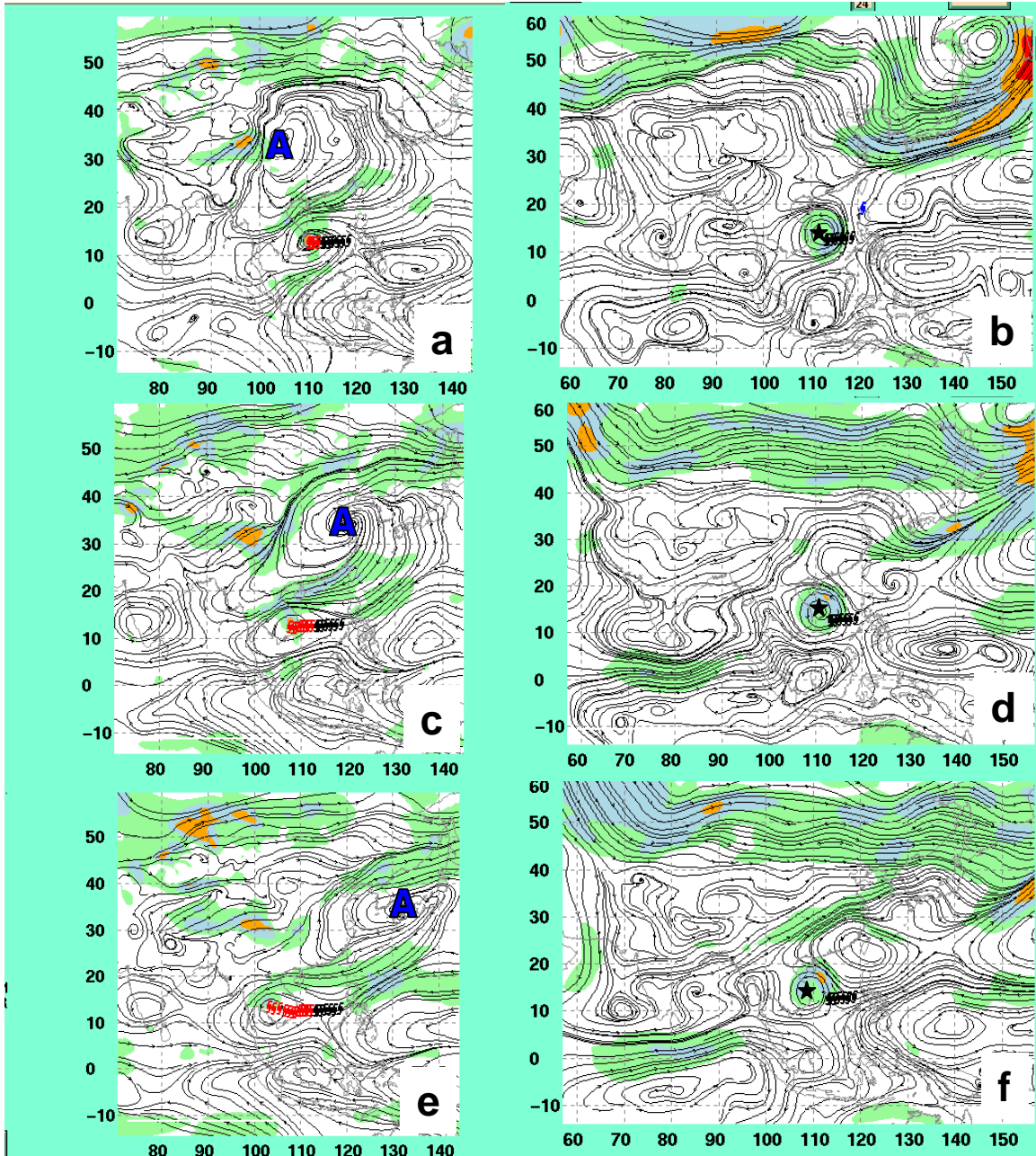
Figure 25.   Forecast 700-mb streamline and isotach (contour interval 20 kt beginning at 20 kt) fields for 22W (Kai-Tak) by GFDN for taus (a) 24 and (c) 48 and (e) 72 for 1200 UTC 29 October 2005, and the corresponding verifying 00-h NOGAPS analyses (b, d, and f). The center of the false anticyclone as depicted in the GFDN is indicated by the blue "A". The verifying TC position is indicated by a black star.

(1) E-RVS. The RVS error mechanism occurs when the vertical depth and intensity of the TC in the model differed from reality in the presence of sheared flow as shown in Fig. 26 (Carr and Elsberry 2000a). In E-RVS, the warm core in the upper to middle levels of the TC is sheared from the low-level vortex, such that the low-level environmental flow becomes the primary steering for the TC. In previous studies (Carr and Elsberry 2000b), E-RVS had been noted to cause a slow bias in the TC track, but Kehoe (2005) also noted an erroneous equatorward track deflection. Carr and Elsberry (2000b) found cases in which the relatively coarse resolution of the global model underestimated the mid-level TC intensity, which makes the TC more susceptible to a sheared environment. In contrast, the higher resolution in the regional model led to a vortex that was not affected by the vertical shear.

(2) E-DCI-m. Similar to the E-DCI characteristic error in the tropics discussed in Chapter III.B, Kehoe (2005) found a similar error mechanism in the midlatitudes, usually as the TC moved north of the subtropical ridge into the midlatitude westerlies. In E-DCI-m, the model incorrectly predicted the TC would rotate counter-clockwise around a midlatitude cyclone to the northwest that had penetrated too deeply into the lower troposphere in comparison to reality. For the large track errors attributed to E-DCI-m during the 2005 season, the midlatitude cyclone was always predicted as overly deep and the structure of the TC was usually under-forecast, which thus exacerbated the large error.

b. Frequency and Characteristics

Incorrect prediction of the TC structure was the most frequent cause of large track errors in the GFS model, and this error occurred to a lesser degree in the NOGAPS model. The most common error mechanisms occurring in the GFS model during the 2005 season (Table 1) were E-DCI-m (12 cases in two TCs) and E-RVS (nine cases in three TCs). In an additional 14 cases during Kirogi (21W), the GFS model substantially weakened the TC in the absence of significant vertical wind shear. In the NOGAPS model, E-RVS occurred in six cases, all in the same TC.

Response to Vertical Wind Shear (RVS)
Error Mechanism Conceptual Model
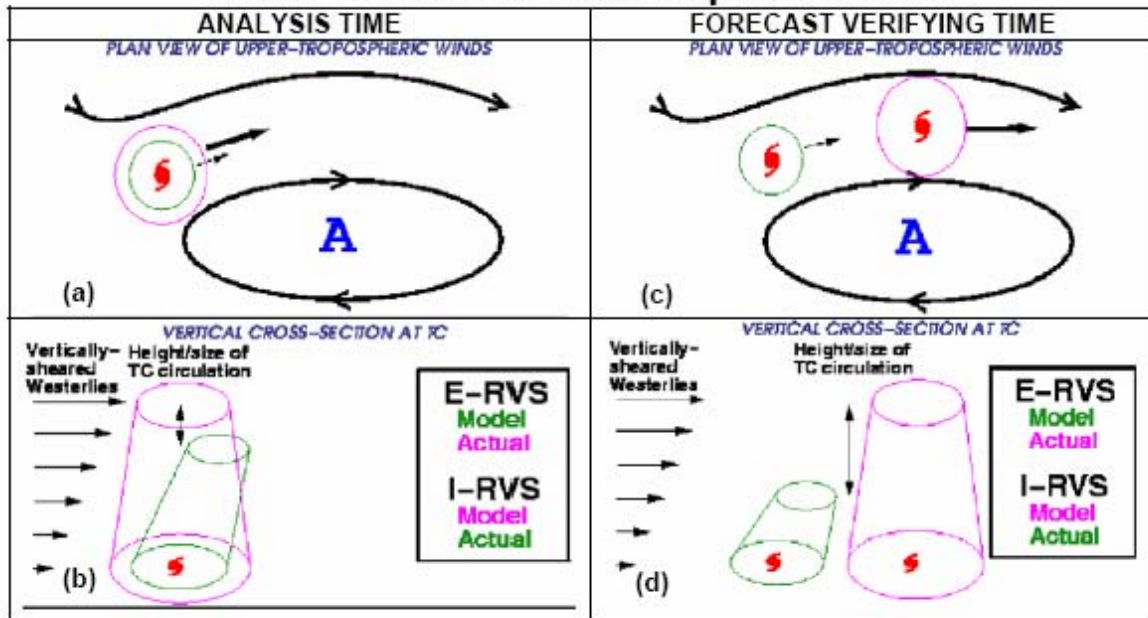
Figure 26.   Conceptual model of RVS (from Carr and Elsberry 2000b). (a) Plan view of
the 500-mb environmental flow and (b) vertical cross-section along the
vertical wind shear vector through the TC with different vertical (and
presumably horizontal) extents in the model and in nature at analysis time.
(c)-(d) Corresponding plan view and vertical cross-section at verification
time in which E-RVS causes the vortex to be too shallow (d, green) and the
track to have a slow bias (c, green). By contrast, an I-RVS error leads to a
vortex that is too deep and a fast track bias [magenta lines in (c) and (d)].

The E-RVS cases in the GFS model occurred in Kulap (01W), Sonca
(03W), and Saola (18W). In each case, the GFS TC was represented as being too weak in
the GFS initial conditions with insufficient vertical extent when compared to the
verifying NOGAPS analyses. In the GFS forecasts, the TCs either failed to intensify or
weakened from the initial intensity. Examination of the 500-mb geopotential height fields
revealed almost no signature of an upper-level vortex, even when the TCs were at
maximum intensity. Instead of a decoupling of the upper-level vortex from the lower-
level vortex as in previous studies of E-RVS (Carr and Elsberry 2000b), the effect of
vertical wind shear on the GFS model forecast was to completely eliminate any trace of
the upper-level vortex. In reality, each of the three TCs accelerated to the northeast under
the influence of a mid-level shortwave trough. Without the appropriate vertical extent of

the vortex, the GFS forecast failed to recurve the TC; rather, the TC meandered in the absence of a strong steering environment.

A further common characteristic of E-RVS cases in the GFS was the elongation of the low-level circulation in the direction of the vertical wind shear. The three TCs actually maintained a more symmetric structure around the center. It is interesting to note that in each of the three cases, the vortex tracker had difficulty following the weak circulation, and thus the interpolated model position did not always agree with the center of the MSL isopleths. The NOGAPS model also predicted six cases of E-RVS occurring in Saola. In contrast to the GFS model, the TC in the NOGAPS model was initialized with accurate depth, but the model then failed to deepen the TC in the first 72 h, and in one case weakened the TC.

Although only four cases of E-DCI-m occurred in the UKMO, these cases still accounted for 10% of UKMO large errors and occurred in two TCs. A key feature in all of the E-DCI-m cases that occurred in the GFS and UKMO models was that in addition to the tropical cyclone being predicted as being too weak, the midlatitude circulation was over-forecast. In some of the cases, the TC merged with the midlatitude cyclone to form one large cyclone. In other cases, the weaker TC was predicted to rotate counter-clockwise around the periphery of the larger cyclone. For the E-DCI-m errors in the UKMO model, the depiction of the TC structure was more accurate than in the GFS model, but was still insufficient. Although the inaccurate forecasts of TC structure were more subtle in the UKMO model than in the GFS model, the discrepancies were significant enough to lead to a false interaction between the TC and the midlatitude low.

For 14 cases in Kirogi (21W), the large track errors are attributed to the GFS model excessively dissipating the TC vortex to the point that it could not be appropriately steered by the environment. It is surprising that the same error occurred for 14 consecutive integrations of the GFS model, including several integrations in which the TC had an initial intensity of 90 kt. In all cases, the initial TC intensity and vertical structure in the GFS were depicted as being far too weak, and then failed to intensify during the integration. At first, the GFS track forecast in Kirogi was very similar to those tracks predicted in the E-RVS cases. That is, the model TC was predicted by the GFS to

50

remain nearly stationary, and then slowly drift equatorward. In these cases, the TC was south of the subtropical ridge and was not being influenced by midlatitude vertical wind shear. A specific example is described in detail in the case study below.

Examination of numerous initial fields has demonstrated that the GFS initialization procedure via a vortex relocation repeatedly fails to properly represent the TC structure in the 0-h analysis, and furthermore the GFS model has difficulty maintaining or intensifying the TC structure. It is concluded that the vortex relocation method used in the GFS model initialization has serious consequences for both the initial TC structure and the spin up of the model TC within the first 24 h. One conclusion from this research is that a proper depiction of TC structure in essential for accurate 96-h and 120-h forecasts. In addition to a 90 kt cyclone appearing in the GFS initial conditions with only one closed mean sea-level pressure isopleth, the fact that the TC fails to intensify in a near-zero vertical wind shear region of the western North Pacific during early October should be a red flag to the forecaster.

In over one-third (23 of 60 cases including tropical influences) of the large NOGAPS track errors, the vertical structure of the TC was incorrectly predicted as being too shallow. Unlike the GFS model, the TCs in the NOGAPS model were generally initialized reasonably well due to the insertion of synthetic observations. However, the TC in the NOGAPS forecast then failed to deepen from this initial structure, or in some cases weakened in comparison to the MSL pressures in the verifying analyses. In some cases, the incorrect vertical structure of the model TC exacerbated large errors when the midlatitude steering environment was already incorrectly predicted. It is interesting that in the vast majority of cases in which the NOGAPS TC failed to appropriately deepen, the initial TC intensity was 55 kt or weaker.

In contrast to the GFS and NOGAPS models, the vertical structure of the TC was properly represented in most UKMO forecasts, which may explain the absence of any E-RVS errors in the UKMO. However, incorrect horizontal structure prediction in UKMO did lead to eight cases of E-DCI in the UKMO model, both in the tropics and the midlatitudes (Table 1).

The regional model GFDN had the opposite problem as the global models because in two cases it over-forecast the TC structure (Table 1). For TC Damrey (17W), the GFDN did not predict a decay of the TC after landfall, even after moving over 500 n mi over land. Rather, the TC was predicted to turn northwestward under the influence of the midlatitude steering ridge. Forecasters should consider any CONW forecast that contains a non-decaying GFDN forecast over land to be suspect.

> *c.* **Case Studies**

> (1) E-DCI-m (GFS) - Mawar (11W). Typhoon Mawar underwent recurvature over Tokyo Bay, and then moved eastward in the midlatitude westerlies (Fig. 27). However, the 0600 UTC 22 August interpolated GFS forecast has Mawar translating due northward to make landfall in southern Japan and then moving into the Sea of Japan. The TC in the GFS model is initialized as being far too weak compared with the verifying NOGAPS analysis (not shown). Although the TC in the GFS model does deepen slightly in the first 24 h, it does not reach the strength depicted in the verifying analysis. The GFS model predicts the development of a midlatitude low in the southern Yellow Sea at 24 h, which is confirmed by the NOGAPS verifying analysis (not shown).

> Although the structure of this midlatitude low in the Yellow Sea is accurately predicted at 54 h in the GFS MSL forecast (Fig. 28a) compared with the verifying NOGAPS analysis (Fig. 28b), the forecast pressure fields have the TC too weak compared to reality. By 66 h, the midlatitude low in the GFS model has deepened and is now stronger than the TC (Fig. 28c). In the verifying analysis, the TC is still the stronger of the two circulations (Fig. 28d).
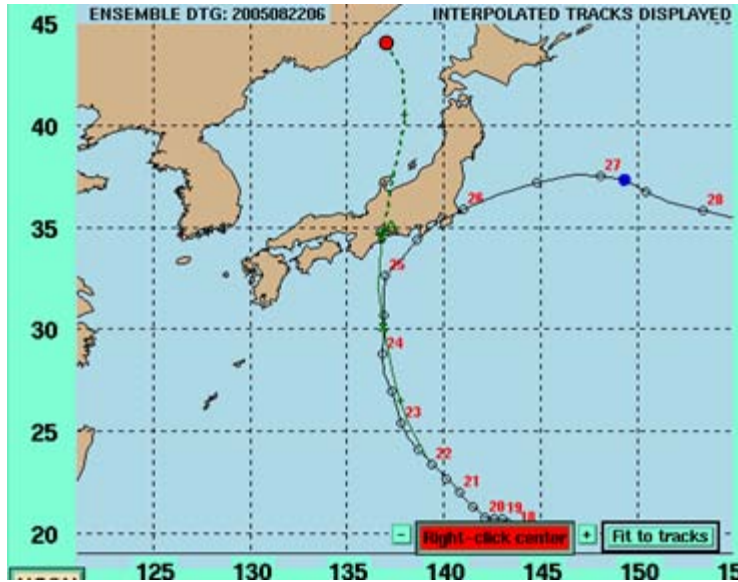
Figure 27. Interpolated GFS (A) forecast track for 11W (Mawar) for the 0600 UTC 22 August 2005 E-DCI-m case study. The solid sections of the forecast tracks represent the 0-h through 72-h forecast while the dashed sections represent the 72-h through 120-h forecast. The solid line with open circles and corresponding dates represents the TC best track. The verifying 120-h position is indicated by the blue circle, while the 120-h interpolated forecast is indicated by the red circle.

In the 66-h 700-mb GPH forecast (Fig. 28e), the weak vortex in the GFS model associated with the TC has already been enveloped by the midlatitude low over the Yellow Sea. In the verifying NOGAPS analysis, Mawar is characterized by several concentric isopleths that are distinctly separate from the midlatitude circulation (Fig. 28f).

At 90 h, the TC in the GFS MSL forecast has been rotated northward and now appears as an appendage on the midlatitude low that has translated across Korea into the Sea of Japan (Fig. 29a). In reality, Mawar has remained separate from the midlatitude low, and is centered over Tokyo (Fig. 29b). Finally, the midlatitude low has the TC as an appendage that is continuing to track to the north in the GFS model at 114 h (Fig. 29c). Interestingly, the GFS vortex tracker has begun to follow the midlatitude low position instead of the weakened TC, which results in the forecast track curving to the northwest (Fig. 27). In the verifying NOGAPS analysis at 114 h, Mawar

has translated eastward on the northern periphery of the subtropical ridge and has actually re-intensified off the coast of Japan, and is clearly a separate entity from the midlatitude low in the northern Sea of Japan (Fig. 29d).
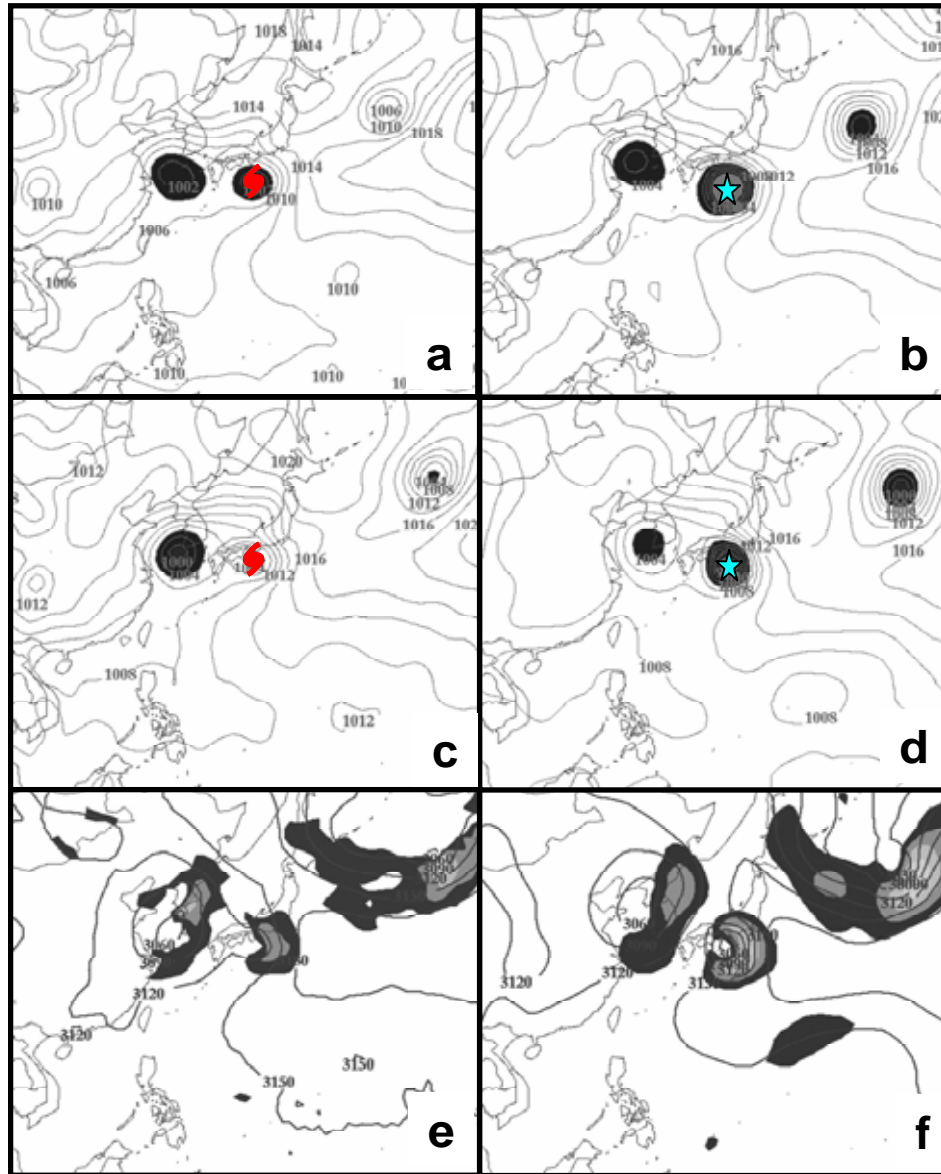
Figure 28.   Forecast mean sea-level pressure (mb) forecast fields for 11W (Mawar) predicted by GFS for taus (a) 54 and (c) 66 for 0600 UTC 22 August 2005 and the corresponding verifying 00-h NOGAPS analyses (b and d). The forecast position is indicated by a red TC symbol, and the verifying TC position is indicated by a blue star. (e) Forecast 700-mb geopotential height and isotach (contour interval 20 kt beginning at 20 kt) field for 11W predicted by GFS for tau 66 and (f) the corresponding verifying NOGAPS analysis.

Figure 29.   Forecast mean sea-level pressure (mb) fields for 11W (Mawar) predicted by GFS for taus (a) 90 and (c) 114 for 0600 UTC 22 August 2005 and the corresponding verifying 00-h NOGAPS analyses (b and d). The forecast position is indicated by a red TC symbol, and the verifying TC position is indicated by a blue star.

In this case study, the incorrectly predicted structures of both the midlatitude low (too strong) and the TC (too weak) in the GFS model contributed to their false interaction via the E-DCI-m error mechanism. Instead of being steered by the subtropical ridge to its south, the TC in the GFS model rotates cyclonically about the midlatitude low to its north. This cyclonic rotation and merger of the smaller TC circulation with the large cyclonic circulation is a characteristic of Excessive Direct Cyclone Interaction (E-DCI-m), which in this case is dominated by a midlatitude circulation. Kehoe (2005) was the first to notice this type of error in the 96-h and 120-h track forecasts during the 2004 western North Pacific season.

(2) E-RVS (GFS) - Saola (18W). The GFS forecast predicts that the TC will continue on a northwestward path, while in reality Saola recurved south of mainland Japan without making landfall (Fig. 30). In comparison to the NOGAPS initial MSL pressure fields, the MSL pressure fields in the GFS depict Saola as appropriately deep (not shown). By 24 h, the TC in the GFS model (Fig. 31a) is inexplicably predicted to weaken while Saola actually continued to deepen (Fig. 31b). Even though the TC in the GFS forecast remained considerably weaker than Saola through the 72-h forecast, the 72-h track error was only 117 n mi. Already by 60 h (Fig. 31c) the TC in the GFS MSL pressure forecast begins to take on an elliptical shape, which indicates it is under the influence of vertical wind shear. The vertical wind shear between850 mb and 200 mb in the GFS forecast was estimated to be approximately 35 kt on the northern periphery of Saola (not shown).
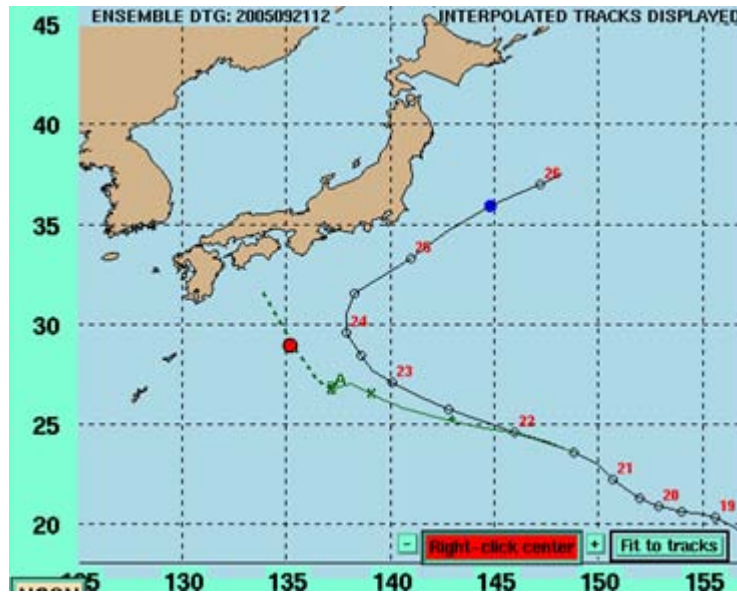
Figure 30.   Interpolated GFS (A) forecast track for 18W (Saola) for the 1200 UTC 21 September 2005 E-RVS case study. The solid sections of the forecast tracks represent the 0-h through 72-h forecast while the dashed sections represent the 72-h through 120-h forecast. The solid line with open circles and corresponding dates represents the TC best track.   The verifying 96-h position is indicated by the blue circle, while the 96-h interpolated forecast is indicated by the red circle.
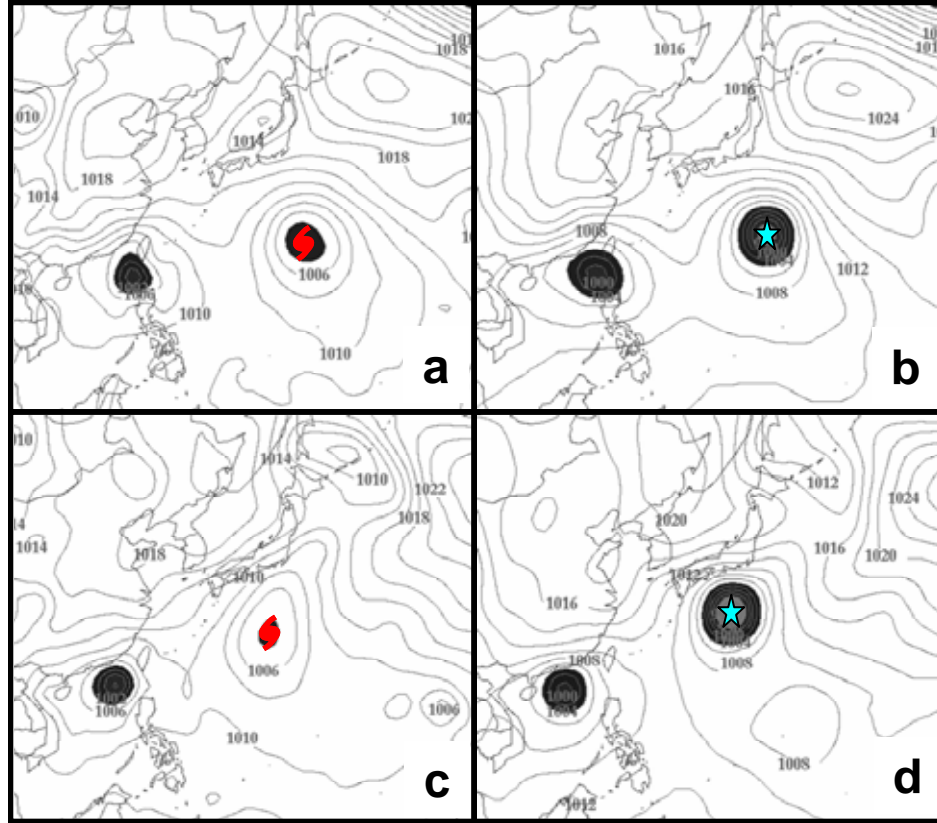
Figure 31.   Forecast mean sea-level pressure (mb) fields for 18W (Saola) predicted by GFS for taus (a) 24 and (c) 60 for 1200 UTC 21 September 2005 and the corresponding verifying 00-h NOGAPS analyses (b and d). The forecast position is indicated by a red TC symbol, and the verifying TC position is indicated by a blue star.

The verifying 500-mb geopotential analyses (not shown) indicate a deepening midlatitude trough to the north of the TC, which the GFS model predicts with reasonable skill. Although some elongation is analyzed to the northwest of Saola, the 500-mb vortex remains coupled with the low-level circulation. In contrast, little or no evidence of a 500-mb vortex exists at 72 h in the GFS model, which is attributed to the shallow extent of the model TC.
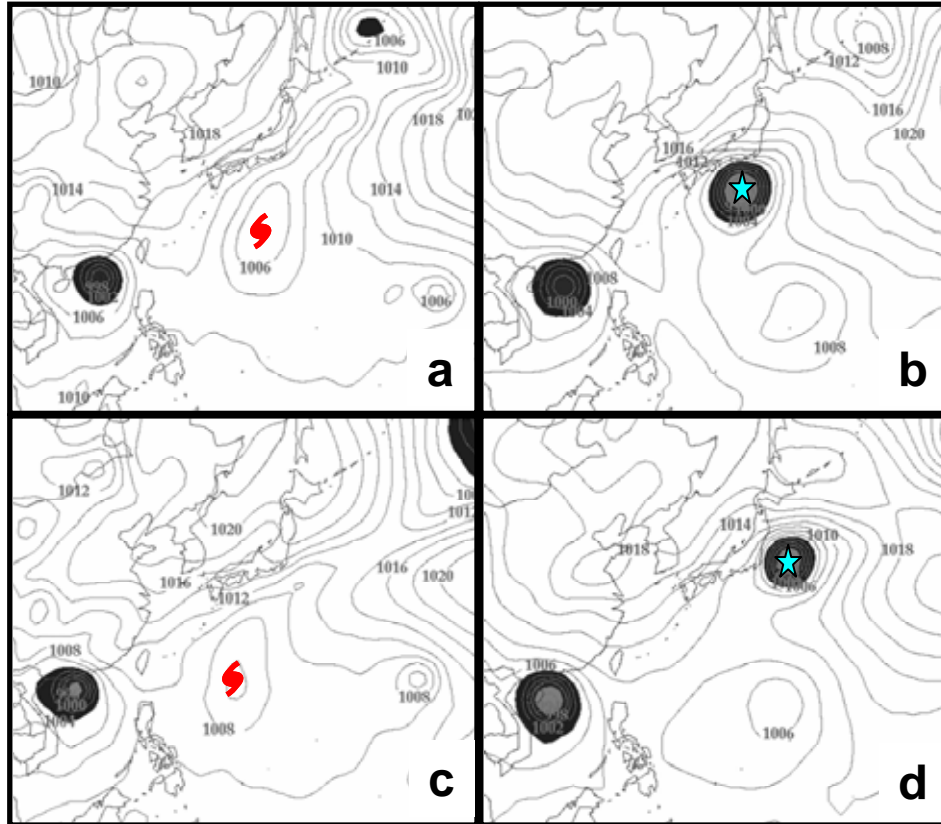
Figure 32.   Forecast mean sea-level pressure (mb) fields for 18W (Saola) predicted by GFS for taus (a) 72 and (c) 96 for 1200 UTC 21 September 2005 and the corresponding verifying 00-h NOGAPS analyses (b and d). The forecast position is indicated by a red TC symbol, and the verifying TC position is indicated by a blue star.

By 72 h in the GFS forecast (Fig. 32a), the TC has a tail-like feature extending to the northeast of the storm along the coast of Japan. In reality, Saola has recurved along the southern coast of Japan and is at its maximum intensity (Fig. 32b). At 96 h (Fig. 32c), the model circulation has barely moved from the 72-h position, since it is too weak to be steered by the 500-mb trough. The TC in the GFS is predicted to migrate southwestward under the influence of a low-level anticyclone over the Yellow Sea and Korea. The GFS TC is so weak at this time that the tracker has difficulty following the TC center. The interpolated track indicates the TC center will be just south of the Japanese island of Shikoku at 96 h (Fig. 30), while in the GFS MSL pressure fields the center is located much further to the south (Fig. 32c). According to the verifying 96-h NOGAPS analysis (Fig. 32d), Saola continued to move parallel to the coast of Japan, and

58

brought heavy rains and strong winds to DOD interests in the Tokyo area. Incidentally, the NOGAPS track forecast for the same period was also degraded due to E-RVS.

(3) Kirogi (21W) dissipation-GFS. The 1200 UTC 13 October GFS interpolated track forecast resulted in an incredible 1454 n mi error at 120 h. Instead of recurving to the northeast, the TC in the GFS forecast actually translated to the southwest toward the Philippines (Fig. 33). As in many other GFS cases, the TC in the MSL pressure field (Fig. 34a) is depicted as being far too weak for a 90-kt storm in comparison to the NOGAPS analysis (Fig. 34b).
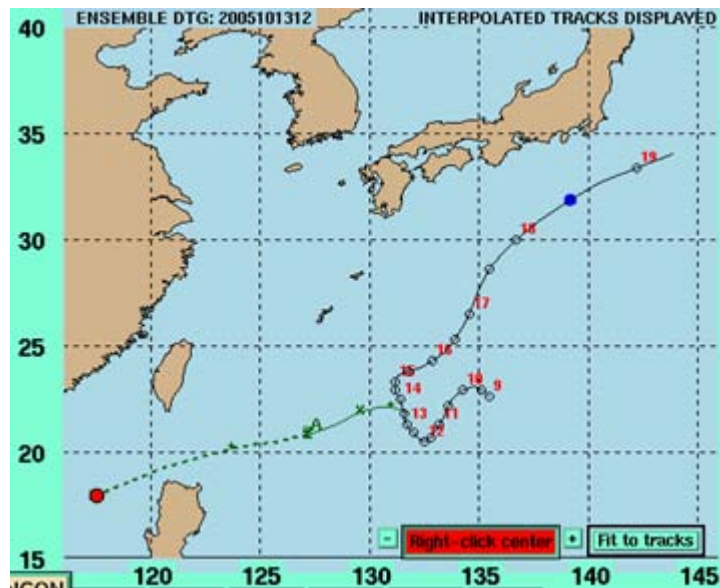
Figure 33. Interpolated GFS (A) forecast track for 21W (Kirogi) for the 1200 UTC 13 October 2005 excessive dissipation case study. The solid sections of the forecast tracks represent the 0-h through 72-h forecast while the dashed sections represent the 72-h through 120-h forecast. The solid line with open circles and corresponding dates represents the TC best track. The verifying 120-h position is indicated by the blue circle, while the 120-h interpolated forecast is indicated by the red circle.

The 500-mb initial GPH fields in the GFS indicate that the forecast TC only constitutes one closed isopleth (Fig. 34c), while in the verifying analysis, three closed isopleths are evident at 500 mb (Fig. 34d), which demonstrates the insufficient depiction of the vertical extent in the GFS model. Similar to the Saola case described above, the TC in the GFS has weakened further after just 24 h (Fig. 34e). The TC had been in a region of weak steering prior to and at the beginning of the forecast period because a ridge centered over central China had blocked its northward progression and the subtropical ridge that was well to the east of Japan (not shown) was not providing significant steering. Between 48 h and 72 h, a midlatitude trough over Korea approached and began to break down the ridge (not shown), so Kirogi began to accelerate to the northeast, as seen in the verifying NOGAPS analyses (Figs. 35 b, d, f).

Even though the midlatitude steering environment is accurately predicted by the GFS model, without the proper vertical extent the TC does not interact properly with the midlatitude trough. Instead of recurving to the northeast as in the verifying analysis, the TC in the GFS (Figs. 35a, c, e) is predicted to move to the southwest under the influence of the low-level anticyclone. In contrast to the E-RVS event described above for Saola, no elongation of the TC circulation or other evidence of vertical shear is predicted. Vertical wind shear between 850 mb and 200 mb in the near vicinity of the TC in the GFS model was approximately 10 kt (not shown). By 96 h in the GFS forecast (Fig. 35c), the TC does not even constitute a closed MSL isopleth. Although the erroneous forecast track in the Kirogi is similar to the E-RVS cases, the lack of vertical shear forces this case to be classified separately ("other" in Table 1) .
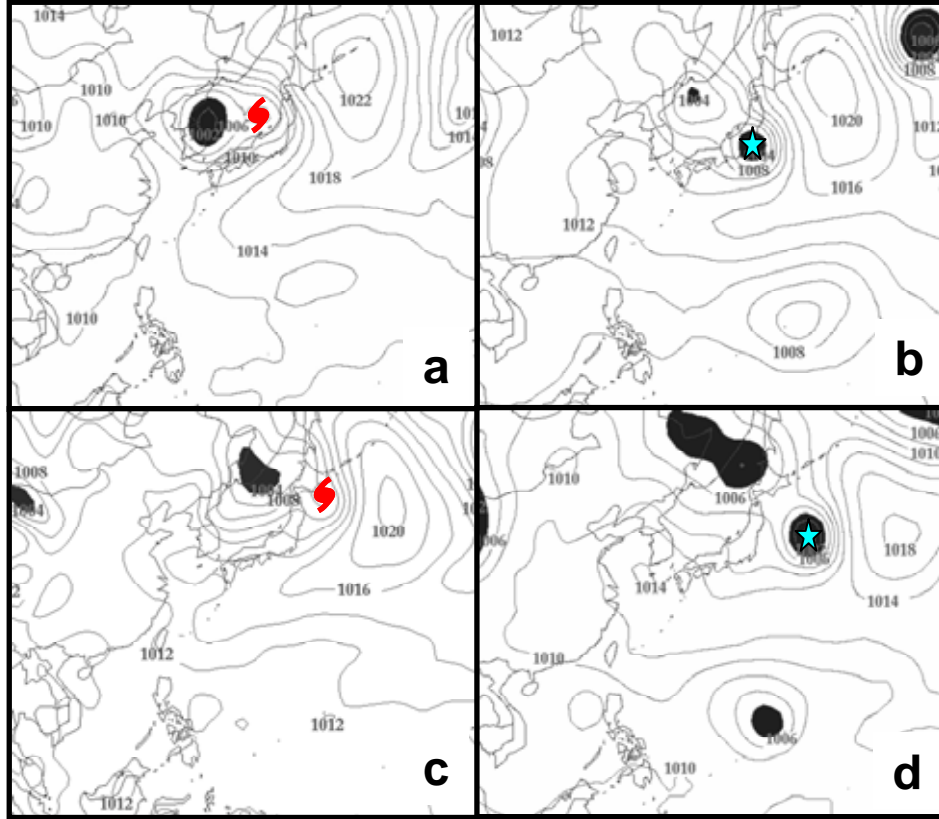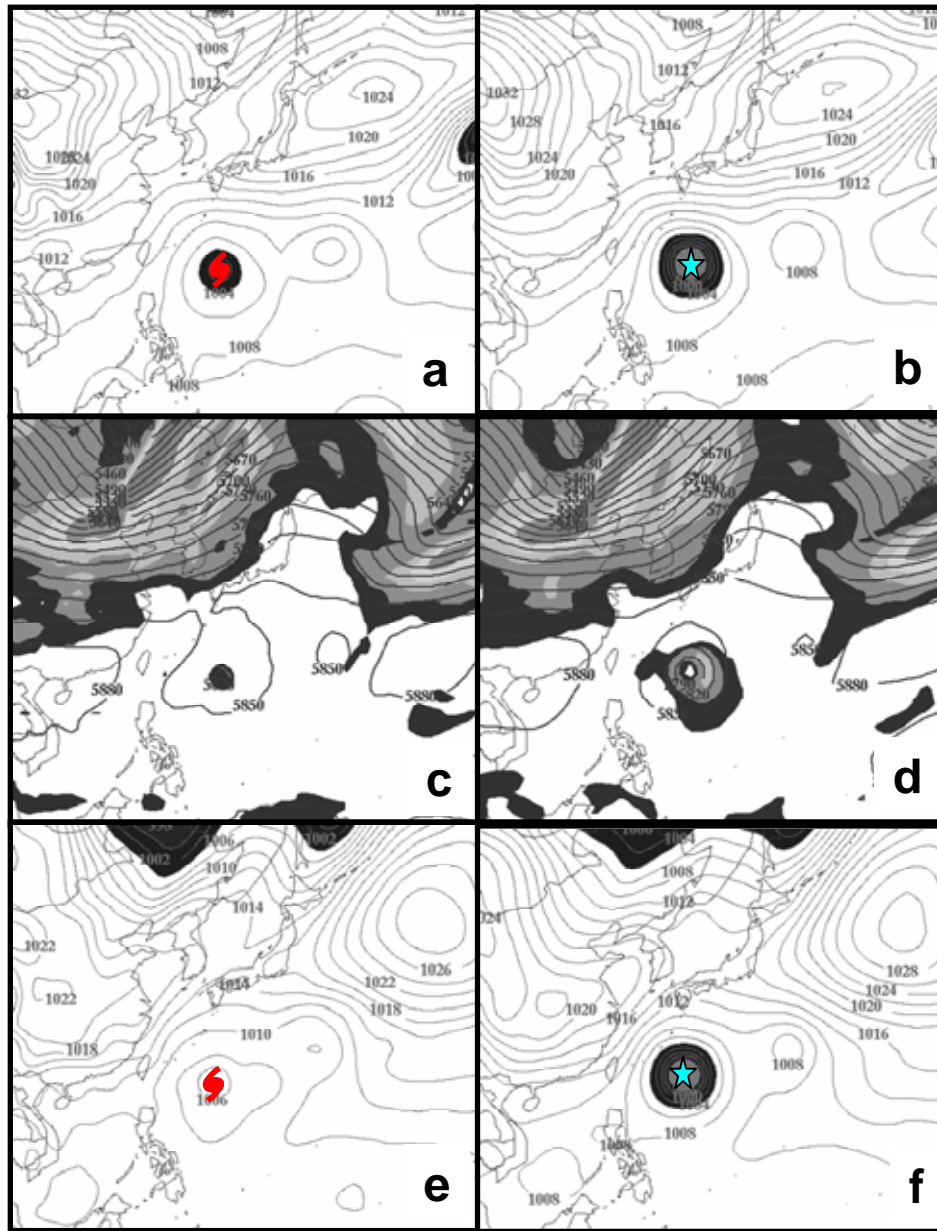
Figure 34. Forecast mean sea-level pressure (mb) fields for 21W (Kirogi) predicted by GFS for taus (a) 00 and (e) 24 for 1200 UTC 13 October 2005 and the corresponding verifying 00-h NOGAPS analyses (b and f). The forecast position is indicated by a red TC symbol, and the verifying TC position is indicated by a blue star. Forecast 500-mb geopotential heights and isotachs (contour interval 20 kt beginning at 20 kt) (c) predicted by GFS for tau 00 and (d) the corresponding verifying NOGAPS analysis.
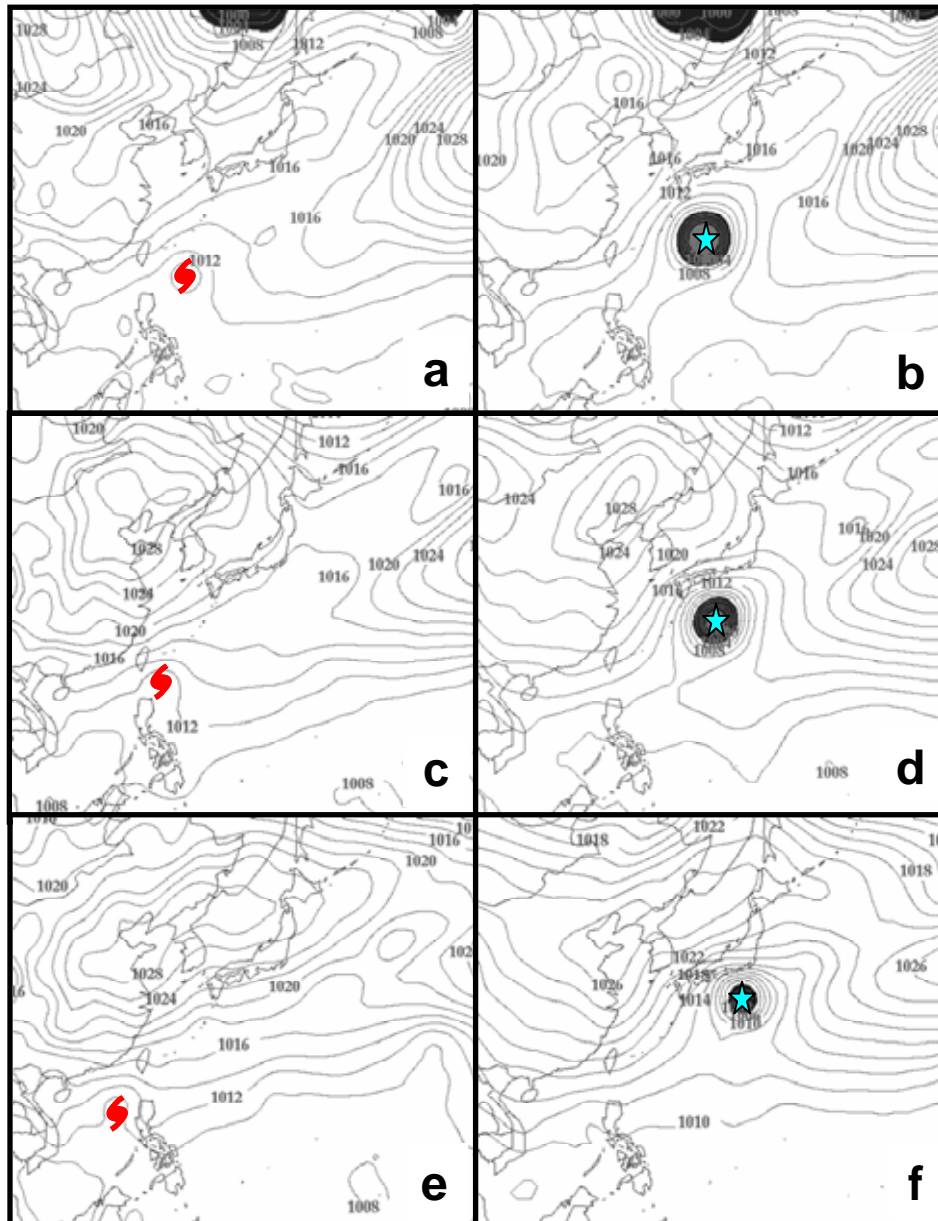
Figure 35.   Forecast mean sea-level pressure (mb) fields for 21W (Kirogi) predicted by GFS for taus (a) 72 (c) 96 and (e) 120 for 1200 UTC 13 October 2005 and the corresponding verifying 00-h NOGAPS analyses (b, d, and f). The forecast position is indicated by a red TC symbol, and the verifying TC position is indicated by a blue star.

IV.   ESTIMATION OF 120-H PREDICTABILITY

A.   ERROR VERSUS SPREAD

The previously determined large track error mechanisms and the consensus spread were used to determine if a 120-h selective consensus (SCON) could be made in each case that would be an improvement relative to the non-selective consensus (NCON) used by JTWC. Elsberry and Carr (2000) defined the spread of the consensus as the largest distance in n mi between the non-selective consensus and a single consensus member. In contrast, Goerss (2000) defined spread as the average distance in n mi between each of the consensus members and the non-selective consensus.

The consensus spread was calculated using both methods and compared for 151 120-h forecasts during the 2005 season. Large spread and large consensus error were defined as > 300 n mi. For each method, all 120-h consensus forecasts were divided into four scenarios: small consensus spread and small consensus error (SSSE); small consensus spread and large consensus error (SSLE); large consensus spread and large consensus error (LSLE); and large consensus spread and small consensus error (LSSE).

A scatter plot of consensus error versus spread using the definition of Elsberry and Carr (2000) is given in Fig. 36. Note that 39% of the 120-h cases fall in the SSSE quadrant. In such cases, all models provide accurate guidance and it is thus inadvisable to attempt to improve upon the non-selective consensus. In 13% of the cases, the consensus error is large (SSLE) even though the consensus spread is small, which means all of the dynamical models provide inaccurate guidance at 120 h.   In such cases, it is normally not advisable to attempt to improve upon the non-selective consensus. Part of the rationale for consensus forecasting is that the errors have a Gaussian distribution about a zero mean (i.e., no systematic error). In a case such as the GFDN false anticyclogenesis, the forecaster may be able to use knowledge of the systematic GFDN error to adjust the forecast away from the GFDN track if it is an outlier. Another 23% of the 120-h cases fall into the LSSE category. In LSSE cases, compensating large errors across the true track tend to cancel out when averaged in the non-selective consensus. To make a selective consensus, it is essential that forecasters assure that compensating errors

are not occurring, since, a selective consensus forecast will be degraded if only one of the compensating track errors is eliminated. The remaining 25% of cases fall into the LSLE quadrant. It is hypothesized that a forecaster will be able to add value to the LSLE cases, if he or she can eliminate one or more dynamical model tracks with a large error to create a SCON of the remaining tracks.
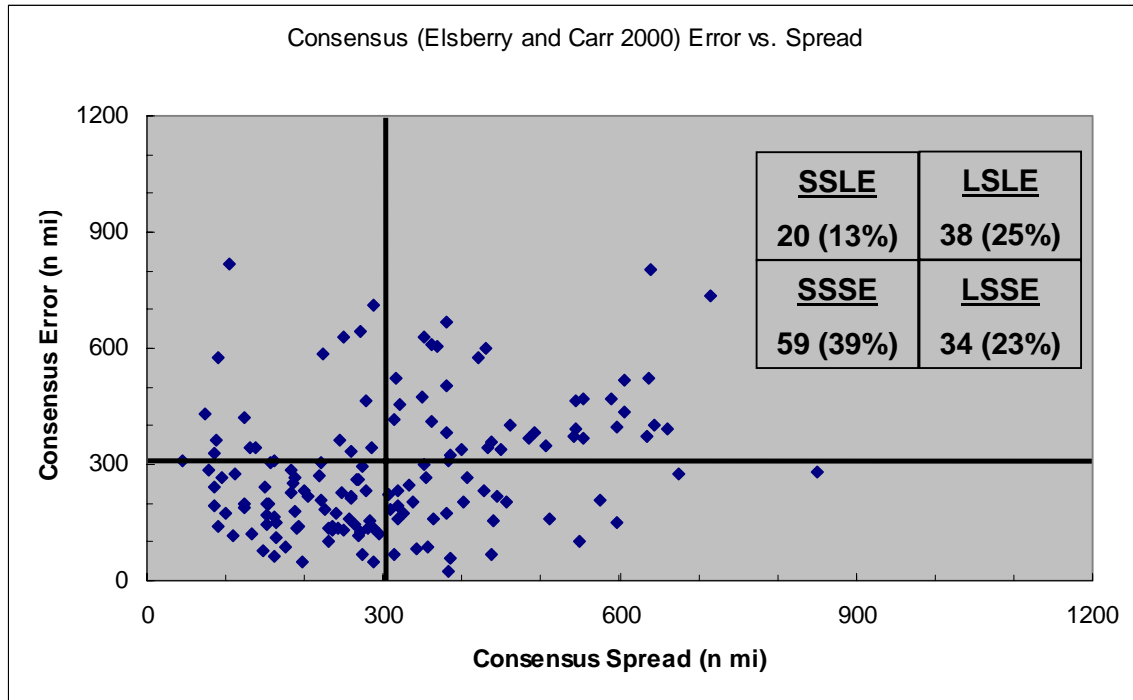
Figure 36. Scatter plot of consensus error (n mi) versus consensus spread (n mi) as defined by Elsberry and Carr (2000) for 151 western North Pacific TC 120-h forecasts during the 2005 season. Spread is defined as the maximum distance of a consensus member track from the consensus track. The thresholds for large and small spreads and errors are 300 n mi. The four quadrants represent four possible scenarios: small spread and large error (SSLE); small spread and small error (SSSE); large spread and large error (LSLE); and large spread and small error (LSSE).

A scatter plot of consensus error versus spread using the definition of Goerss (2000) is given in Fig. 37. The numbers/percentages of the cases in the four error versus spread scenarios using the Elsberry and Carr versus the Goerss methods can be compared from the insets to Figs. 36 and 37, respectively. By averaging the distance of each member from the NCON (as opposed to taking the distance of the largest member from NCON), the number of large spread cases is drastically reduced compared with the Elsberry and Carr method. This result is expected given that averaging will reduce the spread value versus taking the distance to the largest outlier. Thus, 16 of the LSLE cases in Elsberry and Carr method become SSLE cases via the Goerss method, and 21 of the LSSE cases become SSSE cases.
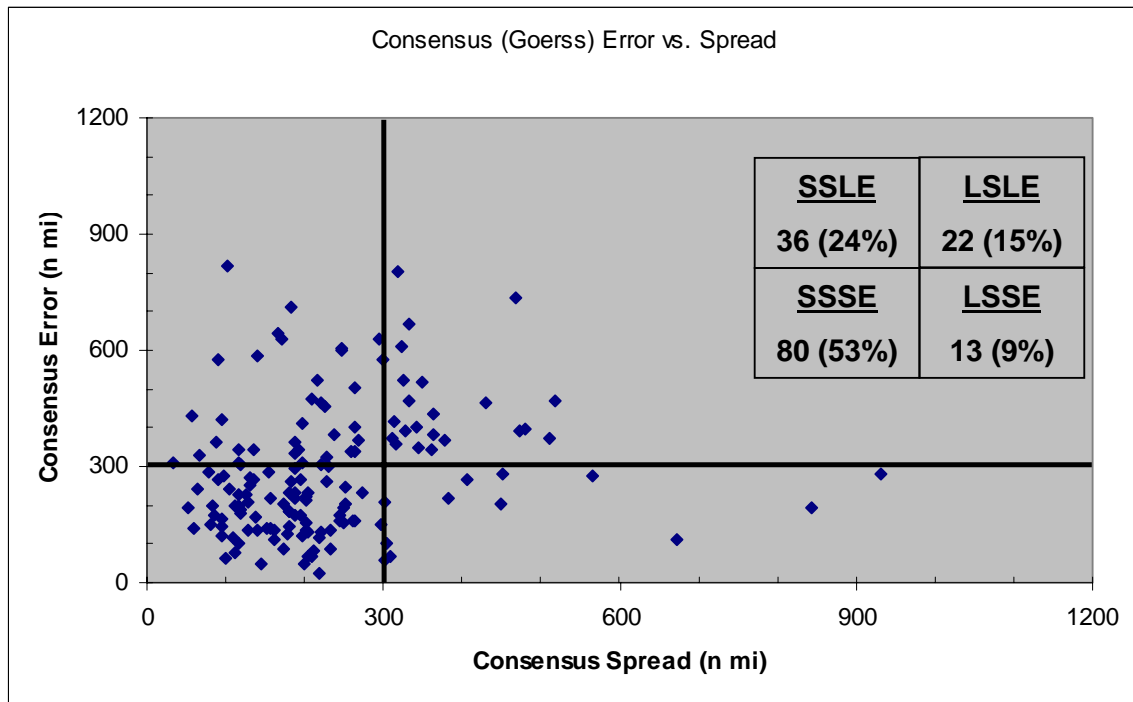
Figure 37.   Scatter plot of consensus error (n mi) versus consensus spread (n mi) as defined by Goerss (2000) for 151 western North Pacific TC 120-h forecasts during the 2005 season. Spread is defined as the average distance of the consensus member tracks from the consensus track. The thresholds for large and small spreads and errors are 300 n mi. The four quadrants represent four possible scenarios: small spread and large error (SSLE); small spread and small error (SSSE); large spread and large error (LSLE); and large spread and small error (LSSE).

65

The rationale of using the Elsberry and Carr spread definition versus that of Goerss is that more LSLE opportunities will potentially exist to improve the SCON track relative to the NCON. All of the LSLE cases determined using the Elsberry and Carr method will be examined for the purposes of creating an SCON.

B.   CREATION OF A SELECTIVE CONSENSUS

The purpose of calculating a selective consensus in hindsight is to estimate the predictability of 120-h TC track forecasts with the present dynamical models assuming that a forecaster can identify a dynamical model track with a large error in real time. While this may not always be possible, the knowledge base of frequently occurring error mechanisms developed in Chapter III serves to aid forecasters in identifying such large track errors.

For each of the 38 LSLE cases in Fig. 36 for the 2005 season, dynamical model tracks were removed based on the large error mechanisms assigned in Chapter III and thus created a selective consensus (SCON). The error of each newly created SCON versus the best-track was calculated and compared to the error of the non-selective consensus (CONW) and the official JTWC forecast (Table 2). In six cases, archived fields were not available so that no error mechanism could be assigned. For these cases, it is assumed that forecasters would have the appropriate fields and thus these erroneous tracks were eliminated when creating the SCON. Although the spread was greater than 300 n mi in one case, no individual model track had a 120-h error of greater than 500 n mi and thus no error mechanism was assigned in Chapter III. A SCON was not created for this case. In three cases, all of the individual models in the consensus had a large track error. In these cases, creation of an SCON was inadvisable, as in the SSLE cases. In one additional case, only two model forecast tracks were available, so no SCON was created. A total of 33 SCON forecasts were created (Table 2). Note that due to model availability, the NCON did not always include tracks from all four dynamical models to 120 h.

The SCON error was smaller than the NCON error in all cases, with the average improvement of 222 n mi. In 10 cases, multiple model tracks contained large errors and had to be removed such that only one model remained in the selective consensus. The SCON error was smaller than the official JTWC forecast error in 22 cases, with an average improvement of 382 n mi. No cases of SCON degradation versus the JTWC

66

forecast existed. Notice that the JTWC did not make an official forecast in 11 of the cases, even though model guidance was available. Many of these omitted cases were for TCs that were forecast to undergo extratropical transition. Even though the responsibility for warnings shifts to another agency when the TC is considered to be extratropical, it is still important for the JTWC to give the best-possible guidance as to the track of the extropical cyclone that may represent a threat to DoD assets.

Table 2.   The 32 cases of 120-h forecasts for which a selective consensus (SCON) was created, and the improvement (n mi) of SCON error relative to the NCON (CONW) error and the JTWC official forecast error. The models used to make the SCON and the NCON are listed from GFS(A), UKMO (E), NOGAPS (N), and GFDN (G).

TC	Date/time group	SCON	CONW	SCON improvement vs. CONW	JTWC	SCON improvement vs. JTWC	models in SCON	models in NCON
04W	2005060206	207.9	338.9	131.0	424.5	216.6	E,N,G	A,E,N,G
	2005060212	169.5	360.4	191.0	509.7	340.3	E,N	A,E,N,G
	2005060218	234.9	392.7	157.8	638.8	403.9	E,N,G	A,E,N,G
	2005060300	205.2	403.1	197.9	707.6	502.4	E,N,G	A,E,N,G
	2005060306	221.9	372.1	150.2	782.8	560.9	E,N,G	A,E,N,G
	2005060312	287.6	384.2	96.7	849.6	562.1	E,N,G	A,E,N,G
	2005060318	211.1	398.1	186.9	1150.5	939.4	E	A,E,N,G
	2005060400	126.0	371.1	245.1	1381.6	1255.6	E,N	A,E,N,G
	2005060406	302.9	412.9	110.0	none	N/A	E,N,G	A,E,N,G
	2005060418	186.4	367.6	181.2	564.1	377.7	A,E	A,E,N,G
	2005060500	217.8	437.1	219.3	698.4	480.6	A,E	A,E,N,G
	2005060506	163.8	464.2	300.4	655.9	492.1	A	A,N,G
	2005060512	209.2	365.5	156.3	577.8	368.6	A	A,N,G
07W	2005072206	381.0	608.8	227.8	none	N/A	A	A,E,N,G
	2005072212	96.6	573.9	477.3	none	N/A	A	A,E,N,G
	2005072218	234.4	604.5	370.1	none	N/A	A	A,E,N,G
	2005072300	394.8	598.0	203.1	none	N/A	A,E	A,E,N,G
	2005072400	299.5	523.2	223.8	none	N/A	A	A,E,N,G
	2005072412	286.8	453.3	166.5	none	N/A	A,N	A,E,N,G
11W	2005082206	151.7	475.7	324.0	none	N/A	E	A,E,N,G
	2005082212	173.2	802.1	628.9	none	N/A	E	A,E,N,G
	2005082218	222.5	604.5	382.0	none	N/A	E,A	A,E,N,G
	2005082300	257.1	598.0	340.9	none	N/A	E,A,N	A,E,N,G
15W	2005090612	80.9	348.6	267.7	350.9	270.0	A, E	A,E,N,G
	2005090618	265.8	521.8	256.0	547.3	281.5	A	A,E,N,G
	2005090700	394.0	504.3	110.3	546.5	152.5	N,G	E,N,G
	2005090706	99.1	391.9	292.8	485.5	386.4	E,N	A,E,N,G
19W	2005092606	224.7	341.7	117.0	315.5	90.8	A,N	A,E,N
	2005092612	149.9	380.6	230.7	332.0	182.1	A,N	A,E,N
	2005092700	196.5	323.2	126.6	349.2	152.7	A,N,G	A,E,N,G
	2005092712	244.1	308.5	64.4	277.4	33.3	A,E,G	A,E,N,G
	2005092800	296.0	467.6	171.6	419.0	123.0	A,E,G	A,E,N,G
21W	2005101112	89.6	337.8	248.3	153.5	64.0	E,N	A,E,N,G
	Average Improvement:			222.2		381.9		

It should be noted that these SCON forecasts produced represent an estimate for 120-h predictability if optimum use is made of the dynamical model guidance. Given

model data availability and time constraints, the creation of an accurate SCON may not always be possible operationally. Some error mechanisms may be more difficult for a forecaster to identify in real time.

C.   CASE STUDIES

The following section will provide examples from the 2005 western North Pacific season of 120-h forecasts for each of the error versus spread scenarios in Fig. 36. The summary of the 120-h track errors for the dynamical models and the consensus methods is given in Table 3.

1.   Small Spread Small Error (SSSE)

The 1200 UTC 12 July forecasts for TC Haitang (05W) indicate a tight grouping of the four dynamical models (Fig. 38), which creates a small spread (165 n mi) from the consensus. Given such a small spread a forecaster should use the NCON as the primary guidance. All the dynamical model tracks were generally accurate in comparison to the best track (Table 3). In this case, the NCON error (150 n mi) is neither the best individual track (AVNI, 66 n mi error) nor the worst (NGPI, 262 n mi error), which is to be expected from previous research (Goerss 2000).

2.   Small Spread Large Error (SSLE)

The model track forecasts for 1800 UTC 1 September for TC Nabi (14W) demonstrate the SSLE scenario (Fig. 39). All of the guidance (223 n mi spread) indicates the TC will recurve later and farther to the west than the best track. In such a scenario, the forecaster has no choice but to go with the provided model guidance and no SCON is created. Even if a forecaster suspects a large error mechanism to be occurring in each of the NCON members, eliminating one of the tracks may degrade the consensus. Again, the NCON (584 n mi error) is neither the best (AVNI, 411 n mi error) nor the worst (EGRI, 800 n mi error) of the forecast tracks (Table 3). Based on the statistics from the 2005 season, approximately 13% of 120-h forecasts will fall into the SSLE scenario (Fig. 36).

Table 3. Nonselective consensus (CONW), SCON (if applicable), and individual interpolated consensus member errors in n mi for the four case studies. Spread is also given in n mi.

Case	CONW error	AVNI error	EGRI error	NGPI error	GFNI error	Spread	SCON error
05W 2005071212	150	66	166	261	168	165	N/A
14W 2005090118	584	411	800	564	579	223	N/A
19W 2005092800	468	374	471	1025	279	589	296
21W 2005101300	196	1119	233	1433	620	1289	N/A
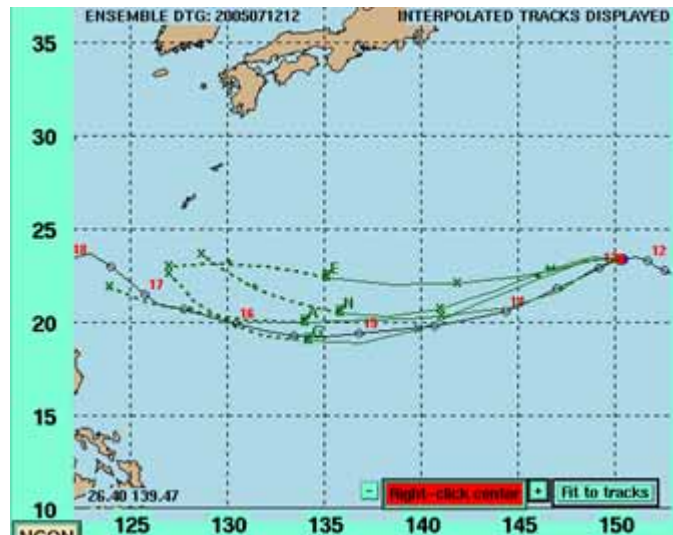
Figure 38. Interpolated GFS (A), UKMO (E), NOGAPS (N), and GFDN (G) forecast tracks for 05W (Haitang) for the 1200 UTC 12 July 2005 forecast. The solid sections of the forecast tracks represent the 0-h through 72-h forecast while the dashed sections represent the 72-h through 120-h forecast. The solid line with open circles and corresponding dates represents the TC best track.
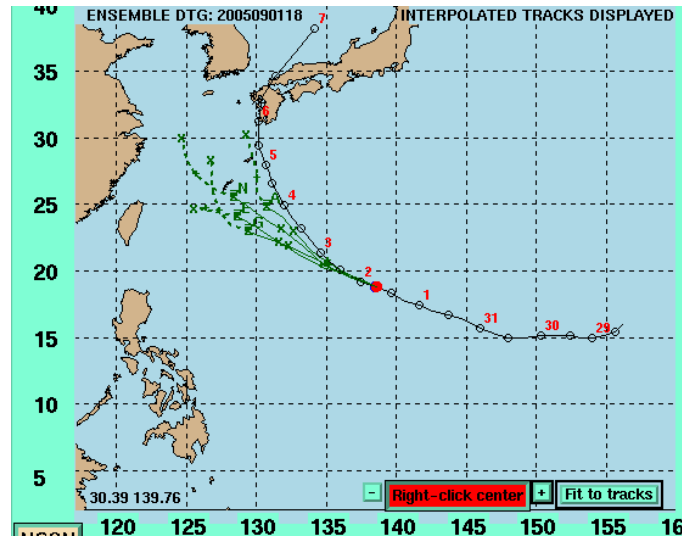
Figure 39.   Interpolated GFS (A), UKMO (E), NOGAPS (N), and GFDN (G) forecast tracks for 14W (Nabi) for the 1800 UTC 1 September 2005 forecast. The solid sections of the forecast tracks represent the 0-h through 72-h forecast while the dashed sections represent the 72-h through 120-h forecast. The solid line with open circles and corresponding dates represents the TC best track.

3.   Large Spread Large Error (LSLE)

As previously noted, forecasters may be able to improve upon LSLE cases by creating an SCON. For the 0000 UTC 28 September forecast for Longwang (19W), NOGAPS is the lone outlier among the consensus members (creating a spread of 589 n mi), while the other track forecasts are closely grouped (Fig. 40). The NOGAPS track forecast was previously reviewed in a case study in Chapter III, where it was determined that the subtropical ridge failed to build and sufficiently block the TC from recurving, which is then an I-MAG error. A forecaster who knows that the NOGAPS model has a tendency to incorrectly handle midlatitude ridges would then eliminate the NOGAPS track and create a SCON from the remaining three track forecasts, as seen in Fig. 41. The SCON now yields an error of 296 n mi, which is a vast improvement over the NCON and three of the four individual model tracks (Table 3).
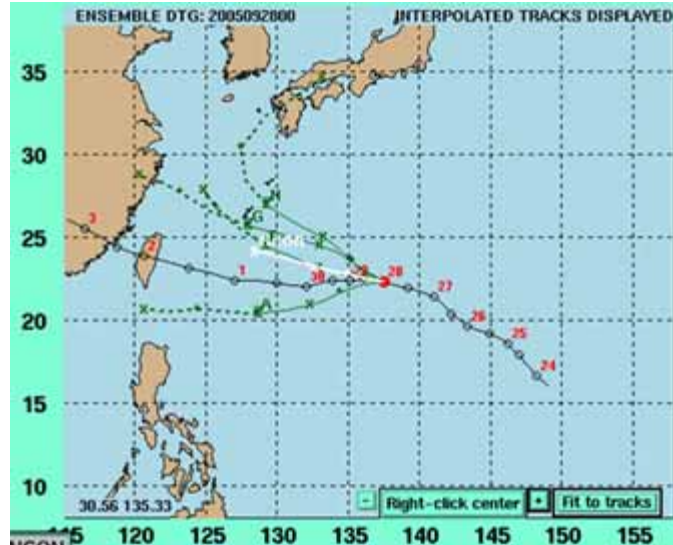
Figure 40.   Interpolated GFS (A), UKMO (E), NOGAPS (N), and GFDN (G) forecast tracks for 19W (Longwang) for the 0000 UTC 28 September 2005 forecast. The solid sections of the forecast tracks represent the 0-h through 72-h forecast while the dashed sections represent the 72-h through 120-h forecast. The solid line with open circles and corresponding dates represents the TC best track.
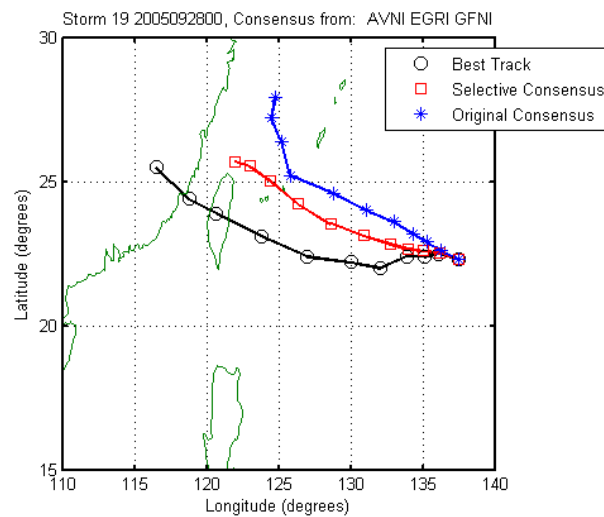
Figure 41.   Selective consensus forecast for 19W Longwang from 0000 UTC 28 September 2005.   The blue forecast track represents the original non-selective conensus (NCON), the red forecast track represents the selective consensus (SCON), and the black track is the best track. Open shapes along the tracks represent every 12 h.

71

4.   Large Spread Small Error (LSSE)

For LSSE cases, a forecaster is advised to use the NCON forecast since models may be making compensating errors such that the average of the forecast tracks still produces an accurate NCON forecast. The 0000 UTC 13 October forecast for Kirogi (21W) demonstrates compensating errors (Fig. 42). The GFS forecast indicates the TC will translate southwestward toward the Philippines. A review of the forecast field indicates the TC is excessively dissipating in a manner similar to a case study in Chapter III, and therefore the GFS track forecast is in error. While a forecaster may be tempted to eliminate the GFS model to create the SCON, a review of the NOGAPS forecast fields indicate the TC is rapidly accelerating to the northeast. The NOGAPS forecast over-deepens an approaching shortwave trough (E-MCG). Although the NOGAPS and GFS forecasts each result in greater than 1000 n mi errors, the errors are in opposite directions. Thus, a NCON that includes both of these forecast tracks produces an error of only 196 n mi, which in this case improves upon all of the individual forecast models (Table 3).

In summary, forecasters should only attempt to produce a SCON when the spread of the consensus is large, or greater than 300 n mi at 120 h. Based on the dataset for the 2005 western North Pacific season, large consensus spread occurred in almost half of the 120-h forecasts (inset, Fig. 36). A forecaster must use the knowledge base of frequently occurring error mechanisms to identify compensating track errors that may be occurring, before attempting to make a SCON. Creating an SCON by eliminating only one erroneous track when compensating track errors exist may greatly degrade the SCON forecast relative to NCON. An examination of each 120-h LSLE case determined that an SCON could be produced that improved on the NCON track error in 33 cases. This represents approximately 20% of the 151 120-h forecasts.

Figure 42.   Interpolated GFS (A), UKMO (E), NOGAPS (N), and GFDN (G) forecast tracks for 21W (Kirogi) for the 0000 UTC 13 October 2005 forecast. The solid sections of the forecast tracks represent the 0-h through 72-h forecast while the dashed sections represent the 72-h through 120-h forecast. The solid line with open circles and corresponding dates represents the TC best track.

THIS PAGE INTENTIONALLY LEFT BLANK

V.   SUMMARY AND CONCLUSIONS

A.   SUMMARY

This research evaluated NOGAPS, GFDN, GFS, and UKMO TC track forecasts with large errors (400 n mi at 96 h and 500 n mi at 120 h) for the 2005 western North Pacific season to determine frequently occurring error mechanisms. Wind, geopotential height, and mean-sea level pressure fields were examined to determine the model steering environment for the TC, and these were compared to the verifying model analysis fields. The large error cases were assigned error mechanisms based on conceptual models defined by Carr and Elsberry (2000 a, b). While Kehoe (2005) had previously examined NOGAPS and GFDN 96-h and 120-h track errors for the 2004 typhoon season, GFS and UKMO track forecasts were examined for the first time.

During 2005, large track errors occurred in 60, 66, 53, and 45 cases for NOGAPS, GFDN, GFS, and UKMO, respectively (Table 1). Error cases were classified as being due to tropical influences or midlatitude influences. Similarly to the 2005 western North Pacific season (Kehoe 2005), midlatitude error mechanisms accounted for the overwhelming majority of cases (95%, 89%, 87%, and 89% in NOGAPS, GFDN, GFS, and UKMO, respectively).

Excessive Direct Cyclone Interaction (E-DCI-t) was the only tropical error mechanism to occur frequently in all four dynamical models. In the three global models, the E-DCI error was exacerbated by an incorrect depiction of TC structure. For the GFDN model, E-DCI occurred due to an interaction of the TC with topography over the Philippines.

Midlatitude System Evolutions were the dominant error mechanisms found in the NOGAPS (82% of cases) and UKMO (74% of cases) models. Midlatitude Cyclogenesis (MCG) was the most frequently occurring error mechanism in both NOGAPS and UKMO, and occurred both excessively and insufficiently. Two-sided frequently occurring error mechanisms are difficult for forecasters to identify in real time. Midlatitude Anticyclogenesis (MAG) was also a two-sided mechanism in NOGAPS, but occurred only excessively in UKMO (Table 1). An incorrect depiction of the

midlatitudes in the NOGAPS and UKMO often led to an incorrect forecast of TC recurvature, and thus resulted in large track errors. Forecasters need to closely monitor the model predicted evolution of midlatitude systems for possible errors.

A systematic error was found in the GFDN model in which a false anticyclone developed downstream of the Tibetan plateau (Excessive Midlatitude Anticyclogenesis) and then propagated eastward. This false anticyclogenesis was present at 500 mb and 700 mb and thus often negatively influenced the environmental steering of the TC. Review of some the 2004 GFDN forecast fields revealed that the false anticyclone was present and contributed to numerous large errors for that season as well.

The false Tibetan anticyclone (always classified as E-MAG) led to four secondary error mechanisms: (i) incorrect steering of the TC on the southern periphery of the false anticyclone (E-MAG, nine cases in four TCs); (ii) incorrect steering of the TC caused by a merger of the false anticyclone and the eastern subtropical ridge (E-MAG, ten cases in three TCs); (iii) insufficient development of the short-wave trough that actually affected the TC (insufficient midlatitude cyclogenesis (I-MCG), six cases in one TC); and (iv) incorrect steering of the TC due to the false eastward displacement of the eastern subtropical ridge (insufficient midlatitude anticyclogenesis (I-MAG), five cases in three TCs). The rapid eastward propagation of the false anticyclone additionally led to four Excessive Midlatitude Anticyclolysis (E-MAL) errors.

The remaining midlatitude error mechanisms (Excessive Response to Vertical Shear, Excessive Direct Cyclone Interaction – Midlatitude, and Excessive Dissipation) were classified as being related to incorrect depiction of vertical structure. For midlatitude errors in the GFS model, 35 of 38 cases could ultimately be attributed to incorrect vertical structure. In each case, the TC in the GFS initialized as being too weak and too shallow and then failed to deepen, making the TC more vulnerable to vertical wind shear or false interaction with another cyclone. In 14 cases, the TC in the GFS falsely dissipated without the presence of vertical shear. In addition, all the errors caused by tropical influences in GFS were also due to improper prediction of vertical structure. It was difficult to accurately assess any erroneous predictions of midlatitude system evolutions in the GFS model since the TC was often too weak to interact with the

76

midlatitude steering environment.   It was hypothesized that the vortex relocation procedure used by GFS instead of bogussing contributed to the incorrect structure.

One third of NOGAPS large track errors could also be explained by incorrect prediction of vertical structure. In contrast to GFS, NOGAPS uses synthetic observations and usually initialized properly, but then the NOGAPS failed to deepen the TC. In the UKMO, the vertical structure of TC was usually properly represented, and therefore no cases of E-RVS occurred. However, the size and strength of the TC in UKMO was often under-predicted. The incorrect size forecasts led to a secondary error mechanism of Insufficient Beta-Effect Propagation (I-BEP) in several UKMO forecasts which exacerbated the TC's false interaction with the midlatitudes. Forecasters should pay close attention of the depiction of size and strength in the model forecast fields, as they have proven to be essential to correct track forecasts.

Forecasters at the JTWC can utilize the knowledge base of frequently occurring error mechanisms to identify when an error is occurring in real time, and by eliminating the offending model forecast(s) create a selective consensus (SCON) that will improve upon the non-selective consensus. A forecaster should only make a SCON if the spread of the consensus is large (greater than 300 n mi at 120 h) and must assure that no compensating errors are occurring that are offsetting and thus may still lead to an accurate NCON track. Based on statistics from the 2005 western North Pacific season, large-spread, large-error (LSLE) scenarios for 120-h track errors occurred approximately 25% of the time. Large-spread, small-error (LSSE) scenarios occurred nearly as frequently (23% of the time), which again underscores the need for forecasters to take care when creating a selective consensus. Previous experience at the JTWC has shown that forecasters at times created a SCON when none was necessary, thus degrading the official track forecast (Jeffries and Fukada 2002).

With the procedure described above, a SCON track that improved upon the NCON track was achieved in 33 cases (Table 3), which represents approximately 20% of all 120-h forecasts for the 2005 season. The average improvement of the SCON over the NCON forecast was 222 n mi and 382 n mi over the JTWC official forecast. Thus, the average track error of JTWC forecasts could be greatly reduced in these approximately

20% of the cases through the perfect elimination of tracks with large error and the creation of a selective consensus. These SCON forecasts represent an ideal for 120-h predictability with the present four dynamical models. However, data availability and time constraints will sometimes inhibit the creation of an accurate SCON in an operational setting. Additionally, forecasters may have difficulty identifying some frequently occurring error mechanisms in real time, especially the two-sided Midlatitude System Evolution (MSE) errors occurring in the UKMO and NOGAPS. Other errors, such as the systematic E-MAG error concerning the false anticyclone found in the GFDN model, and the numerous TC structure errors found in the GFS model should be easier for forecasters to identify.

B. FUTURE WORK

Evaluation of large error cases in the dynamical models serves a two-fold purpose. First, improving the knowledge base of frequently occurring error mechanisms can help forecasters identify when an error is occurring in real time, and possibly produce a selective consensus that improves upon the non-selective consensus. Second, feedback on the model performance can be provided to the model development teams to address the frequently occurring errors.

Dynamical models are constantly being upgraded and improved, and frequently occurring error mechanisms may change from year to year. For instance, if the vortex relocation scheme is modified in the GFS model, the vertical structure-related errors may be reduced or eliminated. However, problems with Midlatitude System Evolutions in the GFS may then become more evident. Consequently, a review of large error cases for each of the models is necessary on a yearly basis. If additional dynamical models become available for 120-h forecasts, an examination of frequently occurring errors will be needed for these new consensus members.

To address the systematic error found in the GFDN model, collaboration is occurring with the developers of the GFDN and the GFDL parent model. It is currently hypothesized that an error in the interpolation of the NOGAPS boundary conditions in the vertical over the topography of the Himalayas is creating a perturbation in the height fields that grows and then propagates downstream. Further cooperation will hopefully resolve the issue before a major upgrade to the GFDN in mid-2006.

APPENDIX A. 2004 WESTERN NORTH PACIFIC TRACK ERRORS

The following is a summary of the results of Kehoe (2005).

A.   METHODS

Following the methods of Carr and Elsberry (2000a,b), Kehoe (2005) used 2004 western North Pacific model forecasts and best-track data to identify characteristic errors of NOGAPS and GFDN models leading to large track errors in 96-h and 120-h forecasts. Large track errors were defined as > 400 n mi at 96 h, and > 500 n mi at 120 h. Kehoe (2005) specifically examined model wind and geopotential height fields to identify error mechanisms, which he divided into tropical and midlatitude interactions. Tropical interactions occurred when the TC was south of the subtropical ridge axis, and midlatitude interactions occurred when the TC was north of or approaching the subtropical ridge axis. Table A-1 lists the error mechanisms identified by Kehoe, and whether they occurred excessively (E) or insufficiently (I). Only the most commonly occurring mechanisms will be reviewed here.

Table A-1.   96-h and 120-h error mechanisms for NOGAPS and GFDN occurring in 2004. *The first (second) number listed is the number of times the phenomenon occurred excessively (insufficiently) (from Kehoe 2005).

2004 96-h and 120-h Error Mechanisms			
Phenomenon name	Acronym	No. of NOGAPS forecasts*	No. of GFDN forecasts*
Large Errors due to Tropical Influences			
Direct cyclone interaction (tropical)	DCI-t	20-0	11-0
Reverse trough formation	RTF	0-0	3-0
Beta effect propagation	BEP	0-5	0-0
Large Errors due to Midlatitude Influences			
Direct cyclone interaction (midlatitude)	DCI-m	6-0	5-0
Response to vertical wind sheer	RVS	26-0	0-0
Baroclinic cyclone interaction	BCI	6-0	0-0
Midlatitude cyclogenesis	MCG	6-53	28-46
Midlatitude cyclolysis	MCL	12-0	2-0
Midlatitude anticyclogenesis	MAG	6-0	9-6
Midlatitude anticyclolysis	MAL	2-4	0-0
False Alarm		6	4
Tracker Error		8	4
Fields not available		2	16
Total of all large-error forecasts		162	135
*The first (second) number listed is the number of times the phenomenon occurred excessively (insufficiently)			

B. FREQUENTLY OCCURRING ERROR MECHANISMS

1. Excessive Direct Cyclone Interaction in the Tropics (E-DCI-t)

The most frequent tropical error mechanism identified by Kehoe (2005) was Excessive Direct Cyclone Interaction (E-DCI-t.) Carr and Elsberry (2000a) previously found that one third of all large track errors at 72 h were due to E-DCI (occurring in both the tropics and in the midlatitudes). For the 2004 season, E-DCI-t occurred 20 times in NOGAPS, and 11 times in GFDN (Table A-1). Kehoe (2005) found three reasons the models falsely predicted E-DCI-t: (i) either the TC or the other tropical cyclone was predicted to have too large a horizontal extent; (ii) either the TC or the other cyclone was misplaced such that the separation distance between the two was too small; or (iii) the TC was predicted by the model to be weaker than reality, such that its steering was controlled by the correctly forecast cyclone. Similarly to Carr and Elsberry (2000a), Kehoe determined that for all cases of model-predicted tropical E-DCI in 2004, DCI failed to occur in reality.

2. Beta Effect Processes

Kehoe (2005) found erroneous model depictions in which beta-effect propagation processes could cause large TC track errors. Kehoe found five cases of Insufficient Beta Effect Propagation (I-BEP) in NOGAPS for the 2004 season, which in each case was due to the TC in NOGAPS being depicted as too small. Although BEP errors appeared only five times in NOGAPS, Kehoe (2005) suggested that it likely occurred more frequently, but was masked by strong environmental flow.

Another beta-effect process that led to significant errors was Reverse Trough Formation (RTF). This mechanism occurs when two TCs are oriented northeast-southwest so their peripheral anticyclones combine to produce one anticyclone, and the TCs then recurve simultaneously. Again, if a TC was depicted to be too large by the model, increased Rossby wave propagation could falsely create a large peripheral anticyclone (Carr and Elsberry 2000a). Kehoe (2005) found cases in which the initial positions of tropical cyclones determined whether the two peripheral anticyclones interact. If the TCs were too close, peripheral anticyclones had greater potential to erroneously merge. While E-RTF occurred only three times as the primary mechanism, Kehoe noted it was often a secondary mechanism in several cases involving E-DCI.

3. Midlatitude System Evolutions (MSE)

Kehoe (2005) found that more than half of the large 120-h track errors in NOGAPS and GFDN were due to Midlatitude System Evolutions (MSE). The most common MSE error found by Kehoe (2005) was I-MCG, which occurred 53 times in NOGAPS and 46 times in GFDN (Table A-1). In this case, the model depiction of the midlatitude trough amplitude was under-forecast versus reality such that it did not affect the steering flow of the TC in question. In reality, the trough would either cause a break in the steering ridge, or influence the TC to recurve. Conversely, E-MCG occurred when the midlatitude trough amplitude was over-forecast by the model such that the steering flow of the TC was erroneously changed. The second most commonly occurring MSE error during the 2004 western North Pacific season was E-MCG (six times in NOGAPS and 28 times in GFDN). Kehoe (2005) also found that E-MAG occurred commonly during the 2004 season (six times in NOGAPS and nine times in GFDN). Case studies showed that E-MAG occurred when the steering ridge was predicted to be too strong in the model compared to reality, which prevented the TC from turning poleward at the appropriate time and location. The final MSE error observed to occur frequently was E-MCL (12 times in NOGAPS and two times in GFDN). The E-MCL errors were observed when a midlatitude trough translated too quickly to appropriately influence the TC as in reality.

Kehoe concluded that both the global model (NOGAPS) and the regional model (GFDN) had difficulty in their depiction of midlatitude trough development and movement, but noted that errors often occurred in successive model integrations and would not switch from an insufficient to excessive error mechanism between two integrations.

4. Excessive Direct Cyclone Interaction in the Midlatitudes (E-DCI-m)

Kehoe (2005) identified an error mechanism in the midlatitudes similar to E-DCI found in the tropics, usually when a TC was north of the subtropical ridge in the midlatitude westerlies. In E-DCI-m, the model incorrectly depicted the TC rotating counterclockwise around a midlatitude cyclone to its northwest, which penetrated too deeply into the low levels in comparison to reality. Kehoe found that E-DCI-m occurred in both models: six times in NOGAPS and five times in GFDN.

81

5. Excessive Response to Vertical Wind Shear (E-RVS)

The final midlatitude error mechanism highlighted by Kehoe (2005) was Excessive Response to Vertical wind Shear (E-RVS). In 2004, E-RVS occurred when the upper to middle levels of the TC in the NOGAPS model were erroneously sheared from the low-level vortex, such that the low-level environmental flow alone steered the TC, whereas in reality the steering level remained higher. All 26 cases of E-RVS found by Kehoe were in NOGAPS.

APPENDIX B. RECENT DYNAMICAL MODEL UPDATES

Constant efforts are underway to increase the accuracy of the numerical weather prediction models. Nevertheless, the models still have the tendency to produce forecasts with large track errors. Some recent changes to the numerical modeling systems will be highlighted below. Special attention is paid to the TC vortex initialization scheme of each model, since TC structure was found to be an important factor in track error for the 2005 western North Pacific season.

A.   NOGAPS

The Navy global spectral model (NOGAPS) began assimilation of synthetic TC observations ("bogussing") to represent the tropical cyclone in 1991. It had been previously shown the NOGAPS would develop and maintain tropical circulations in the vicinity of actual TCs (even in data-sparse regions.) The NOGAPS bogus consisted of 13 synthetic soundings: one at the storm center; four at 220 km north, south, east, and west of the center; four at 440 km northeast, southeast, southwest, and northwest of the center; and four at 660 km north, south, east, and west of the center. The background flow was produced from filtering the first-guess fields to permit only the first 20 waves. Goerss and Jeffries (1994) noted marked improvements in 72-h forecasts attributed to the bogus scheme. Most recently, Goerss and Hogan (2006) found degradation to 24-h through 96-h TC track forecasts without synthetic observations (statistically significant to 95%). Degradations due to lack of synthetic observations at 120 h were less statistically significant.

In 2003, a 3-D variational assimilation (3-D VAR) scheme known as Naval Research Laboratory Atmospheric Variational Data Assimilation System (NAVDAS) was introduced. The implementation of NAVDAS allowed the assimilation of AMSU-A satellite radiances (beginning in June 2004) versus retrievals. Baker and Campbell (2004) found statistically significant improvement to TC 24-h to 120-h track forecasts when using AMSU-A radiances as opposed to retrievals. Goerss and Hogan (2006) also studied the impact on TC track forecasts of assimilation of various satellite observations in NOGAPS. They found that AMSU-A radiances had the largest impact at 120 h, while assimilation of feature-track winds had the greatest impact from 24 h to 96 h.

In 2002, the resolution of NOGAPS was increased from 159 to 239 waves (equivalent to 0.5º lat. horizontal resolution) and 30 vertical levels. Tests indicated that the new resolution led to a slight decrease in TC track error, especially at 96 h and 120 h (Hogan and Clune 2002). Unfortunately with the change in resolution, model developers noticed a fast bias in low-level tropical winds, which led to an adjustment in the convective momentum transport parameter of the Emanuel cumulus parameterization scheme. The update led to a reduction in track error at 72, 96, and 120 h (Hogan et al. 2004). The convective momentum transport parameter had to be adjusted again in September 2004 after it was determined that the introduction of satellite radiance data assimilation caused an over-deepening of Atlantic TCs (T. Hogan, NRL- Monterey personal communication). Kehoe (2005) found no differences in the 2004 track forecasts in the western North Pacific from before to after the change.

B. UKMO

In 1995, the UKMO introduced a bogussing scheme similar to that of NOGAPS. However, four, six, eight, and 10 synthetic observations where placed at 2, 4, 6, and 8 degree intervals respectively around the storm center (Heming et al. 1995). Heming et al. noted increased model skill after implementation, which they attributed to a representation of the vortex that could more correctly interact with its surrounding environment. The current bogus scheme has replaced the previous inner two rings at 1.25 degrees and 2.5 degrees radius each containing four bogus points (J. Heming, UKMO personal communication).

The UKMO introduced a new dynamics and physics package to the global model in 2002. It was noted that these changes reduced a previous systematic error in which the model failed to properly maintain the intensity of TCs at longer forecast intervals. This change not only improved intensity forecasting, but track forecasting performance as well (Met Office 2002).

In October 2004, the UKMO implemented a new four-dimensional variational data assimilation technique (4D-Var). The goal of 4D-Var was to improve initial conditions of the model forecast by including a time dimension. The previous forecast for a six-hour window surrounding the new forecast time is used as a guess forecast. The guess forecast is refined by running the model forward, then backward (usually through

50 iterations) to minimize changes between later observations and the guess state. The refined guess forecast then becomes the new analysis at the 0-hour. Implementation of the 4D-Var has not led to consistent improvement in TC track forecasting, but has further improved the ability of the model to maintain TC intensity at longer lead times (Met Office 2004).

In addition to minor changes in data assimilation, the UKMO has introduced a new physics package in 2005, although details are not currently available externally. The reduction in the UKMO TC track forecast average error at 120 h between 2004 and 2005 in the western North Pacific is notable. It is hypothesized that the addition of 4D-Var and the updated physics package have attributed to this improvement (J. Heming, UKMO personal communication).

C.   GFDN

The GFDN model is the Navy's version of the National Centers for Environmental Prediction (NCEP) GFDL model, although with several differences. The GFDN is an uncoupled, static sea-surface temperature field, while the GFDL is a coupled ocean-atmosphere model. Additionally, the resolution of the GFDL has been increased in 2005 to add a third inner grid, while this change has yet to be implemented in the GFDN (T. Marchok, NOAA/GFDL, personal communication). The GFDN also uses NOGAPS (as opposed to the GFS fields used in GFDL) for periodic updates to boundary conditions.   In August 2004, the GFDN forecast cycle was updated to run four times daily, up from twice a day at 0600 and 1800 UTC (Dickerman 2006).

For the 2005 season, a change in the mass initialization was implemented in the GFDN. Formerly, the NOGAPS TC vortex was removed from the GFDN and a 2-D integration of the model produced a TC that was constrained to fit the tangential profile defined by the TC warning from JTWC. Now, GFDN uses the vortex representation from the parent model NOGAPS instead of the internally generated TC vortex (Dickerman 2006).

In addition, the axisymmetric model used to specify the initial vortex structure in the GFDN was updated for the 2005 season. Included were updates to the physics and to the vortex initialization package previously implemented in the GFDL model for the

2004 season (Bender et al. 2005). These changes decreased spin-up and spin-down problems with the TC vortex in the early part of the GFDN forecast (Dickerman 2006).

Finally, researchers discovered a major bug in the 2004 GFDN model that affected the initialization of the TC background field. The bug led to errors in initial storm motion that were corrected for the 2005 season (C. Dickerman, FNMOC, personal communication).

D.   GFS

Prior to 2000, the GFS model (previously known as the AVN before September 2002) did not use any form of synthetic observations, and thus track forecast skill lagged behind UKMO and NOGAPS. The guess field (from the prior 6-h forecast) and available observation data were used to produce the model analysis package. Thus, NCEP adopted a procedure to relocate the TC vortex within the model-guess field. This process involved locating the TC vortex in the guess field, separating it from the environmental flow, and then moving the TC vortex to the official warning position. If the vortex was not adequately represented by the model, bogus observations were added before the analysis fields were updated. This vortex relocation procedure led to almost a 30% reduction in average forecast errors, which were then comparable to NOGAPS and UKMO (Liu et al. 2000). The most recent change to the GFS has been a resolution upgrade to T382L64 that is integrated to 180 h, which should have an obvious impact on 96-h and 120-h TC forecasts as this is a significant upgrade in resolution. It is noted that the previous upgrade in resolution in 2002 (T254L64 to 84 h, and T170L42 to 180 h) did not affect four- and five-day forecast accuracy.

LIST OF REFERENCES

Baker, N.L., and W.F. Campbell, 2004: The impact of AMSU-A radiance assimilation in the U.S. Navy's Operational Global Atmospheric Prediction System (NOGAPS). Preprints, *13th Conference on Satellite Meteorology and Oceanography*, Norfolk, VA, Amer. Meteor. Soc., CD-ROM, P3.1.

Bender, M., 2005, cited 2006: A proposal for transition of research to operations: upgrades to the operational GFDL hurricane prediction system, NOAA/Geophysical Fluid Dynamics Laboratory, Princeton, NJ, [available from http://www.nhc.noaa.gov/jht/20032005reports/GFDLbender_JHTfinalreport.pdf]

Carr, L.E., III, and R.L. Elsberry, 1997: Models of tropical cyclone wind distribution and beta-effect propagation for application to tropical cyclone track forecasting. *Mon. Wea. Rev.*, **125**, 3190-3209.

Carr, L.E., III, and R.L. Elsberry, 2000a: Dynamical tropical cyclone track forecast errors. Part I: Tropical region errors. *Wea. Forecasting*, **15**, 641-661.

Carr, L.E., and R.L. Elsberry, 2000b: Dynamical tropical cyclone track forecast errors. Part II: Midlatitude circulation influences. *Wea. Forecasting*, **15**, 662-681.

Carr, L.E., R.L. Elsberry, and J.E. Peak, 2001: Beta test of the systematic approach expert system prototype as a tropical cyclone track forecasting aid. *Wea. Forecasting*, **16**, 355-368.

Dickerman, C.L., 2006: A recent history of the GFDN tropical cyclone forecast model. Preprints, *27th Conference on Hurricanes and Tropical Meteorology*, Monterey, CA, Amer. Meteor. Soc., CD-ROM, P5.8.

Elsberry, R.L., and L.E. Carr, 2000: Consensus of dynamical tropical cyclone track forecasts — error versus spread. *Mon. Wea. Rev.*, **128**, 4131-4138.

Goerss, J., 2000: Tropical cyclone track forecasts using an ensemble of dynamical models. *Mon. Wea. Rev.*, **128**, 1187-1193.

Goerss, J., and R. Jeffries, 1994: Assimilation of synthetic tropical cyclone observations into the Navy Operational Global Atmospheric Prediction System. *Wea. Forecasting*, **9**, 557-576.

Goerss, J., and T. Hogan, 2006: Impact of satellite observations and forecast model improvements on tropical cyclone track forecasts. Preprints, *27th Conference on Hurricanes and Tropical Meteorology*, Monterey, CA, Amer. Meteor. Soc., CD-ROM, P5.2.

Goerss, J., C. Sampson, and J. Gross, 2004: A history of western North Pacific tropical cyclone track forecast skill. *Wea. Forecasting*, **19**, 633-638.

Heming, J. T., J. C. L. Chan, and A. M Radford, 1995: A new scheme for the initialization of tropical cyclones in the UK Meteorological Office global model. *Meteorol. Appl.*, **2**, 171-184.

Hogan, T., and W. Clune, 2002,cited 2006: A description of the impact of the increase in NOGAPS resolution to T239 with 30 levels. [Available at https://www.fnmoc.navy.mil/PUBLIC/MODEL_REPORTS/index.html.]

Hogan, T., M. Peng, J. Ridout, Y.-J. Kim, J. Teixeira, and R. Pauley, 2004: The Navy Operational Global Atmospheric Prediction System: Current status and testing of convective momentum transport in the Emanuel cumulus parameterization. Proceedings, *16th Conference on Numerical Weather Prediction*, 11-15 Jan. 2004, Amer. Meteor. Soc., Seattle, WA, CD-ROM, J14.1.

Jeffries, R. A., and E.J. Fukada, 2002: Consensus approach to track forecasting. Paper TP3.2, Extended Abstracts, *Fifth International Workshop on Tropical Cyclones*, Cairns, Australia, World Meteorological Organization (Geneva).

Kehoe, R. M., 2005: Characteristic errors in 120-h tropical cyclone track forecasts in the western North Pacific. M. S. thesis, Naval Postgraduate School, 115 pp. [available at http://thesis.nps.navy.mil/05Mar_Kehoe.pdf.]

Liu, Q., T. Marchok, H-L Pan, M. Bender, and S. Lord, 2000: Improvements in hurricane initialization and forecasting at NCEP with global and regional (GFDL) models. NCEP Tech. Proc. Bulletin, No. **472**.

Met Office, 2002, cited 2006: A new Unified Model, NWP Gazette. [available from http://www.metoffice.com/research/nwp/publications/nwp_gazette/jun02/index.html]

Met Office, 2004, cited 2006: 4D-Var: A new method of data assimilation, NWP Gazette. [available from http://www.metoffice.gov.uk/research/nwp/publications/nwp_gazette/oct04/4d_var.html]

INITIAL DISTRIBUTION LIST

1.   Defense Technical Information Center
      Ft. Belvoir, Virginia

2.   Dudley Knox Library
      Naval Postgraduate School
      Monterey, California

3.   Air Force Institute of Technology
      Wright-Patterson Air Force Base, Ohio

4.   Director, Joint Typhoon Warning Center
      Naval Pacific Meteorology and Oceanography Center
      Pearl Harbor, Hawaii

5.   Office of Naval Research
      Arlington, Virginia

6.   R. L. Elsberry
      Naval Postgraduate School
      Monterey, California

7.   M. A. Boothe
      Naval Postgraduate School
      Monterey, California

8.   K. A. Payne
      Joint Typhoon Warning Center
      Pearl Harbor, Hawaii

9.   Technical Director
      Fleet Numerical Meteorological and Oceanography Center
      Monterey, California

10.   Director, Environmental Modeling Center
      NOAA/NCEP/EMC
      Washington, D.C.

11.   Julian Heming
      UK Met Office
      Exeter, England